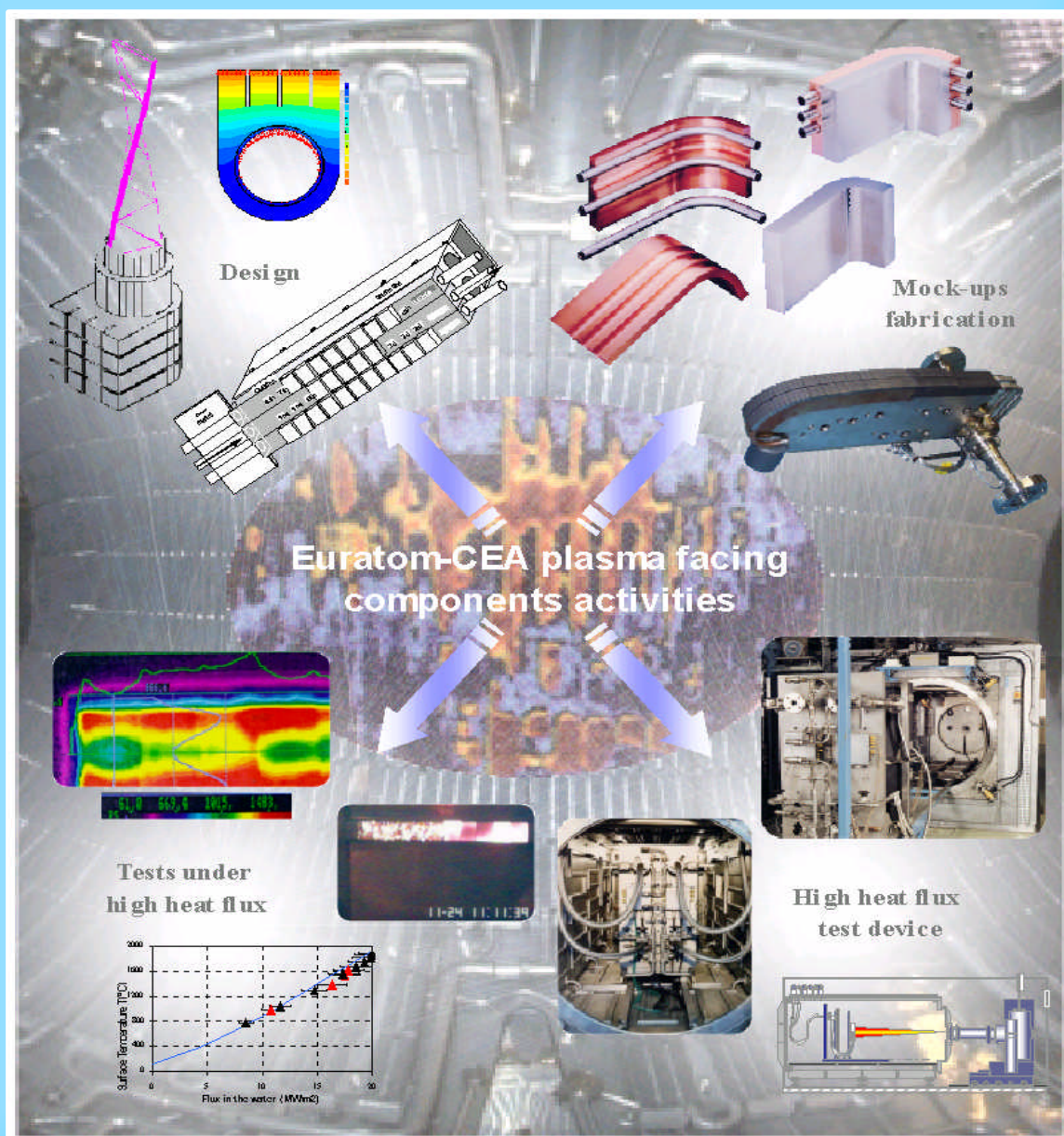


FUSION TECHNOLOGY

Annual Report of the Association EURATOM/CEA 2000

Compiled by : Ph. MAGAUD and F. Le VAGUERES



ASSOCIATION CEA/EURATOM
DSM/DRFC
CEA/CADARACHE
13108 Saint-Paul-Lez-Durance (France)

CONTENTS

INTRODUCTION	1
---------------------------	---

EFDA TECHNOLOGY PROGRAMME	3
--	---

Physics Integration

Diagnostics

TW0-DIAG-DEV	ITER diagnostic window development	5
--------------	--	---

Heating and Current Drive

TW0-ICRF/ANT	ICRF Antenna and vacuum transmission line development - ICRH Antenna coupling: Near field computations.....	7
CEFDA 00-519	Neutral beam heating design for EDA extension	11
TW0-NB.DEV.1	Neutral beam development for EDA extension - EU-JA collaborative experiment on KAMABOKO source.....	15
TW0-NB.DEV.3	Neutral beam development for EDA extension - 1 MeV SINGAP accelerator	19
TW0-NB.DEV.4	Neutral beam development for EDA extension - Manufacture and testing of a prototype 1 MeV bushing for SINGAP	23

Vessel/In Vessel

Plasma Facing Components

CEFDA 99-501	Critical heat flux and thermal fatigue testing of CFC monoblocks - 200 kW electron beam gun test	27
CNET 98-480	Thermal fatigue testing of divertor full scale prototype - 200 kW electron beam gun test	29
CNET 98-485	Thermal fatigue testing of baffle full scale prototype - 200 kW electron beam gun test	35
DV4.3	Optimisation and manufacture of HHF components - Study of flat tile cascade failure possibility for high heat flux components.....	37
TW0-DV4/01	Optimisation of manufacture of HHF components	41
TW0-DV4/02	Optimisation of Cu-SS-Tube Joints	43
TW0-T438-01	Development and testing of time resolved erosion detecting techniques	45

Vessel/Mechanical structure

T216-GB8	Small scale testing of FW/BS modules	49
TW0-LASER/CUT	VV intersector maintenance - Further development of high power Nd YAG - Improvement of YAG laser back-plate cutting using powder injection	51
TW0-LASER/HYD	YAG laser process for cutting and welding of the hydraulic module blanket - CW YAG laser process for cutting and welding of the hydraulic connections	53
TW0-LASER/REWELD	VV intersector maintenance - Further development of high power Nd YAG - Laser rewelding after cutting	55
TW0-LASER/WELD	VV intersector joining - Further development of high power Nd YAG - Laser welding with multipass filler wire	59
TW0-T301/01	Ultrasonic inspection for vessel inter-sector weld - Completion of ultrasonic inspection process development - Optimisation of the ultrasonic inspection method : effect of the wave polarity and frequency on the signal to noise ratio	61
TW0-T420/06	Fabrication of a first wall panel with HIP'ed beryllium armor	65
TW0-T420/08	Development of HIP fabrication technique - Faisability of using HIP for the manufacturing of Primary First Wall Panel (PFWP)	69
TW0-T427/03	Development and characterization of one-step SS/SS and CuCrZr/SS HIP joints including mock-up fabrication.....	73
TW0-T508/04	Development of Be/CuCrZr HIPping technique	75
TW0-T508/05	Development of Be/CuCrZr brazing techniques	77
TW0-T519/01	Low temperature water radiolysis	79
V63	Detailed investigation of CuAl25 (IG1) - Its joints with 316LN stainless steel and joints testing procedure	81

Assembly & Maintenance

T252	Radiation tolerance assessment of standard components for remote handling and process instrumentation	85
T329-5	In vessel RH dexterous operations - Task extension 2	91
TW0-DTP/1.1 T329-4	Carrier and bore tools for 4" bend pipes	95
TW0-DTP/1.2 TW0-DTP/1.4	Prototypical manipulator for access through IVVS	99

Magnet Structure

CEFDA 00-517	Design of cryogenic transfer lines and ring manifolds for ITER-FEAT	103
CEFDA 00-541	PF correction coils : conceptual design and analysis, CS cooling inlets, conductor analysis tools	105
M40	Design work on magnet R&D	109

M50	Conductor R&D - Development of NbTi conductors for ITER PF coils	111
TW0-T400-1	CSMC and TFMC installation and test	113

Tritium Breeding and Materials

Breeding Blanket

Water Cooled Lithium Lead (WCLL) Blanket

TTBA-1.1	TBM Adaptation to Next Step.....	117
TTBA-2.1	Blanket Manufacturing Techniques - Definition of specifications for demonstrators	121
TTBA-2.2	Blanket Manufacturing Techniques - Solid HIP demonstrator for fabrication and coating, fabrication of double wall tubes	125
TTBA-2.4	Blanket Manufacturing Techniques - Feasibility of powder HIP fabrication for TBM or TBM components	129
TTBA-2.5	Blanket Manufacturing Techniques - Double-wall tube out-of-pile testing (DIADEMO experimental program)	133
TTBA-3.1	Coating qualification and irradiation tests - Permeation barrier qualification - Fabrication and characterization of CVD specimens	137
TTBA-3.5 WPA4.2.3	Coating qualification and irradiation tests - Permeation out-of-pile testing	141
TTBA-4.1	Processes and components - Tritium extraction from Pb-17Li	143
TTBA-5.3	Safety and Licensing - Modelling of the lithium/lead water interaction	147
TTBA-5.4	Safety and Licensing - Development of minor components & instrumentation.....	149
TTBA-6.2	MHD Effects - Test and modeling of natural convection MHD	153

Helium Cooled Pebble Bed (HCPB) Blanket

TTBB-2.3	Blanket Manufacturing Techniques - First wall manufacturing by HIP forming technique	157
TTBB-5.D3	Development of ceramic breeder pebble beds - Characterization of Li_2TiO_3 pebble beds	159
TTBB-5.D4	Development of ceramic breeder pebble beds - Validation of Li_2TiO_3 fabrication with pre-industrial means of the lab fabrication steps - Mastering/Optimizing	163

Structural Materials development

Advanced materials

TTMA-1.2	SiC/SiC ceramic composites - SiC/SiC composite development and characterization	167
TTMA-1.4	SiC/SiC ceramic composites - Compatibility of SiC/SiC composite with liquid Pb-17Li alloy	169

TTMA-1.6	SiC/SiC ceramic composites - Brazing of SiC/SiC composites with thermo-mechanical testing	173
Reduced Activation Ferritic Martensitic (RAFM) Steels		
SM-2-3-1	Mechanical properties of F82H weldments	177
SM-3-3	Corrosion in water conditions - Corrosion water with additives	181
SM-3-5.1	Compatibility with hydrogen and liquid - SCC behaviour of Eurofer in aqueous environments	185
SM-4-3	F82H weldability with filler metal	187
SM-5-7	Small size specimen technology	191
SM-6-1	Development of high dose high temperature - Low temperature, high dose irradiation test with ISTC.....	193
TTMS-1.1	RAFM steels - Irradiation performance - Neutron irradiation of RAFM steels to 30-35 dpa at 325°C.....	197
TTMS-2.1 SM-2-1	RAFM steels - Metallurgical and mechanical characterization - Metallurgical characterization of EUROFER 97 steel	199
TTMS-2.2	RAFM steels - Metallurgical and mechanical characterization - Mechanical characterization of Eurofer 97 : tensile and impact properties.....	203
TTMS-2.3.1	RAFM steels - Metallurgical and mechanical characterization - Mechanical properties of diffusion bonded welds (RAFM/RAFM HIP joint)	207
TTMS-2.3.2	RAFM steels - Metallurgical and mechanical characterization - Mechanical properties of weldments	211
TTMS-2.4	RAFM steels - Metallurgical and mechanical characterization - Mechanical properties of powder HIP Eurofer.....	215
TTMS-4.1	RAFM steels - Qualification fabrication processes - Eurofer powder HIP development and characterization.....	217
TTMS-4.2	RAFM steels - Qualification fabrication processes - Mechanical alloying including ODS	221
TTMS-4.3	RAFM steels - Qualification fabrication processes - RAFM weldability.....	225
TTMS-4.4	RAFM steels - Qualification fabrication processes - Dissimilar welding RAFM/316LN	229
TTMS-4.5	RAFM steels - Qualification fabrication processes - Solid HIP process and qualification	231
TTMS-5.1	RAFM steels - Rules for design and inspection - Design code assessment and development	235
TTMS-5.4	RAFM steels - Rules for design and inspection - Data collection and data base maintenance	239
TTMS-6.3.1	RAFM steels - Qualification of high performance steels - Development of RAFM-ODS steels.....	243
Neutron Source		
TTMI-001	IFMIF - Accelerator facility	245

Safety and Environment

CEFDA 00-539	French contribution to ITER licensing working group.....	249
SEA1-14	Assist JCT on safety documentation	251
SEA4-4	Plant safety assessment - ITER-FEAT design CAT V accident analysis : H ₂ production via delayed plasma shutdown.....	253
SEA5-2	Validation of computer codes and models - ISAS maintenance.....	255
SEA5-3	Validation of computer codes and models - Thermohydraulical code validate experiments	257
TSW-2.1	Waste and Decommissioning Strategy - Detritiation of structural material and management of tritiated waste.....	259
TSW-2.6	Waste and Decommissioning Strategy - Development and assessment of overall strategies.....	263
TW0-SEA3.5	Hydrogen deflagration/detonation analysis	265
TW0-SEA4	Plant safety assessment.....	267

System Studies

Power Plant Conceptual Studies (PPCS)

TW0-TRP-1.1	Safety and environmental requirements	271
TW0-TRP-2.4	Economic and operational requirements	273
TW0-TRP-2.5	Supply requirements	277
TW0-TRP-3D4	Reactor integration	279
TW0-TRP-4D5	High heat flux components.....	283
TW0-TRP-4D7	Economics and operational analyses - Maintenance schemes	285

Socio-Economics Studies

SERF2	Externalities of fusion - Accident external costs and sensitivity analysis on the site location.....	289
-------	---	-----

<i>UNDERLYING TECHNOLOGY PROGRAMME</i>	293
---	------------

Vessel/In Vessel

Plasma Facing Components

UT-PFC&C-HFW	Transparent polycrystalline ceramics	295
UT-PFC&C-HIP	Mechanical behaviour of HIP joints	299

UT-PFC&C-SiC	C-SiC and boron doped graphite	303
UT-PFC&C-SiC/MJ	Development of SiC/metal joining technology	307
UT-SM&C-VVI	Design and analysis of vacuum vessel and internals	309

Vessel/ Mechanical Structure

UT-SM&C-BIM	Dissimilar diffusion-bonded joints mechanical testing	313
-------------	---	-----

Assembly and Maintenance

UT-RH1	Remote Handling Techniques - Technology and control for remote handling systems	317
UT-RH2	Remote Handling Techniques - Graphical programming for remote handling	319
UT-RH3	Remote Handling Techniques - Advanced technologies for high performances actuators	323
UT-RH4	Remote Handling Techniques - Radiation tolerance assessment of electronic components from specific industrial technologies for remote handling and process instrumentation.....	327

Tritium Breeding and Materials

Breeding Blanket

UT-SM&C-BLK	Development of breeding blankets	333
UT-SM&C-COAT	Development of an oxide layer on Fe-Al coatings	337
UT-SM&C-LM/DC	Diffusion coefficient measurements in liquid metals	341
UT-SM&C-LM/MAG	Liquid metal corrosion under magnetic field.....	345
UT-SM&C-LM/Refrac	Compatibility of refractory materials with liquid alloys	349
UT-SM&C-LM/WET	Wetting of materials by liquid metals.....	353

Materials Development

Structural Materials

UT-SM&C-LAM/Mic	Influence of the martensite morphology on the plasticity behaviour of the Eurofer steel	357
UT-SM&C-LAM/Weld	Laser weldability of LAM steels (Eurofer97)	361
UT-SM&C-LAM2	Irradiated behaviour of Reduced Activation (RA) martensitic steels after neutron irradiation at 325°C.....	363
UT-SM&C-LAM3	Microstructural investigation of Reduced Activation Ferritic-Martensitic (RAFM) steels by Small Angle Neutron Scattering (SANS)	367
UT-SM&C-ODS	Development of forming and joining technologies for ODS steels	371

Nuclear Data

UT-N-NDA	Nuclear data assessment	375
----------	-------------------------------	-----

Fuel Cycle

UT-T1	Separation of the D/T mixture from helium in fusion reactors using superpermeable membranes - Development of superpermeable membranes suitable to operate under ion bombardment	379
-------	---	-----

Safety and Environment

UT-S-BLK	Blanket Safety	383
UT-S-MITIG	Evaluation and mitigation of the risk connected with air or water ingress	385

System Studies

UT-SM&C-REL	Reliability modeling & assessment	389
UT-SM&C-TDC	Innovative Thermo-Dynamic Cycles studies (TDC)	393
UT-SM&C-TMNC	Thermal-hydraulic models for nuclear components	397

<i>INERTIAL CONFINEMENT FUSION PROGRAMME</i>	399
---	-----

ICF01	Intense laser and particle beams dynamics for ICF applications	401
ICF02	Civil applications of inertial confinement fusion - Cryogenic targets production using magnetic levitation	405
ICF03	Laser-matter interaction at relativistic intensities and fast igniter studies	411
ICF-KiT-PRC	Overview on power reactor concepts	415

<i>APPENDIX 1 : Directions contribution to the fusion programme</i>	419
--	-----

<i>APPENDIX 2 : Allocations of tasks</i>	423
---	-----

<i>APPENDIX 3 : Reports and publications</i>	429
---	-----

<i>APPENDIX 4 : CEA tasks in alphabetical order</i>	441
--	-----

<i>APPENDIX 5 : CEA sites</i>	445
--	-----

Task Title : TBM ADAPTATION TO NEXT STEP

INTRODUCTION

Considering the specification of ITER-FEAT [1], thermo-mechanical and tritium-related analyses of the WCLL Test Blanket Module (TBM) have been carried out. This enabled to investigate whether temperature and stress levels relevant to those of DEMO and tritium permeation tests could be achieved despite the lower heat flux and neutron wall loading in ITER-FEAT. Minor modifications of the design were made and the cooling conditions were adjusted. The overall test program has been also re-evaluated in collaboration with the ITER Joint Central Team (JCT).

2000 ACTIVITIES

TEST BLANKET MODULE DESCRIPTION

The WCLL TBM, the main body of which is similar to the equatorial part of an inboard segment of the corresponding DEMO blanket, is expected to use all technologies required for that concept: ferritic-martensitic steel as structural material, liquid Pb-17Li as breeder and neutron multiplier, and light water at typical PWR conditions as coolant. ITER-FEAT, as a test bed, provides a unique opportunity to operate, for the first time, a DEMO-relevant TBM system in a combination of magnetic field, surface heat flux and 14.1 MeV neutron wall loading.

The WCLL TBM (Figure 1) is essentially formed by a directly cooled steel box having the function of Pb-17Li container and by a double-walled C-shaped tube bundle, immersed in the liquid metal, in which the water coolant circulates. The module box is reinforced by radial and toroidal stiffeners to withstand the disruption-induced forces and the full water pressure under faulted conditions. Two independent water-coolant circuits are present, one cooling the module box, the other cooling the breeder region. As foreseen for DEMO, double-wall cooling tubes and tritium permeation barriers are used. The tube bundle is maintained in place with one spacer grid at about TBM mid-plane level.

The segment box cooling tubes are collected in the rear by two vertical half tubes, welded to the back-plate of the segment box, one for the inlet water, the other for the outlet. Two coolant headers for the breeder zone cooling circuit, one at the top for outlet water and one at the bottom for inlet water, are also welded to the back-plate of the TBM. Water at PWR conditions ($p = 15.5$ MPa and T between 290 and 325°C) will be used as coolant. During normal operation, the removed heat shall be dissipated into a low temperature, low pressure secondary cooling circuit provided by ITER.

The TBM is cased in one vertical half of the ITER-FEAT mid-plane Port #18 and is supported by a water-cooled stainless steel frame. The other half of Port #18 is occupied by the Japanese Ceramic/water-cooled TBM. At present, the EU WCLL TBM is assumed to be straight without FW protection and is attached to the back wall of the frame, which in turn is directly supported by the ITER-FEAT vacuum vessel.

Different fabrication techniques with different degrees of performances and required R&D are being considered for the EU WCLL TBM [2]. The fabrication based on the use of a machined monolithic steel block and solid hot isostatic pressing (HIP) is, at present, the preferred option for the manufacturing of a straight TBM, because it requires only limited extrapolation from present-day industrial technology.

Table 1 : Main characteristics of the EU WCLL-TBM to be tested in ITER-FEAT (surface heat flux 0.25 MW/m², neutron wall loading 1.1 MW/m²)

Dimensions	1.72 m high x 0.514 m wide x 0.585 m deep
Mass in operation	Be 8.75 kg, steel 950 kg, water 60 kg, Pb-17Li 2575 kg, total 3594 kg
Deposited power in the whole TBM	1.07 MW (assuming 0.25 MW/m ² surface heat flux and 1.1 MW/m ² neutron wall loading)
Tritium production	36 mg/day (22 % duty cycle, 90% ⁶ Li enrichment; 1.1 MW/m ² NWL)
Breeder zone water cooling circuit	Pressure 15.5 MPa, inlet/outlet temperatures 315/325 °C, mass flow rate 7.8 kg/s, extracted power 0.48 MW
Segment box water cooling circuit	Pressure 15.5 MPa, inlet/outlet temperatures 303/325 °C, mass flow rate 4.4 kg/s, extracted power 0.58 MW, number of cooling tubes 48
Maximum temperatures	Pb-17Li/steel interface 450°C, Be armor 458 °C, FW steel 449 °C, Pb-17Li 459°C
Maximum stress levels	FW steel 290 MPa

DESIGN OF THE TBM ANCILLARY CIRCUITS

The Pb-17Li ancillary circuit has been designed in an integrated way in a sealed housing located just behind the ITER bioshield plug (Figure 2). It is placed as close as possible to the TBM in order to reduce tritium permeation, enabling a measurable concentration in the tritium extraction system. Due to space requirements for allowing the personnel to perform the maintenance operations, the integrated Pb-17Li circuit has been reduced to the minimum size (2.315 m high x 2.19 m deep x 1.6 m wide). It includes the following major components: circulation pump, storage/drain tank with a pump for filling, tritium extraction unit, valves for circuit isolation and flow control and trace heating on all pipework.

- E.U WCLL TBM MODULE -

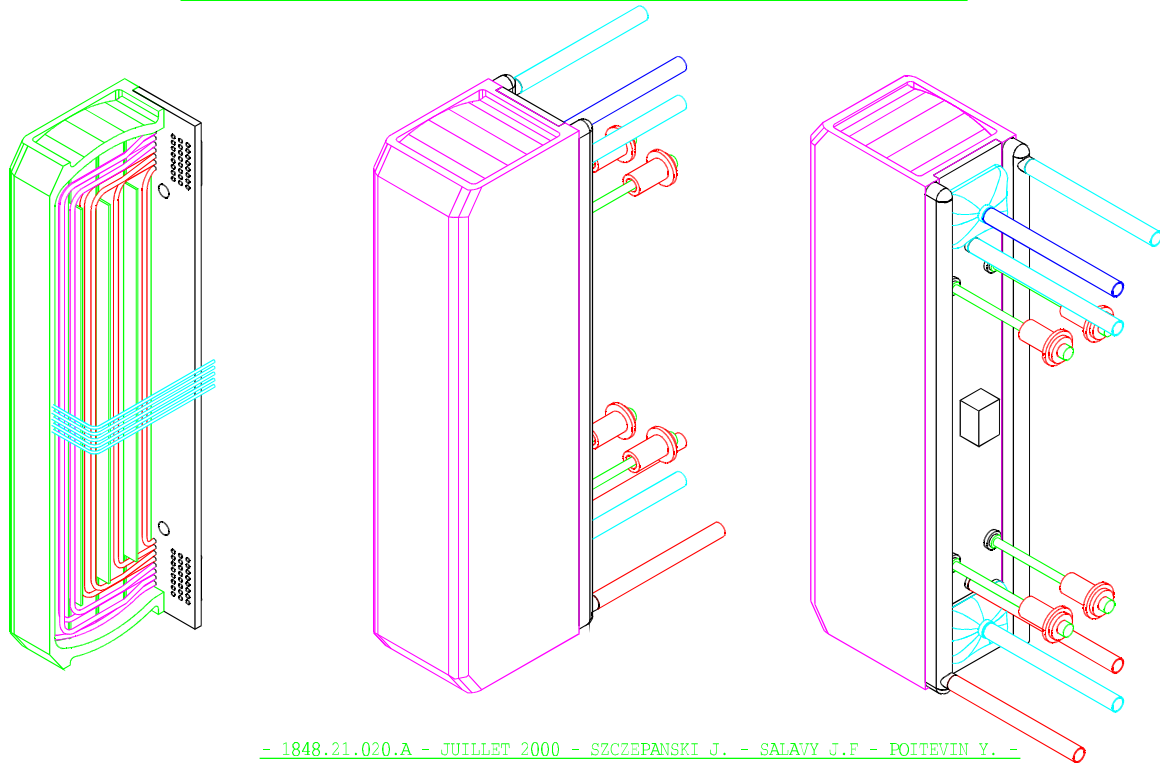


Figure 1 : EU WCLL-TBM for testing in ITER-FEAT

- E.U WCLL TBM LAYOUT IN ITER FEAT "PORT 18" -

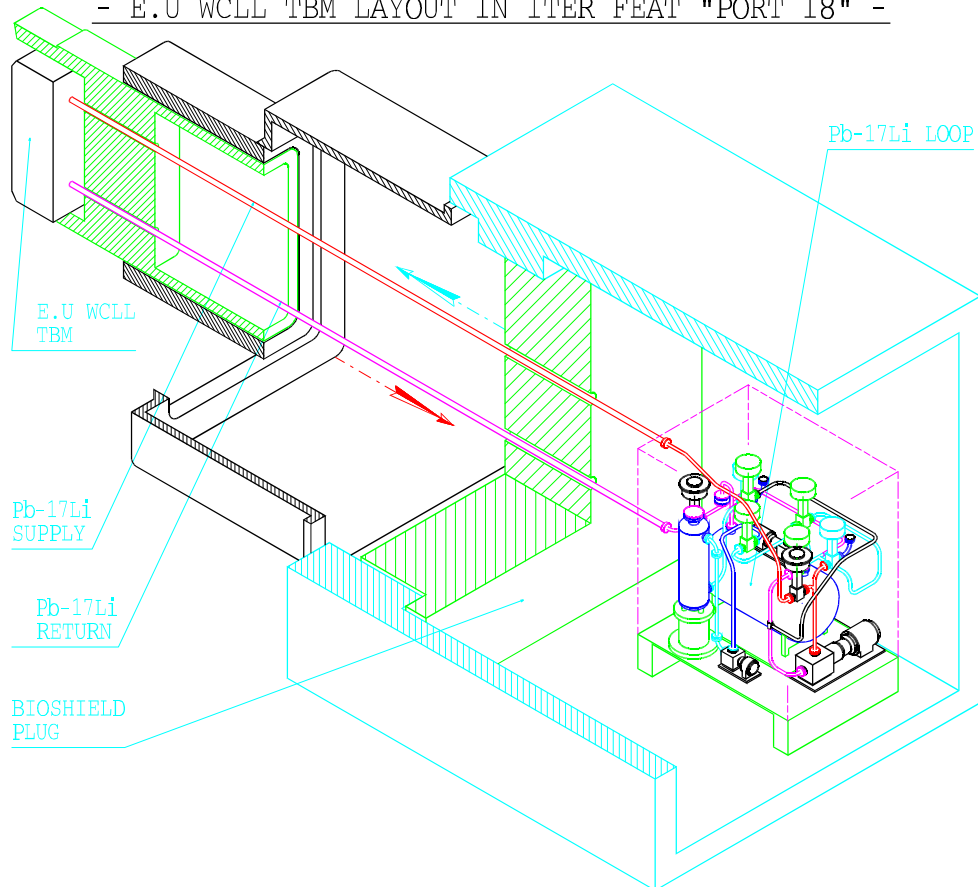


Figure 2 : ITER-FEAT Port #18 layout showing location of the EU Pb-17Li loop behind the Bioshield Plug

The tritium extraction unit consists of a packed vertical column extractor with purge gas supply. This system can be bypassed, but in nominal conditions the entire flow rate will go through it. The tritium extraction from the purge-gas will be performed in the ITER Tritium Building. In order to avoid Pb-17Li freezing, during extended periods of system shutdown and in accidental situations, the Pb-17Li in the circuit will be gravity-drained into the storage tank. All the pipework will be thermally insulated. The Pb-17Li flow rate for the TBM will be kept adjustable in the range of [0.1 – 1] kg/s in order to be able to obtain high tritium partial pressures, to reproduce 10 recirculations per day (0.4 kg/s) or to study MHD effects at higher flow rates. The two independent water coolant ancillary circuits have been located in the ITER-FEAT TCWS vault and detritiation is assumed to be performed by the ITER cooling system to which the tritiated water will be diverted. A limited space of (4.5 m high \times 4 m wide \times 4 m deep) has been attributed to the two WCLL-TBM water cooling ancillary circuits. One half of the allocated space will be attributed to either circuit. The basic components of each cooling system have been preliminary designed: storage/drain tank, pressurizer, heat exchanger to the secondary coolant system, pumps and connecting pipework. A counter-current straight tube bundle exchanger was chosen, in order to minimize the exchange surface. Nevertheless, the exchanger dimensions will be \sim 2 m long. Fluctuations of the coolant inlet temperature (pulsed operation) will be damped by a controlled heat exchanger bypass or an additional heater. Additional valves will allow the isolation of the cooling system and heating/cooling of the system at start-up and shut-down.

TESTING STRATEGY FOR THE EU WCLL TBM

The overall objective of the WCLL TBM test in ITER-FEAT during the BPP is to evaluate its behavior (e.g., functional, thermal, mechanical, neutronic) under conditions which are, as much as possible, relevant to DEMO, either through extrapolation of the results or through direct interpretation. The validation of computer codes is expected to be one of the most valuable achievements. It is intended to leave the same WCLL-TBM in place from its installation until the end of the BPP. It has been indeed demonstrated (cf. Table 1) that, despite the lower heat flux and neutron wall loading in ITER-FEAT, temperature and stress levels relevant to those of DEMO can be obtained by properly choosing coolant parameters. The only exceptions are: i) long maintenance periods in which the TBM might be removed from the Vacuum Vessel if required; ii) the insertion for a limited duration of a specifically instrumented TBM for neutronic measurements, iii) in case of TBM failure where the TBM has to be removed and replaced; and iv) if a newly developed preferred technology has to be tested.

CONCLUSION

Considering the specifications of ITER-FEAT, thermo-mechanical and tritium analyzes of the WCLL Test Blanket Module have shown that, despite the lower heat flux and neutron wall loading in ITER-FEAT, temperature and stress

level relevant to those of DEMO and tritium permeation tests could be achieved considering minor modifications of the design and by properly adjusting the cooling conditions. In order to keep measurable concentration in the tritium extraction system, the Pb-17Li ancillary circuit has been located as close as possible to the TBM, after the bioshield plug. It has been designed in an integrated leak-tight housing taking into account space and remote handling constraints of the ITER machine. The two water cooling loops (one for the breeder zone and one for the First Wall) have been also designed to fit properly in the allocated space in the TCWS vault of ITER.

The overall test program of the WCLL TBM has been re-evaluated in collaboration with JCT. It has been shown in particular that a unique WCLL TBM design could be considered for all phases of ITER-FEAT operation and testing sequences considering proper adjustment of cooling conditions and adapted instrumentation. The same TBM design will then be specifically instrumented according to the envisaged test sequence.

REFERENCES

- [1] S. Booth, Minutes of the 7th meeting of the Test Blanket Working Group, ITER JWS Garching, February 22-23, 2000.
- [2] M. Fütterer et al., Design development and manufacturing sequence of the European water-cooled Pb-17Li Test Blanket Module, Proceedings of the ISFNT-4, 6-11 April 1997, Tokyo, Japan.

REPORTS

Y. Poitevin, M. Fütterer et al. «First status of the conceptual design and testing sequence of the WCLL Test Blanket Module for ITER-FEAT», CEA internal report SERMA/LCA/RT/01-2917/A, February 2001.

TASK LEADER

Yves POITEVIN

DRN/DMT/SERMA
CEA Saclay
91191 Gif-sur-Yvette Cedex

Tél. : 33 1 69 08 31 86
Fax : 33 1 69 08 99 35

E-mail : ypoitevin@cea.fr

Task Title : BLANKET MANUFACTURING TECHNIQUES

Definition of specifications for demonstrators

INTRODUCTION

The 2000 activities performed in the framework of task TTBA-1.1 [1] have lead to an update of the conceptual design and operating conditions of the Test Blanket Module (TBM) for a testing in ITER-FEAT on the basis of the design previously envisaged for ITER-FDR [2].

The work carried out in the framework of Task TTBA-2.1 consisted in assessing the impact of these modifications on the definition of TBM demonstrators. The key elements to be included in TBM demonstrators have been also specified.

2000 ACTIVITIES

TBM DESIGN EVOLUTION AND IMPACT ON DEMONSTRATORS

The overall dimensions of the TBM have changed with regard to the previous TBM designed for ITER-FDR (1.72 m high x 0.514 m wide x 0.585 m deep instead of 2.12 m high x 0.44 m wide x 0.585 m deep). Radial and toroidal stiffeners delimit 12 rectangular (126 mm x 148 mm) sectors inside the TBM (Cf. Figure 1).

These overall dimensions remain of the same order of magnitude than those for ITER-FDR and should have a limited impact on the demonstrators specifications and manufacturing route.

However, due to the change in size of the sectors delimited by stiffeners, it has appeared necessary to reinforce the First Wall (FW) corners and the side walls in order to withstand the accidental pressurization of the segment box at 15.5 MPa.

Thermo-mechanical calculations have shown that a side wall thickness of 26 mm (instead of 21 mm) would lead to acceptable temperature and stress level during normal and accidental situations. The thickness of the FW remains unchanged at 21 mm as well as the one of radial and toroidal stiffeners (8 mm).

It is also envisaged to drill small holes (dimensions to be defined) in the stiffeners (Cf. Figure 2) in order to allow mixing of the Pb-17Li between the front sectors, where the tritium production is higher (~57% of the tritium is produced there), and sectors at the rear, where tritium production is lower. This should ensure higher average tritium concentration during testing at the return tube located at the back of the module.

The Pb-17Li supply/return system of the TBM has been slightly modified (Figure 2). In order to favor flowing in the front sectors, the Pb-17Li inlet tube which is connected to the TBM backplate is prolonging inside the TBM up to the front part. The Pb-17Li outlet tube is plunging up to the bottom of the TBM in order to allow complete drainout of the TBM during maintenance or standby phases.

C-shape Double Wall Tubes (DWTs) have been preferred [3] instead of the previous U-shape tubes as they allow significant reduction of steel inventory at the top of the TBM (the water header are reported on the external side of the backplate). This implies that DWTs could not be inserted, as previously with U-tubes, after welding of stiffeners inside the segment box. They must be put in place before this operation.

An optimisation of the Breeder Zone (BZ) cooling conditions under ITER-FEAT operating conditions has also permitted to reduce the total number of C-shape DWTs to 35 instead of 48 in the first C-shape version [3]. The DWT cooling in the front part of the breeder zone has to be located with a precision of about 1 mm with regard to the reference drawings. This implies the use of a spacer grid at midplane of the TBM. In the upper and lower part of the module, connection of the DWTs to the backplate requires 3-dimensional bending which could be performed with lower precision (to be defined) than for the front region. However, the preliminary announced precision of +/-2 mm on classical 3-dimensional bending obtained on U-shape DWT appears too low and has to be improved in the future. Some fabrication techniques using a 3D model shape could permit to reach higher precision on curvature radius of 3d-bent DWTs.

KEY ELEMENTS OF A DEMONSTRATOR

On the basis of the reference WCLL TBM design, demonstrator mock-ups should be designed with the final aim of demonstrating the possibility to manufacture and integrate the following elements of the TBM:

- Eurofer Steel box with internal double-wall cooling tubes. The external size of the box should be representative of the reference TBM (several tens of cm).
- Connection of FW cooling DWT to the backplate with continuity of the double-wall function between water and Pb-17Li regions.
- FW water cooling header welded on back-plate.
- Internal stiffeners (thickness 8 mm) delimiting rectangular sectors of about 10-15 cm width.

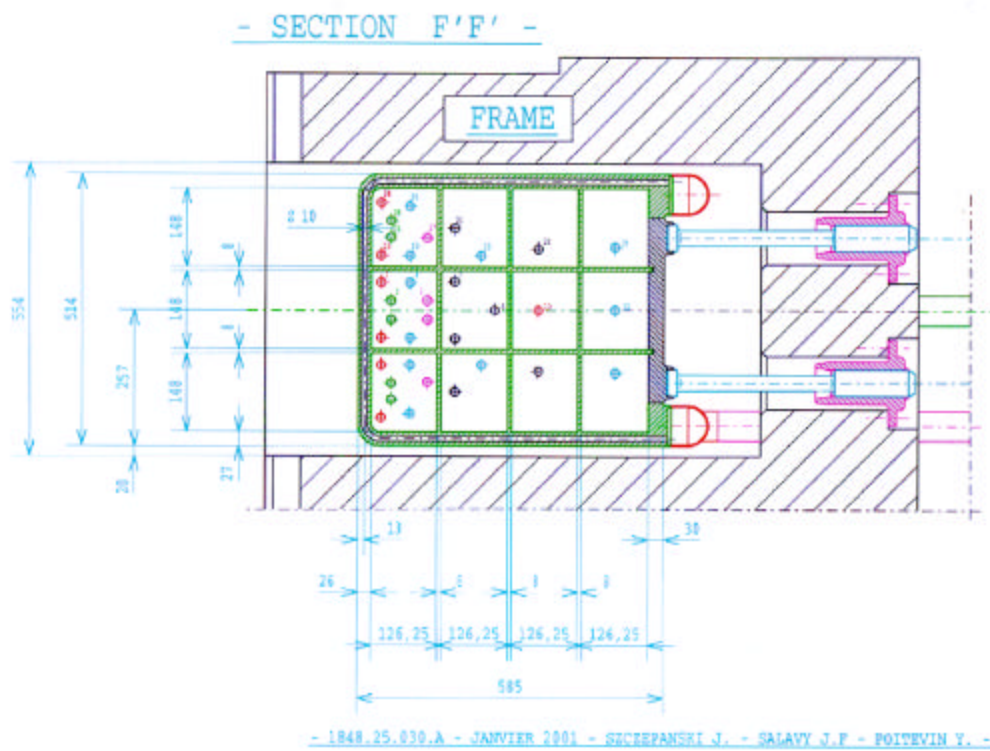


Figure 1 : Equatorial section of the WCLL TBM for ITER-FEAT

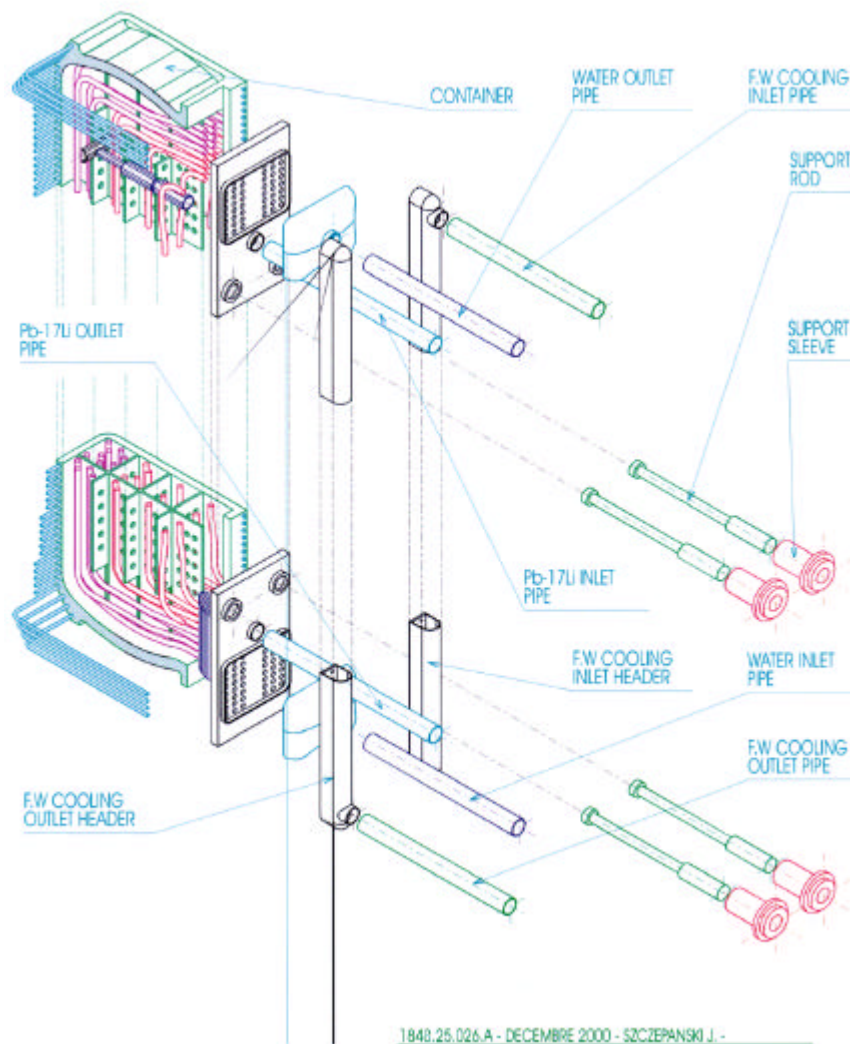


Figure 2 : WCLL TBM for ITER-FEAT

- C-shape DWTs inserted inside stiffeners sectors with connection to the backplate (double wall function continuity) and spacer grid.
- Breeder zone water cooling header welded on backplate.
- Top or bottom closing of the segment box.

The final demonstration could be achieved through several mock-ups as long as the integration of all sub-elements in the foreseen reference TBM is ensured.

CONCLUSION

The design modifications induced by testing of the WCLL TBM in ITER-FEAT have been analysed for a re-definition of specification for demonstrators. They appear however relatively limited and should not lead to strong modifications of the foreseen manufacturing route [3].

REFERENCES

- [1] Y. Poitevin, P. Fütterer et al., "First status of the conceptual design and testing sequence of the WCLL Test Blanket Module for ITER-FEAT", CEA internal report SERMA/LCA/RT/01-2917/A, February 2001.
- [2] M. Fütterer et al., "Design Description Document (DDD) for the European Water-cooled Pb-17Li Test Blanket Module", CEA internal report SERMA/LCA/2125, 1997.
- [3] M. Fütterer et al., "Design modifications of the WCLL Test Blanket Module for ITER: reduction of header space", CEA internal report SERMA/LCA/TR/00-2761/A, February 2000.

REPORTS

Y. Poitevin et al., "Definition of specifications for a demonstrator of the WCLL Test Blanket Module for ITER-FEAT", CEA report SERMA/LCA/RT/01-2916, March 2001.

TASK LEADER

Yves POITEVIN

DRN/DMT/SERMA
CEA Saclay
91191 Gif-sur-Yvette Cedex

Tél. : 33 1 69 08 31 86
Fax : 33 1 69 08 99 35

E-mail : ypoitevin@cea.fr

Task Title : **BLANKET MANUFACTURING TECHNIQUES** **Solid HIP demonstrator for fabrication and coating,** **fabrication of double wall tubes**

INTRODUCTION

The fabrication of WCLL modules relies on Hot Isostatic Pressing process of reduced activation ferritic martensitic steel. Either powder or “solid” material can be used as starting point for the fabrication. This task was devoted to the study of the latter case.

2000 ACTIVITIES

FIRST WALL MOCK UP

A first wall mock up was fabricated using two U-bent T91 plates and five copper-coated SS304L tubes. Views of the mock up are presented on figure 1.

The two plates were bent separately. The adjustment was obtained by properly machining the mating surfaces. In a similar manner, adjustment of tubes was obtained by enlarging the grooves. The purpose of such operations was to avoid copper layer damage during HIP.

Despite these operations, it was necessary to use a press to achieve stacking. After press fitting, the plates slightly opened to a few tenth mm gap. The tube-plate gap was also a few tenth mm. After HIPing at 1050°C, 120MPa for 4h and tempering at 750°C, 2h, the mock up was machined to remove TIG welds and to obtain the specified curvature on the plasma side.

Tube/plate interfaces were examined. The elimination of gaps occurred through tube expansion rather than plate deformation, as could be expected.

No clear discontinuity of the copper layer was noticed. However the copper layer is very thin at some places and specially along the plate/plate joint, as shown on figure 2. In some places, the final thickness of the copper layer is only about 20-30% of its initial value.

The plate/plate joints were examined (figure 3). The joint recrystallisation is not complete. Small grains are visible in the joint area. A higher HIP temperature would be needed to achieve perfect joining, which is not possible due to the copper melting point.

DOUBLE WALL TUBES

Double wall tubes (DWTs) are made of two concentric tubes separated by a copper compliant layer. The fabrication of these components involves the coating of the smallest tube with copper and subsequent HIP.

Several DWTs were fabricated with Eurofer tubes. A 2,5m long mock up was supplied to DIADEMO for thermal fatigue testing. Other mock-ups were used for the demonstrator fabrication. A short DWT was used for destructive characterization.

The Vickers hardness of the material is $HV5 = 250 \pm 1$, which is slightly above the specifications. The interface microstructure shows a very large quantity of oxide particles on the outer tube side.

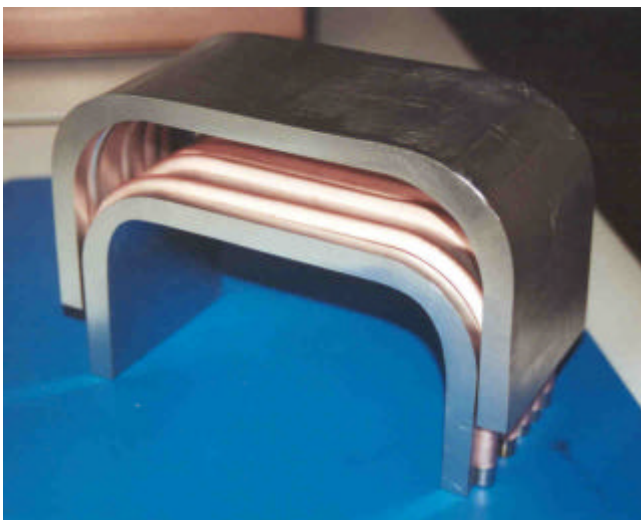


Figure 1 : First wall “solid HIP” mock up (stacking and after HIP and machining)

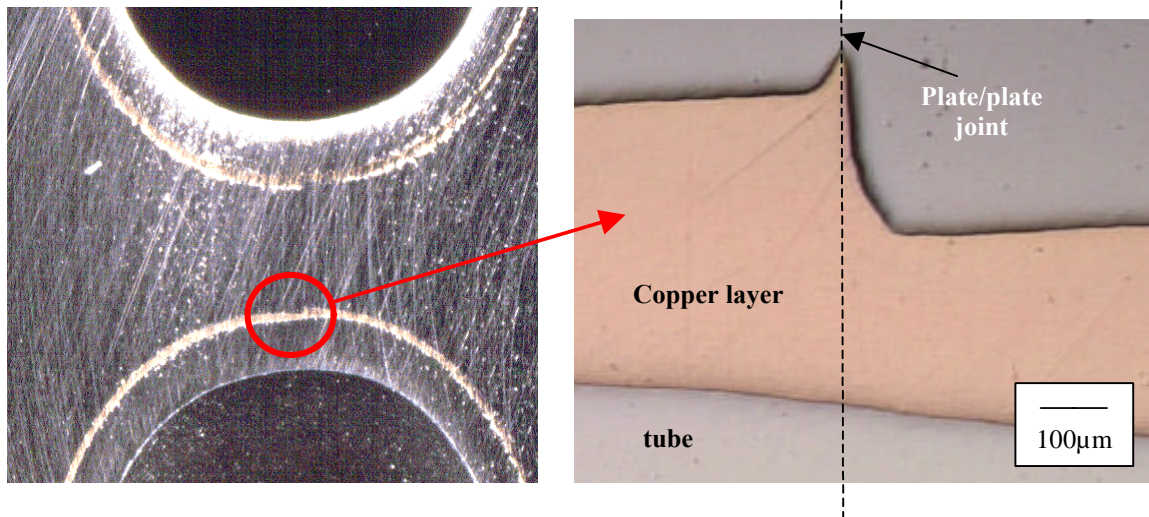


Figure 2 : Evidence of copper layer damage

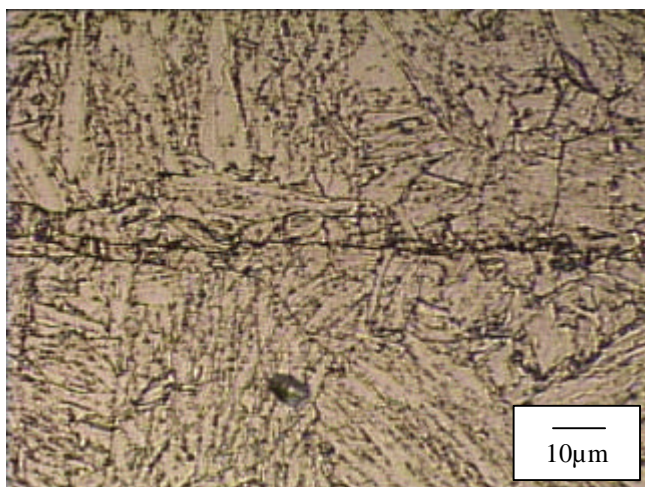


Figure 3 : Plate/plate HIP joint

This is due to the very fast re-oxidation of the inner surface of the tube after acid pickling (acid pickling was necessary due to the bad surface condition of as received tubes). On the inner tube side, the interface is almost particle-free. Copper and Eurofer are separated by a layer, 55µm thick, which results from the diffusion of the nickel underlayer towards steel and copper. The copper layer itself is about 260µm thick, which is much higher than what was specified.

Die-and-plug shear testing was used to evaluate the joint strength in the same way than during past studies [1], [2]. The mean rupture force was 513daN/mm for 1mm thick slices. For all specimens, the rupture occurred at the copper / outer tube interface. This result is coherent with the joint microstructure. The strength value can be compared to previous results valid for the short straight DWT mock ups that were manufactured in the past with T91 tubes (630daN/mm).

DEMONSTRATOR DEFINITION AND FABRICATION

A WCLL demonstrator was defined on the basis of work performed within task WPA3.1 (1999), [1]. It is made of a steel block 320x170x520mm (steel 56T5 from Aubert & Duval was used due to the unavailability of Eurofer forged block) and a Eurofer bent plate as first wall material.

The maximum capacity of the press used for bending the first wall plate led to the choice of a 300mm high first wall. Five diameter 8/10mm, copper-coated Eurofer tubes are inserted between the block and the plate.

The block comprises two LiPb containers. For costs reasons, they were drilled, resulting in a round shape instead of a square shape. The demonstrator comprises two double wall tubes with different curvatures. The first one has the minimum bending radius achievable by cold bending while the second has twice this radius. Based on [1], the DWT/plate attachment is to be achieved by conical fitting and tube expansion. The cone angle was reduced from 6° to 4° while the cone height was kept at 20mm in order to avoid DWT end damage during expansion. Top, open boxes represent DWT water supply. LiPb supplies are drilled at the mid-thickness of the plate.

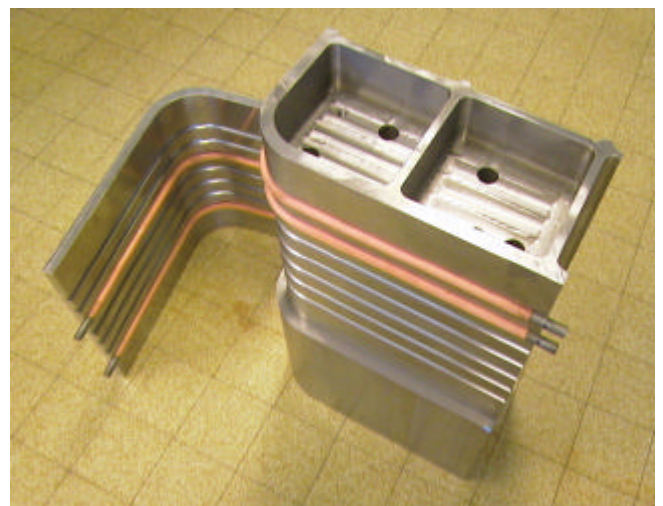


Figure 4 : WCLL demonstrator

The demonstrator was HIPed at 1040°C. Unfortunately, during HIP, the block / first wall plate weld cracked. The mock up was expertised. In some places, filler metal was needed to weld the periphery of the joints. ER316 was used and these welds did not crack. In some others places, only little filler metal was needed and Eurofer filler metal was used. Cracks were observed in these zones. They arose from martensitic transformation on cooling, as can be deduced from the well-known Schaeffler diagram.

JOINTS DEVELOPMENT

The microstructure and properties of Eurofer / SS316LN HIPed joints were further assessed. The diffusion-affected zone is much thicker on the SS316LN side than on the Eurofer side of the interface. The good mechanical properties of such joints were confirmed. The microstructure of Eurofer joints brazed with a TiZrBe-based amorphous braze was also characterised. The microstructure is satisfactory in terms of absence of cracks and porosity. Mechanical characterisation would be required to assess whether the braze joint could be used for the DWT/plate connection.

CONCLUSIONS

It is difficult to insure the absence of copper layer damaging during the fabrication of first wall by solid HIP. Furthermore, the martensitic steel / martensitic steel joint is incompletely bonded due to the limited HIP temperature. Recent results show that powder HIP could be a more suitable solution for FW fabrication.

Double wall tubes were fabricated with Eurofer tubes. The copper/Eurofer diffusion welded joints in the DWTs present a high density of oxides due to the bad surface condition of Eurofer tubes. The copper /outer tube joint is weaker than that of previous DIADEMO mock-ups.

A module demonstrator was defined and the TBM fabrication sequence was adapted to this fabrication. A forged block with two LiPb containers was machined. A FW eurofer plate and copper-coated eurofer tubes were tentatively HIPed on the block. Unfortunately the filler metal used to seal the plate / block interface periphery was inadequately chosen : the weld cracked during HIP before diffusion welding was effective. Reparation is in progress in the frame of task TW1-TTBA2.2.

Further investigation about the microstructure and properties of Eurofer/316LN HIP joints and Eurofer brazed joints were made.

REFERENCES

- [1] E. Rigal, C. Chabrol, task WPA3.1, NT DEM 92/99
- [2] E. Rigal, task WPA3.1.1, NT DEM 68/98

REPORTS AND PUBLICATION

- [1] E. Rigal, task TTBB2.2 final report, NT DEM n°108/2000

TASK LEADER

Emmanuel RIGAL

DRT/DTEN/SMP/LS2M
CEA Grenoble
17, rue des Martyrs
38054 Grenoble Cedex 9

Tél. : 33 4 76 88 97 22
Fax : 33 4 76 88 54 79

E-mail : rigal@chartreuse.cea.fr

Task Title : **BLANKET MANUFACTURING TECHNIQUES**

Feasibility of powder HIP fabrication for TBM or TBM components

INTRODUCTION

Water Cooled Lithium Lead blanket modules (WCLL) have complex shapes and geometries with double curvature and embedded cooling channels. Conventional techniques such as forging, bending and welding result in very complex fabrication routes. Hot Isostatic Pressing (HIP) techniques appear to be one of the most suitable route for the manufacturing of such complex shape components. This task was devoted to the fabrication route of the WCLL blanket modules. In 2000 we were interested in the conception and fabrication route of the WCLL blanket modules skeleton in one step. To forecast the large channels deformation during the HIP cycle, we have used the PreCAD modelling tool, developed by CEA/CEREM.

2000 ACTIVITIES

HOT ISOSTATIC PRESSING

Hot isostatic pressing (HIP) is a process in which powder consolidation is effected by the application of high pressure and high temperature. The optimisation of the process parameters has been achieved for the Eurofer powder consolidation in [1] and [2] relative to its mechanical properties.

Hip cycle

The HIP cycle for the manufacturing of the mock-ups is slightly different in the sense that pressure is applied only when the temperature reaches 1060°C. In this case, the maximum deformation is authorized when the yield stress of

the Eurofer is the lowest. The HIP cycle retained is this study is the following one :

- from 20°C to 1400°C in 4 hours,
- step during 3 hours at 0.2MPa, then from 0.2 MPa to 100 MPa in 1 hour,
- 1060°C/100 MPa step during 4 hours,
- from 1060°C/100 MPa to room temperature and pressure in 4 hours.

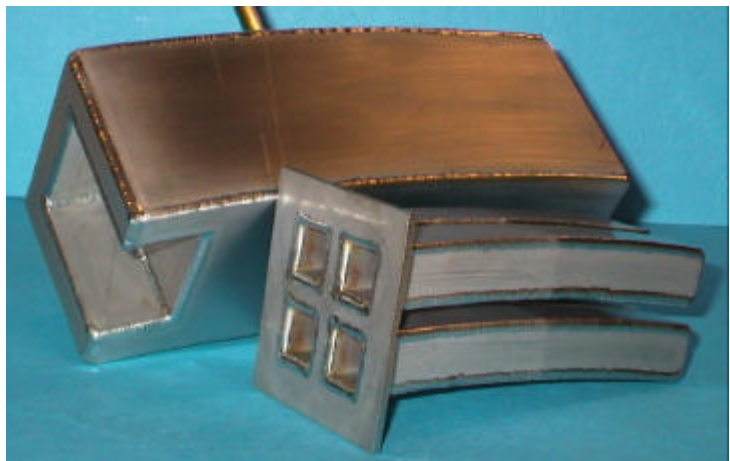
FABRICATION ROUTE

To qualify the WCLL fabrication route based on the HIP technique, a WCLL module will be manufactured in 2001. During the 1999 work, the manufacturing route has been criticized and a possible simplification has been proposed. This simplification concerns the manufacturing route of the skeleton which would be manufactured by powder HIP instead of welding square tubes. This modification has a positive consequence on the cost of the fabrication step. During this study four mock-ups representative of the skeleton of the WCLL module were manufactured. As Eurofer plates and square tubes were not available, we used SS304L material. The powder used for the manufacture of the WCLL skeleton is produced by Osprey. This powder is gas atomised. Its chemical composition is given in [3].

To manufacture the straight shape WCLL skeleton module, we used for the external shape a square tube of 60 mm and for the coolant channels square tubes of 16 mm. These tubes were closed up by small plates (fig. 1a). To get the canister of the skeleton the coolant channels and the external shape were welded. For manufacturing the curved mock-up, we decided to manufacture the model starting from parts cut off from plates by laser cutting. Some plates were then bent and assembled by welding (fig. 1b).



a) Straight shape



b) Curved shape

Figure 1 : Skeleton at a reduced scale

After HIPing, a control has been done on the cooling channels geometry of the straight and curved shape (fig. 2). These different values are reported in table 1 and table 2.

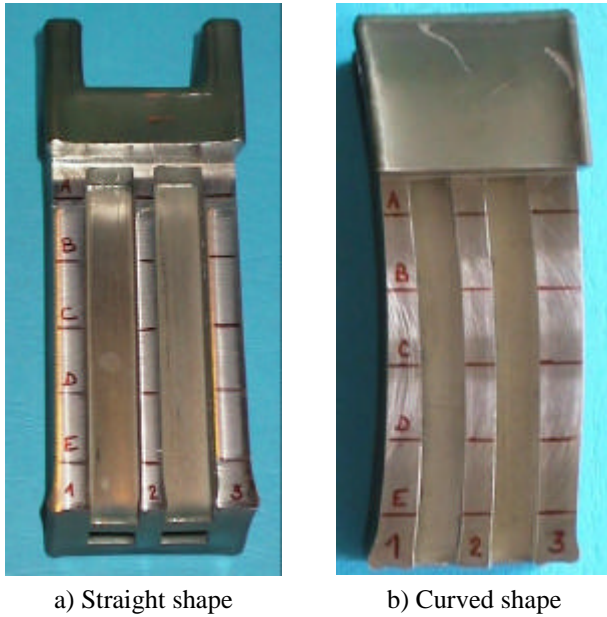


Figure 2 : Position of measured points

Table 1 : Measurements done
on the straight shape cooling channels

	before hipping	after hippping				
		A	B	C	D	E
Total width (mm)	60	53.2	53.2	53.2	53.4	53.5
Rib 1 (mm)	12.25	9.6	9.6	9.6	9.6	9.7
Channel 1 (mm)	14	14	14	14	14	14.2
Rib 2 (mm)	7.5	6	6	6	6	6.1
Channel 2 (mm)	14	14	14	14	14	14
Rib 3 (mm)	12.25	9.8	9.8	9.7	9.7	9.6

Table 2 : Measurements done
on the curved shape cooling channels

	before hipping	after hippping				
		A	B	C	D	E
Total width (mm)	60	53	52.5	52.5	52.5	52.8
Rib 1 (mm)	13.25	7.7	8.2	8.8	9.5	10.2
Channel 1 (mm)	12	11.8	11.9	11.9	11.9	11.9
Rib 2 (mm)	8.5	8.5	8.4	8.2	8.1	8
Channel 2 (mm)	12	12	12	12	12	12
Rib 3 (mm)	13.25	13	12.1	11.8	11	10.5

For the straight mock-up, the distortion of channels is symmetrical and faces of the cooling channels remain parallel between them. One can also notice that the inner dimensions of channels remain unchanged after the HIP cycle.

For the curved mock-up the distortion is not symmetrical. However, faces of the cooling channels remain parallel between them. As previously, the inner dimensions of channels (rib 1 and 2) remain unchanged after the HIP cycle.

NUMERICAL SIMULATION

A numerical analysis of the compaction of the WCLL skeleton has been performed and the simulated deformed mesh compared to the experiments.

The higher and the lower part of the mock-up became deformed in a significant way in the simulation whereas this deformation is very low on the experiment (fig. 3).

The discrepancies between the experimental results and the simulation lead to the conclusion that the numerical model is not accurate enough to be used in a predictive manner.

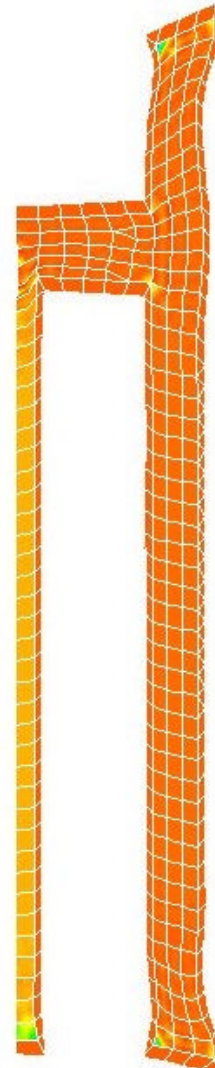


Figure 3: Simulated shape during the HIP cycle

CONCLUSION

Two manufacturing routes based on the HIP process have been studied in view of WCLL blanket skeleton fabrication. The main conclusions are the following :

- HIP parameters are defined to manufacture the skeleton of the WCLL module.
- Skeleton of the WCLL module at a reduced scale was manufactured using square tubes of various sections.
- Curved skeleton of the WCLL modules at a reduced scale was manufactured using parts machined by laser cutting. With this original concept we can manufacture very complex parts with a limited number of machining operations. This concept avoids numerous time consuming controls as in a case of a classical manufacturing route.
- The numerical model is not good enough to predict correctly the deformation related to the HIP process.

REPORTS AND PUBLICATIONS

- [1] L. Federzoni : Powder HIP development and characterization. TASK SM-4.1, Note technique DEM N° 80/99.
- [2] J.M. Gentzbittel, I. Chu : Eurofer powder HIP development and characterization. TASK TTMS-4.1, Note technique DEM N° 120/2000.
- [3] Ph. Bucci, J.M. Leibold, T. Portra : Blanket manufacturing techniques, feasibility of powder HIP fabrication for TBM or TBM components. TASK TWO-TTBA-2.4, Note technique DEM N° 110/2000.
- [4] L. Federzoni, Ph. Bucci : Test Blanket Module, Manufacturing route and manufacturing of modules. TASK WP-A3.4, Note technique DEM N° 88/99.

TASK LEADER

Ph. BUCCI

DRT/DTEN/SMP/LS2M
CEA Grenoble
17, rue des Martyrs
38054 Grenoble Cedex 9

Tél. : 33 4 76 88 38 39

Fax : 33 4 76 88 54 79

E-mail : bucci@cea.fr

Task Title : **BLANKET MANUFACTURING TECHNIQUES**

Double-wall tube out-of-pile testing (DIADEMO experimental program)

INTRODUCTION

Within the framework of the study on Water-Cooled Lithium-Lead tritigenous Blankets for a fusion reactor, technological choices on cooling tubes must be validated. Within this context, tests on Double-Wall Tubes (DWT's) through which reactor power will be transferred must be carried out.

The state of the art technology of these tubes is of utmost importance as it conditions the concept and must be validated from both mechanical and thermal point of view. Before considering industrial manufacturing, samples have to be tested under fusion reactor nominal.

The main objective of DIADEMO experimental device is to validate, in close collaboration with the task TTBA.2 (Double-Wall tube fabrication), the choice of the double-walled tube for the future Fusion reactor.

2000 ACTIVITIES

This task has been launched in 1996. Following that :

- A preliminary feasibility study, concerning an experimental device in order to test DWTs, has been performed by mid of 1996.
- A pre-design study has been, then, performed during the second half of 1996 in order to launch, beginning of 1997.
- A call for tender for the fabrication study.
- Following this fabrication study, a call for tender has been launched for the manufacturing of the mechanical part of the experimental device.
- In the mean time (summer 1997), a call for tender has been launched in order to perform the study and the manufacturing concerning the 'Instrumentation and Control of the experimental device.
- The end of the year 97 and the year 98 have been devoted to the fabrication of the experimental device (mechanical part, instrumentation and control, thermal isolation).
- During the year 99, an experimental program have been lead on a straight Double-Wall Tube (DWT) sample.

- *During the year 2000, the DIADEMO Pb-Li test section has became operational, the instrumentation of the U bent DWT was made and cycling thermal tests began and continued in 2001.*

This subtask is included in task TTBA.2, driven by CEA/ CEREM, responsible of the fabrication of the DWTs (choice of the DWT fabrication procedure, DWT manufacturing).

The U bent DWT, manufactured by CEA/ CEREM has been delivered to Cadarache at the end of the year. So the major part of the experimental program is made in 2001.

DIADEMO EXPERIMENTAL DEVICE

The experimental device "DIADEMO" has to satisfy to fusion reactor operating conditions.

So the circuit has been designed for pulsed conditions (in order to perform thermal fatigue tests on the DWTs) and for long time thermal steady-state operating conditions (in order to perform endurance tests).

The final experimental device is as follow : Two test sections :

- the first one called "*Air Test section*", using only the pressurized water cooling circuit. The test samples are electrically heated (not use of Pb-17Li loop),
- the second one called "*Pb-17Li Test section*", using the entire circuit; the Pb-17Li being also electrically heated.

The "Air Test Section" has been used for the tests of small size samples (program 1999).

The "Pb-17Li Test section" is available for the final qualification of the DWTs in presence of the eutectic.

Pb-17Li Test section

A drawing of the Pb-17Li test section is shown in appendix 2.

The maximum operating temperature in the Pb-17Li is 500°C (DEMO operating condition in the blanket).

Nevertheless it will be possible to perform thermal transient in the liquid metal for ITER operating conditions.

The operating temperatures will be between 300 and 390°C.

The main components of the Pb-17Li loops are the following :

✦ **a test vessel**, filled up with Pb-17Li, in which will be located two large size DWTs for the qualification tests. Due to the weak quantity of eutectic and for safety reason, the storage tank is located just under the test vessel. The level of Pb-17Li in the test vessel will be maintained by a gas overpressure in the storage. This experimental arrangement allows a fast gravity dumping.

The main size of the test vessel is about : ϕ 220 mm, height 1500 mm.

The main size of the storage is about : ϕ 250 mm, height 350 mm, volume ~15 l.

In the test vessel the Pb-17Li will be heated by 2 x 37 Kw immersed electrical heaters. In order to preheat the test section before fill up, other heaters will be located directly on the wall of the structure (test vessel and storage).

- ✦ **a melting vessel** in order to prepare the liquid Pb-17Li.
- ✦ **an atmosphere discharge circuit** (with rupture disc), connected to the upper part of the test vessel, in case of Pb-17Li/ water interaction.
- ✦ **a gas circuit (argon)**, in order to realize the neutral atmosphere in the test vessel.

Due to the very low velocity of the liquid metal in the DEMO or ITER blanket, it is not forecasted to perform liquid metal forced flow.

Primary Water Cooling Loop

The operating conditions of the primary water cooling circuit will simulate reactor conditions :

- Maximum water temperature : 325°C,
- Minimum water temperature : 265°C,
- Mean water temperature : 300°C
(test loop operating temperature),
- Water pressure : 15.5 MPa,
- Water tube flow rate : 0.37 kg/s.

Secondary Water Cooling Loop

The nominal operating conditions of the secondary water cooling circuit are the following :

- Mean water temperature : 55°C,
- Water pressure : 1.5 MPa,
- Water tube flow rate : 1.5 kg/s.

The secondary water loop is connected to an external air cooler, in order to remove the final thermal power.

Double-wall tube mock-up

The U bent DWT mock-up material is martensitic steel (EUROFER 97). The developed length of the mock-up is 2500 mm. The inner tube dimensions are ϕ 11/13.5 mm ; the outer tube dimensions are ϕ 14/17mm (after HIPping). The inner tube has been coated by electroplating with copper on the outer surface. The deposited pure copper layer has a thickness between 0.15 - 0.20 mm.

In order to weld the DWT mock-up to austenitic steel tube, the U bent DWT were equipped with austenitic tubular connections (304 L stainless steel ends and the DWT were diffusion welded simultaneously).

The following sketch shows the thermocouple instrumentation performed on the U bent DWT mock-up. 18 thermocouples of 1 mm diameter and laminated at 0.3 mm are located on the surface of the external tube. They are located on 9 sections (2 thermocouples per section) (figure 1).

They are diametrically opposite on the tube, one of them face to an electrical heater in order to evaluate the influence of the electrical heaters on the temperature homogeneity in the vicinity of the tube.

It has not been possible to braze the thermocouples in the tube thickness (specification given by the Double-Wall tube manufacturer), in order to measure the real temperature of the external surface.

For this reason, laminated thermocouples are used and are placed on the external wall and covered by a little piece of stainless steel electrically welded on the surface.

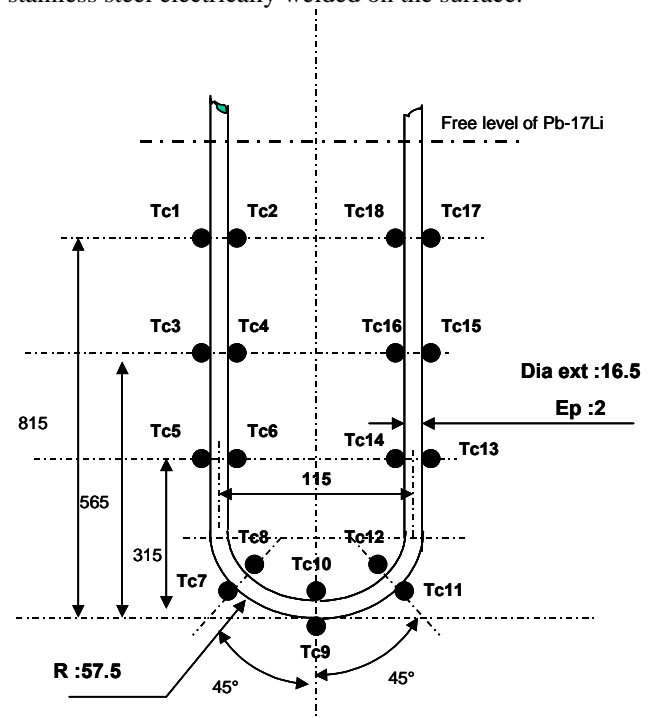


Figure 1 : Situation of thermocouples on the U bent DWT

To control the level of Pb-17Li and also to show the thermal stratification or thermal heterogeneity of Pb-17Li, a “central tube” is instrumented with thermocouples of 1 mm diameter (figure 2).

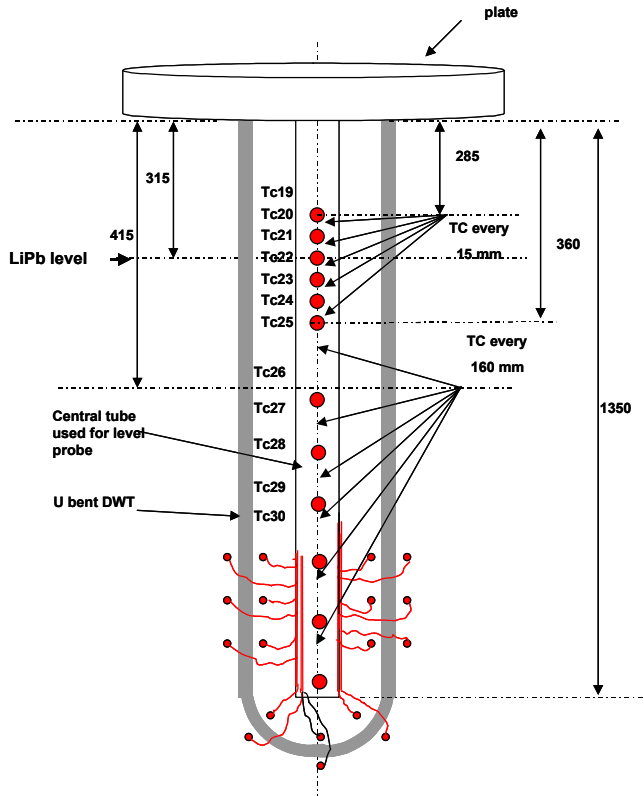


Figure 2 : Instrumentation of “central tube”

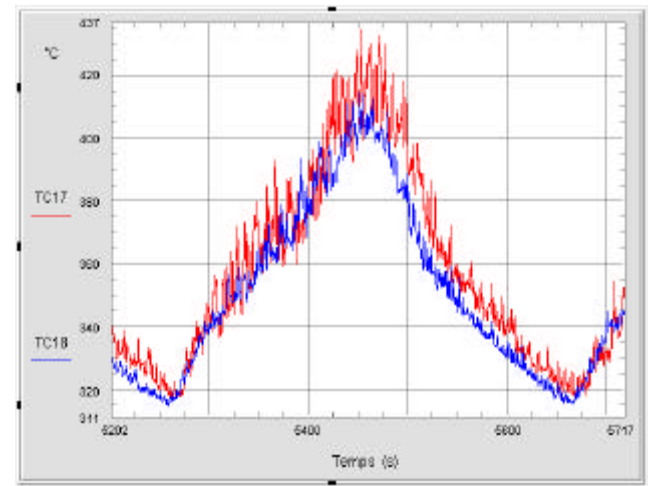
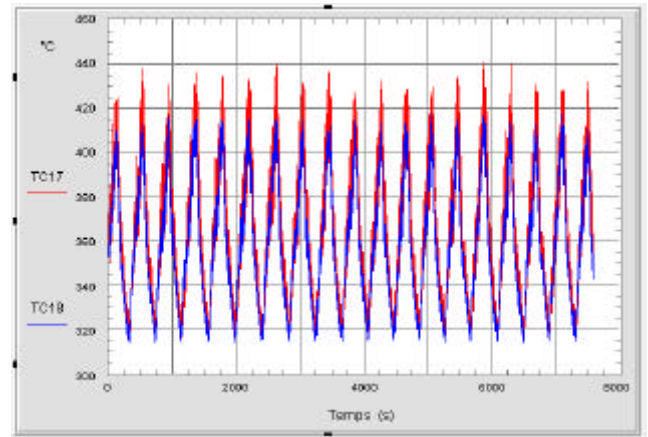
TEST CAMPAIGN.

On the U bent DWT, the experimental program performed on the “Pb-17Li test section”, is composed of two phases :

	Phase 1 thermal fatigue cycling	Phase2 endurance tests
Framework of the study	ITER Test Module	DEMO (reactor component),
Test objective	thermal fatigue in Pb-17Li	endurance test (500°C)
Max. length of the tubes (2 tubes)	2500 mm	(developed length),
Tube water flow rate	0.37 kg/s	
Electrical heating of the Pb-17Li	2 x 37 Kw immersed	electrical heaters
Operating tests	Transient between 300-390°C	Pb-17Li temperature~500°C

TEST RESULTS.

The first cycles of the phase 1 can be illustrated as followed :



CONCLUSION

We are at the beginning of the program and no conclusion on the results can be made.

2001 ACTIVITIES

In 2001, the experimental program will be continued on the Pb-17Li Test Station :

- The program of the year 2000 will be ended.
- If no damage will be observed on the U bent tube, another cycling and endurance tests will be performed (programme 2001).

REFERENCES

- [1] L. CACHON et al -
"DIADEMO EXPERIMENTAL PROGRAM (TTBA-
2.5) - Technical report"
NT. DER/ STPI/ LCFI - 00-058.

TASK LEADER

Lionel CACHON

DRN/ DER/ STPI/ LCFI
CEA Cadarache
13108 St Paul Lez Durance Cedex

Tél. : 33 4 42 25 74 25

Fax : 33 4 42 25 66 38

E-mail : lionel.cachon@drncad.cea.fr

Task Title : COATING QUALIFICATION AND IRRADIATION TESTS

Permeation barrier qualification

Fabrication and Characterization of CVD specimens

INTRODUCTION

This work concerns the development of the Chemical Vapor Deposition (CVD) technique which is one of the route studied for the fabrication of the Tritium Permeation Barriers (TPB) for the Water Cooled Lithium Lead (WCLL) blanket concept. The coating procedure for the Fe-Al/Al₂O₃ CVD coating using respectively the pack-cementation and the Pyrosol processes has been described in [1,2].

This report presents the work that has been carried out for two actions:

- the fabrication of specimens devoted to the evaluation of the properties and the behavior of the CVD coating by different in-pile and out-of-pile tests that are defined in the Barrier Qualification Procedure and scheduled in the other milestones of the TTBA-003 task,
- the deposition feasibility of Fe-Al coatings starting from a Cr-Al base cement which is tested in the frame of the CVD optimization in the view of the process industrialization.

2000 ACTIVITIES

COATING OF SPECIMENS FOR THE QUALIFICATION OF THE BARRIER

The fabrication of TPB on different specimens has been required for the qualification of the Fe-Al/Al₂O₃ CVD coating in out-of-pile and in-pile tests. All the coating operations have been performed in the standard conditions described in the Coating Qualification Report relative to the CVD route [1].

Tubes for irradiation tests (Kazakhstan)

The purpose of these tests is to evaluate the tritium permeation through coated and bare steel under neutron irradiation and in presence of eutectic Pb-17Li alloy. The experiments will be carried out in a high flux reactor in Kazakhstan in the framework of the K-39 ISTC project [3]. The deposition has been performed on two MANET II steel tubes completely assembled the surface to be coated being outside only.

The pack-cementation operation has required the fabrication of a specific tubular box to contain the cement and of particular caps to avoid a treatment of the internal surface of the tube.

Tubes for permeation tests (ENEA)

The aim of these tests is to measure the hydrogen permeation rate through coated steel in gas and in liquid lithium-lead. The experiments will be carried out in the new experimental device Vivaldi of ENEA [4]. The deposition has been performed on two EUROFER steel tubes (usefull part : length ~ 250 mm – Φ 10 mm). The surface to be coated is only the outside of the tube. The fabrication of another box and caps with a shape and a volume well-adapted to the tube geometry has been necessary to perform the pack-cementation operation.

Informations about the CVD barrier behaviour during Exotic experiments (NRG Petten)

A T91 martensitic steel tube (Φ 17/14 mm x L 185 mm) was coated with a Fe-Al/Al₂O₃ CVD barrier last year in the framework of the WPA4 task for evaluation of the barrier behavior and efficiency under irradiation in in-pile experiments at the High Flux Reactor (HFR) of Petten [5]. The experiments performed in EXOTIC-8.10 were devoted to the measurement of the tritium release behavior of a Li₄SiO₄ pebble bed, which is studied as candidate ceramic breeder for the HCPB blanket. The TPB-coated T91 tube formed the primary containment for the pebble bed. The tritium permeation rate through the T91 tube was measured at different temperatures. The results obtained after 100 irradiation days confirm that the coating presents a rather low tritium permeability even under realistic thermal-hydraulic and neutronic conditions. Further quantitative analyses will be made when more in-pile data become available and post-irradiation examination will be performed on the CVD TPB.

DEVELOPMENT of the CVD PROCESS

In the procedure qualified up to now for the CVD deposition of the Fe-Al/Al₂O₃ barrier, the pack-cementation treatment uses a Fe-Al base cement which is prepared by spray-drying [1]. This operation enables to form a fine and homogeneous powder in which each grain contains the Fe-Al donor, the activator (NH₄Cl) and the inert filler (Al₂O₃) which are intimately mixed.

The economical purpose is considered in the industrial development of the CVD process. The possibility of avoiding the spray-drying operation can be interesting in that context by simplifying the cement fabrication defined in the Coating Qualification Procedure. The choice of a new donor is proposed for the cement : aluminum alloys with higher melting point have been naturally considered. Chromium is an interesting element since it enters the substrate composition and since shots of Cr-Al material are commercially available (Starck).

Thermochemical calculations have been carried out to study the vapor phase created during the CVD reaction. The results are given in the following parts that also describe the characteristics of the Al-Cr base cement that has been tested and the metallurgical characterization of the coatings obtained by preliminary deposition tests.

The Cr-Al alloy has a composition of 50/50 wt%. The shots have been grinded to get a powder with a granulation compatible with the other powders consisting the cement, in order to form a rather homogeneous mixture and to get a good covering of the pieces to be treated.

The cement used for the preliminary tests has been prepared by a simple mixing of , 50 wt% of Cr-Al grinded shots (donor), 6 wt% of NH_4Cl powder (activator) and 44 wt% of Al_2O_3 powder (inert filler).

In addition, the price of the Cr-Al alloy shots is rather attractive in comparison with the Fe and Al powders. On that basis, the cost saving on the raw material is significant.

Thermochemical calculations

Thermochemical calculations have been performed to simulate the vapor phase starting from this new cement. The aim is to study the possibility of finding particular conditions respecting the temperature range (700 – 750°C) where only aluminum chlorides and no chromium chlorides are formed starting from the Cr-Al alloy. With some assumptions, the simulation describes the nature and the quantity of the solid or gaseous species present at the equilibrium. Such calculations only give tendencies of the possible reactions but they do not inform about the kinetics of the reactions.

The calculation program (GEMINI II code) is based on the minimization of the total Gibbs energy of the chemical system. The gaseous phase has been studied with the Al–Cr–Cl–H–N–O system in order to take into account all the elements present in the cement.

The calculations results give the following tendencies for all the tested temperatures:

- the solid phases that are formed are mainly consisted of Al_8Cr_5 and AlN : there is no evolution of the cement during the reaction, which is very important for the stability of the process ; this is not the case when using the Fe-Al base cement because an alloying of Al and Fe occurs as shown by the XRD characterization of the cement powder after the pack cementation treatment [5].
- Cr is not transported during the reaction and only different aluminum chlorides are formed in the gaseous phase ; the amount of AlCl increases with temperature : this chloride is responsible for the dismutation reaction which produces the aluminisation treatment as follows : $3 \text{ AlCl} \Rightarrow \text{AlCl}_3 + 2 \text{ Al}$, AlCl_3 being decomposed at higher temperatures.

These results show that the aluminisation is thermodynamically possible using the Cr-Al base cement. They enable to choose the highest temperature of 750°C for the experimental tests.

Deposition tests and metallurgical characterization

T91 steel specimens with a mirror polished surface finishing have been coated for comparison with the Fe-Al coatings obtained in the Coating Qualification Procedure. The deposition has been carried out in the laboratory-scale reactor devoted for the pack-cementation treatments.

The surface morphology observed by SEM appears very fine . The coating is homogenous and presents a good covering capability according to these observations.

The SEM observation after chemical attack of the polished cross-section of the specimen confirms that the coating is very homogeneous with a total thickness of about 5 μm .

In addition, no brittle intermetallic phases seem to be formed, which is very encouraging with regards to what was obtained in the past. That means that an improvement of the coating quality can be obtained thanks to a process parameters optimization.

CONCLUSION

Different specimens have been coated with the Fe-Al/ Al_2O_3 CVD barrier according to the procedure described in the Coating Qualification Report.

They have been delivered for evaluation of the coating properties in out-of-pile tests (EUROFER steel tubes for permeation tests in gas and liquid lithium-lead in Vivaldi experiment) and in-pile tests (MANET II steel tubes for permeation tests in liquid Pb-17Li under irradiation conditions in the high flux reactor in Kazakhstan in the framework of the K-39 ISTC project).

This part contributes to complete the recommendations expressed in the Coated TPB Fabrication Assessment which declares that the CVD deposition technique offers good industrial potential.

The optimization of the Fe-Al deposition using the new Cr-Al base cement must be studied further on, because the preliminary tests lead to encouraging results.

The possibility of oxidizing in situ the Fe-Al coating by using a CO_2 reactive atmosphere in the last step of the pack cementation operation is also a route to be studied.

Both actions should present economical benefits in the view of a process industrialization for the TPB deposition:

- the use of the Cr-Al base cement should suppress the spray-drying operation now necessary for the preparation of the Fe-Al base cement,
- the in situ oxidization should suppress the operation of the Pyrosol alumina deposition, provided that the oxidized Fe-Al coating presents a barrier efficiency and behavior as good as that of the Fe-Al/ Al_2O_3 which is now qualified.

REPORT AND PUBLICATION

- [1] C. CHABROL, F. SCHUSTER “Coating qualification report”, Note Technique DEM n° 98/32, 15/07/98
- [2] C. CHABROL, F. SCHUSTER “Tritium permeation barrier fabrication by chemical vapor deposition”, Note Technique DEM n° 98/67, 1/12/98
- [3] M. TITKOV, I. RICAPITO, G. BENAMATI “Preliminary and general evaluations of a possible design for an irradiation experiment on tritium permeation barriers (K-39 ISTC)”, ENEA report HI-A-N-001, 19/04/1999
- [4] A. AIELLO, C. FAZIO, M. CHINI, Z. YAO, D. LEVTCHOUK, E. SERRA “PRF measurement in Pb-17Li / gas”, Annual report on the EU tasks WPA 4.2.1, ENEA report LB-A-R-008, 31/03/00
- [5] C. CHABROL, F. SCHUSTER, E. ROUVIERE, V. BENEVENT “Permeation barrier qualification – Fabrication and characterization of optimized CVD samples”, Note Technique DEM n° 99/97, 23/12/99

TASK LEADER

Claude CHABROL

DRT/DTEN/SMP/LPTS
CEA Grenoble
17, rue des Martyrs
38054 Grenoble Cedex 9

Tél. : 33 4 76 88 99 77
Fax : 33 4 76 88 99 85

E-mail : chabrol@cea.fr

Task Title : COATING QUALIFICATION AND IRRADIATION TESTS
Permeation out-of-pile testing

INTRODUCTION

In the water-cooled Pb-17Li blanket concept developed in Europe, the cooling is insured by pressurised water flowing in tubes immersed in Pb-17Li [1]. Due to its mechanical properties, behaviour under irradiation and compatibility with flowing Pb-17Li, the material constituting the tube could be a martensitic steel (Fe with 7 to 10% Cr). For safety and economical reasons, the permeation through these tubes of the tritium produced in Pb-17Li has to be evaluated and minimised. One way considered to decrease tritium permeation is the use of coatings.

In order to measure the tritium which permeates from Pb-17Li towards water of the bare material and of a coated one, a special loop was designed [2,3] and built [4]. Moreover this device can be used to perform corrosion test in pressurised water.

The work performed this year concerns on one hand the water circuit of the loop, cleaning and qualification of hydrogen introduction procedure, and on the other hand the gas system analysis.

As the priority has been given by the project leader, M. Fütterer, to perform the corrosion test of low activation materials in water [5] of the TTMS 3.3 task, the main part of the work to perform in the frame of TTBA3.5 in 2000 has been delayed and will be performed in 2001.

2000 ACTIVITIES

THE MAIN FEATURES OF THE LOOP

The loop consists of an autoclave full of pressurised water at 17 MPa and 350°C respectively maximum pressure and temperature. The autoclave is linked to a water circuit allowing to insure a continuous water flow and to control the water chemistry. Some corrosion specimens can be placed in the autoclave.

In the autoclave, there is a martensitic steel permeation membrane, which can be filled with some Pb-17Li and linked to a gas circuit to dissolve hydrogen in Pb-17Li by bubbling.

This loop allows to perform corrosion tests in water and hydrogen permeation measurements from Pb-17Li towards water.

WATER CIRCUIT CLEANING

Before performing any test in the loop, it is necessary to clean the water circuit. The aim of the cleaning is to passivate the circuit and to eliminate the impurities.

- The cleaning consists in several steps including a first washed of the circuit with cold demineralised water; and few sequences of filling the loop with water, increasing the water pressure and temperature (up to 320°C) and running the loop for one or a few weeks with a water flow rate between 7 and 15 L h⁻¹ and emptying the loop. During all the sequences water samples have been taken for analyse.

The water control consists in measuring its resistivity and analysing its chemical composition by ionic chromatography in order to measure the Cl⁻, SO₄⁻ and F⁻ concentrations. At the end of the cleaning process, the water resistivity was 390 kΩ cm and the Cl⁻, SO₄⁻ and F⁻ concentrations were each less than 150 µg kg⁻¹.

HYDROGEN INTRODUCTION AND CONTROL IN WATER

The aim of the hydrogen introduction in the water is to remove the dissolved oxygen.

Hydrogen gas is introduced in the loop by the reservoir. It is done when all the loop is cold and full of water flowing with a 10 L h⁻¹ flow rate at atmospheric pressure. Hydrogen gas circulation is established at countercurrent to the water flow by bubbling in the reservoir. The hydrogen enters the bottom of the reservoir under a 3 bar pressure and leaves it at its top. This operation lasts for a few hours.

The hydrogen content in the water is measured by means of Pd/Ag sensors placed in the autoclave and at the water entrance and exit of the autoclave.

GAS ANALYSES

The gas analyses will be performed by means of a chromatograph. The detector used in this device consists in a Discharge Ionisation Detector (DID) sensitive enough to detect components with a concentration of a few tens vppb. The whole gas analysis device is composed of several parts:

- a sample and calibration line: the sampling loop has a volume of 3 mL;

- a back-flush column to avoid some gases different from hydrogen or its isotopes to contaminate the separation column. It is a 4 m long column full of molecular sieve running at 80°C;
- a separation column (4 m long column full of molecular sieve) placed in a cryogenic chamber (temperature as low as -150°C);
- a line equipped with a DID detector to analyse hydrogen and deuterium in Ar or He.

The optimal temperature of the cryogenic column is a compromise between a sufficiently low temperature to separate the hydrogen isotopes but not too low to obtain the analysis results in a reasonable time (about 15 minutes).

During tests performed with the chromatograph, some problems arose and led to change some components : a ventilator (used to have a uniform temperature in the cryogenic chamber), an electric valve (for the liquid nitrogen admission in the cryogenic chamber), the gas ionisation cell. The analyses performed after repairing were correct.

CONCLUSION

Before operating, the loop has been cleaned in order to passivate the water circuit and remove the impurities. The procedure to remove the dissolved oxygen in water by hydrogen bubbling has been established. After, the loop has been used to perform a corrosion test in pressurised water for the TTMS3.3 programme [5]. The specimens, made of low activation martensitic steels, are in the autoclave. The experimental conditions are the following:

- temperature: 320°C,
- water pressure: 150 bars,
- water flow rate: 10 L h⁻¹,
- hydrogen pressure in the reservoir: 1.8 bar,
- hydrogen pressure in the Pd/Ag of the autoclave: 250 mbar,
- water chemistry: H₂O with 160 ppb Li.

The corrosion test will last up to about mid 2001.

The gas circuit, after replacing the faulty parts, is now operational for future permeation tests.

REFERENCES

- [1] L.GIANCARLI et al., Development of the EU Water Cooled Pb-17Li blanket, Proc. ISFNT-4, Tokyo, Japan, April 6-11, 1997
- [2] A.TERLAIN, T.DUFRENOY, Tritium permeation barrier testing devices, CEA report, RT SCECF 448 (December 1997)
- [3] T. DUFRENOY, A.TERLAIN, Hydrogen permeation measurements with an aluminised martensitic steel, CEA Report, RT-SCECF 487 (December 1998)
- [4] T. DUFRENOY, A. TERLAIN, Tritium permeation from Pb-17Li towards water and corrosion loop, CEA Report, RT SCECF 513 (December 1999)
- [5] O. RAQUET, C. DUFOUR, L. SEJOURNE, Material compatibility in fusion environment, WP SM 3.3: aqueous corrosion of low activation steels, Final report, CEA Report, RT 540 rev.1, (November 2000)

REPORT

T. DUFRENOY, V. LORENTZ, O. RAQUET, A. TERLAIN,
Tritium permeation from Pb-17Li towards water, RT SCECF 552(December 2000)

TASK LEADER

Anne TERLAIN

DEN/DPC/SCCME/LECNA
CEA Saclay
91191 Gif-sur-Yvette Cedex

Tél. : 33 1 69 08 16 18
Fax : 33 1 69 08 15 86

E-mail : anne.terlain@cea.fr

Task Title : PROCESSES AND COMPONENTS

Tritium extraction from Pb-17Li

INTRODUCTION

In the reference Water Cooled Lithium Lead Blanket design for the DEMO reactor, the eutectic Pb-17Li liquid alloy mainly acts as the tritium breeder. The thermal power generated in the blanket by the nuclear reactions is removed by means of tubes in which flows pressurised water operating in conditions similar to those of a PWR primary circuit.

The tritium generated in Pb-17Li is removed from Pb-17Li in an external tritium extractor. Many activities during last years have been devoted to provide data to design a tritium extraction process.

A review of the relevant data on tritium extraction from liquid Pb-17Li has been performed in order to show the experience which can be used to design such a process but also to point out the lacking data necessary for a process extrapolation to an industrial scale.

2000 ACTIVITIES

The report reviews the data on the tritium extraction from the Pb-17Li liquid alloy. It includes: the main characteristics of the system and the consequences on the design of a tritium extraction system, some models which have been developed, experimental data with their analysis and finally some trends to go from a small scale extractor to an industrial one

THE MAIN CHARACTERISTICS OF THE Pb-17Li/H₂ SYSTEM

The reported values of the tritium solubility in Pb-17Li are very scattered. However, it emerges from all the results that the solubility is very low, of the order of 0.01 appm at 1Pa, and shows a weak temperature dependence. All the workers have assumed that the Sievert's law applies. The low tritium solubility in Pb-17Li means a low tritium inventory in the blanket.

But the high tritium partial pressure in equilibrium with the dissolved tritium is the driving force for tritium permeation towards the water coolant circuit and the tritium management is a key issue for the water-cooled blanket. From the low diffusivity of tritium in Pb-17Li, it is expected that the transport of tritium in the Pb-17Li liquid could be a limiting step. It leads to prefer tritium extraction process in which the diffusion of tritium in Pb-17Li is minimised and therefore in which Pb-17Li flows as a film or small droplets.

THE MAIN DATA OBTAINED ON THE H₂ EXTRACTION FROM Pb-17Li

Different mathematical models, mainly based on data obtained with very different systems, have been used to design a tritium extraction from Pb-17Li process by means of gas-liquid contactors. Two main types of extractors have been considered. In the bubble type contactor, the gas is introduced as bubbles in a Pb-17Li bath and creates the mass transfer surface. Large gas flow rates are expected to achieve a significant efficiency at low tritium concentration in Pb-17Li. Even if the results of these calculations must be considered with a great care, they show the sensitivity of the design to the K_s (Sievert's constant) values and the necessity to use several columns with a gas recycling to achieve an acceptable (>60%) extraction efficiency without prohibitive gas consumption.

The droplet spray extractor as well as the multi stage tray column seems better because the liquid flows as a rain of droplets. But the feasibility and the efficiency of this kind of extractor depend on the possible way to form small droplets without superficial oxide layer.

The calculation of a tritium extraction unit requires the knowledge of the tritium retention, transport and release mechanisms in Pb-17Li. Experiments have been carried out in order to determine the hydrogen (or its isotopes) adsorption/desorption rate. They have been performed either by sweeping a stagnant Pb-17Li surface with a gas or by using a bubbling gas in Pb-17Li. The results are scattered but nevertheless it appears that the mass transfer coefficient in the 400°C-600°C temperature range is low (between $5 \cdot 10^{-6}$ and 10^{-4} m s⁻¹). A large interfacial mass transfer area is necessary to achieve high extraction efficiency.

Experimental data on hydrogen extraction from Pb-17Li were carried out with the MELODIE loop [1, 2]. Three types of gas-liquid extractors have been installed on this loop: a plate column, a bubble column and two packed columns.

The plate column consisted of a cascade of 20 unperforated plates. The Pb-17Li flew down while the carrier gas flew at counter current, sweeping each plate.

The experiments were conducted in the 370°C-500°C temperature range and with hydrogen partial pressure of dissolved hydrogen in Pb-17Li between 100 Pa and 1000 Pa. A mass transfer coefficient of 10^{-5} m s⁻¹ has been determined.

The maximum efficiency achieved with this column (15%) is low but is in relation with the low mass transfer interfacial area.

A bubble column consisting of a cylindrical container full of flowing Pb-17Li in which was injected at counter current the carrier gas through two stainless steel sinters with a low porosity in order to limit the bubbles size. Owing to the poor gas hold-up and probably to an insufficient mixing of Pb-17Li and perhaps bubble coalescence, the efficiency of this extractor was very low (less than 13%). However, the investigated gas flow rates were probably too low.

Two extractors with structured packing have been installed on MELODIE loop and tested. The first one was equipped with three 54.7 mm diameter cylinders of AISI 410S stainless steel, Sulzer Mellapak 750Y, structured packing. Each cylinder was 20 cm high and was supported by a perforated plate. At the top of the packing, a liquid distributor was placed to favour the liquid distribution. In this extractor, a counter-current flow of pure argon in flowing Pb-17Li was processed at two different temperatures, 673 and 713 K. The respective gas and liquid flow rate ranges were 3 to 9 $10^{-3} \text{ Nm}^3 \text{ h}^{-1}$ and 70 to 100 $10^{-3} \text{ m}^3 \text{ h}^{-1}$. The tests were performed with a 1000 Pa equilibrium hydrogen partial pressure at the extractor entrance.

The hydrogen exchanged between the liquid and the gas can be considered either as the hydrogen flux extracted from Pb-17Li, F_{LH} or as the atomic hydrogen flux in the gas at the extractor outlet F_{GH} . The values of F_{LH} have been calculated using the K_s values given by REITER et al. [3]. The $F_{\text{LH}} / F_{\text{GH}}$ ratios for the different experiments, were between 1.9 and 3.6 at 713 K and between 2.7 and 4.7 at 673 K and are therefore different from 1 which is the value expected to satisfy the hydrogen mass balance.

The studies have shown that the tested 600 mm high packed column decreased the inlet hydrogen atomic concentration in Pb-17Li of about 22 and 25 % respectively at 673 and 713 K. For each temperature, the efficiency was nearly constant in the investigated ranges of liquid and gas flow rates.

A second extractor, an 800 mm high packed column (with the same Mellapak 750Y packing) was studied in the MELODIE loop. Up to 30% efficiency was reached at 673 K for an inlet hydrogen pressure of 1000 Pa. This improvement, in regards to the 22% efficiency obtained with the previous extractor, was achieved thanks to a reduction of the liquid load on the packing (the lowest one tested, $2.8 \cdot 10^{-3} \text{ m}^3 \text{ s}^{-1} \text{ m}^{-2}$, being still not the optimal one). Concerning the impact of the packing height, an experiment, performed with this extractor, pointed out that an increase of 400 mm leads to at least 10% of supplementary efficiency (for an hydrogen pressure in the 400 to 1000 Pa range). Due to the probable mass transfer limitation in the liquid phase, the contactor behaviour in an immersed configuration is always less efficient than in non-immersed configuration. Incoherence of H_2 mass balance was also observed.

ANALYSIS OF THE DATA

The efficiencies achieved with the bubble column are lower than those obtained with the packed columns for the same gas and liquid flow rates.

The mass transfer coefficient for the bubble column is lower. It can be attributed to:

- the suitability of the liquid film flow for the kinetics of mass transfer (diffusion of atomic hydrogen in the liquid as the limiting step),
- the difficulty to generate interfacial area via bubbles.

The data obtained with the packed columns show that high gas flow rate are not very beneficial for the mass transfer. At the opposite to the classical uses of the structured packing, it seems that to work just before the column flooding would lead to work with high gas flow rates due to the high density of the liquid with no guaranty to increase the mass exchange area. However a minimum gas flow rate must be introduced in the column to avoid any thermodynamical limitation.

The liquid load in the column is a very important factor to control due to its high influence on the efficiency of the transfer. This parameter must be in a range limited by two values:

- a minimum value below which the packing is not completely used because some parts are not wetted by the liquid (the liquid is as trickles or droplets for example),
- a maximum value beyond which the liquid film thickness increases and therefore the mass transfer kinetics is slowed down.

The liquid load values well suited for Pb-17Li/ H_2 system and the Mellapak 750Y packing have to be determined. However, the recommended range for this parameter given by the supplier for organic liquids is large. Experiments in MELODIE loop have been performed with a liquid load between 10 and 32 $\text{m}^3 \text{ m}^{-2} \text{ h}^{-1}$ while the recommended values for petroleum liquids are between 10 and 14 $\text{m}^3 \text{ m}^{-2} \text{ h}^{-1}$.

The efficiency of a packed column is closely related to mass transfer surface area and therefore to the wetting of the packing by the liquid. The wetting of a smooth surface by a liquid can be evaluated by measuring the contact angle of a drop deposited on this surface (sessile drop technique).

This angle is linked to the different surface tensions between the gas, the liquid and the solid. Some experimental studies on the wetting of a Fe-7Cr steel by liquid Pb-17Li [4] have shown that the Fe-7Cr steel (with or without preliminary high temperature heat treatment under controlled atmosphere to modify the natural oxide layer) is partially wetted by Pb-17Li, the contact angle being between 61° and 68°. To increase the wettability of the packing different parameters must be considered:

- the material: the contact angle of Pb-17Li on a smooth Fe substrate is between 40° and 50° [4]. This difference between Fe and Fe-7Cr has to be related to the difference of oxides developed on these substrates and their relative stability. A low chromium steel will be probably a more suitable material for the packing;

- the rugosity of the packing surface: different experimental studies report that a better wettability of the packing can be achieved by increasing the surface roughness;
- preliminary heat treatments can modify the surface state and therefore the wettability.

The tests performed in MELODIE loop have shown the feasibility of the hydrogen extraction from Pb-17Li by means of a packed column. However the data do not allow to know the characteristics of the liquid flow (film or droplets...) on the packing and in particular the part of the surface effectively used.

For a given Pb-17Li liquid flow rate, in addition to determine the optimum running conditions associated to the suitable dimensions of a column with the Mellapak 750 Y packing, different ways have to be investigated in order to increase the efficiency as for example a liquid or gas recirculation, the type of packing or the presence of liquid redistributors inside the column.

EXTRAPOLATION FROM PILOT SCALE TO AN INDUSTRIAL SCALE TRITIUM EXTRACTOR FROM Pb-17Li

If the data, which have been obtained up to now, allow to assess the feasibility of the tritium extraction from Pb-17Li by a gas liquid contactor, they are not sufficient to design industrial scale extractor. If we consider a packed column, which is the more efficient type of tested contactor, different models are available in the literature to predict the mass transfer coefficient, interfacial surface area, the pressure drop, the characteristics of the liquid flow on the packing. They have been developed from data obtained with very different systems, mainly organic liquids or water, and sometimes in conditions very far from those of the Pb-17Li/H₂ system (vacuum distillation for example). These models cannot be used without any verification and without any characterisation of the liquid flow on the packing. Moreover, the origin of H₂ mass balance incoherence must be found: new determinations of the Ks Sievert's constant could help to reach goal.

CONCLUSION

Lot of data have been gained during last years on the liquid Pb-17Li/H₂ system and the extraction of H₂ from Pb-17Li. In the frame of the water-cooled Pb-17Li blanket development, the most investigated process is the gas/liquid contactor system. Among the different types of existing contactors, the packed column has allowed to reach the best efficiency (up to 30%).

However, the data have been obtained with laboratory scale devices and for a too small parameter (gas and liquid flow rates, H₂ content in Pb-17Li) range to determine the optimum running conditions. Moreover, they cannot allow to make some reliable extrapolation to larger size process and liquid flow rates.

The development of a model taking into account the specificities of the Pb-17Li/H₂ system is necessary. Such a development requires in particular to characterise the liquid flow on the packing and to solve the H₂ mass balance incoherence.

REFERENCES

- [1] A. TERLAIN, T. SAMPLE, M.A. FÜTTERER, Hydrogen Extraction Tests from Liquid Pb-17Li using Gas-Liquid Contactors, Fusion Technology (1994) 165-168
- [2] N. ALPY, T. DUFRENOY, A. TERLAIN, Hydrogen Extraction from Pb-17Li: Tests with a Packed Column, Fusion Engineering and Design 39-40 (1998) 787-792
- [3] F. REITER, J. CAMPOSILVAN, G. GERVAISINI, R. ROTA, Interactions of Hydrogen Isotopes with the Liquid Eutectic Alloy 17Li-83Pb, Fusion Technology (1986) 1185
- [4] P. PROTSSENKO, M. JEYMOND, N. EUSTATHOPOULOS, A. TERLAIN, Wetting and reactivity in the Pb-17Li/Fe and Pb-17Li/Fe-7Cr systems, RT SCECF 550 (November 2000)

REPORT

A. TERLAIN, N. ALPY
Tritium extraction from Pb-17Li- Synthesis of the data
RT SCCME (March 2001)

TASK LEADER

Anne TERLAIN

DEN/DPC/SCCME/LECNA
CEA Saclay
91191 Gif-sur-Yvette Cedex

Tél. : 33 1 69 08 16 18
Fax : 33 1 69 08 15 86

E-mail : anne.terlain@cea.fr

Task Title : SAFETY AND LICENSING

Modelling of the lithium/lead water interaction

INTRODUCTION

The general objective of this action is to validate the code models in order to be able to perform safety analyses for licensing.

In that frame, safety studies are specifically devoted to the transient behavior of a liquid metal breeder blanket module under accidental conditions.

The accident scenario considers the complete failure of a water tube (coolant) into the Lithium/Lead (Li/Pb) blanket which was previously investigated through the experimental BLAST tests and which is under analysing through the new and more detailed experimental LIFUS programme at Brasimone.

During the first part of the accident scenario the violent thermal interaction between “hot” Li/Pb and injected “cold” water leads to a pressure transient, due to a rapid water vaporization, which is analysed using the Simmer-III code (multi-phase and multi-component thermalhydraulics in a 2D/Rz geometry).

In a first study, code physical models and code options are widely investigated upon the BLAST experiments numerical simulation in order to select the most appropriate code parameters to correctly reproduce the involved key phenomena ; in a second study, the selected code parameters are applied to the LIFUS 5 test numerical simulation.

The general experimental device provides for:

- a cylindrical reaction vessel containing or not tube bundles and filled with liquid Li/Pb,
- a pressurised water injector into the reaction tank at the bottom of the vessel,
- an expansion tube joining the top of the reaction vessel to a cylindrical expansion tank partially filled with liquid Li/Pb.

The main experimental parameters concern the water injection conditions (temperature and pressure), the Li/Pb temperature and the presence of obstacles inside the reaction vessel, the expansion tube diameter.

The pressure evolution in the reaction tank is recorded during the test.

2000 ACTIVITIES

BLAST TESTS ANALYSES

A general meshing has been selected in order to represent the different geometric characteristics (injector position, expansion tube diameter, tube bundle,...) of the Blast 2, 3, 4, 5 and 7 tests. This meshing is chosen sufficiently fine to correctly represent the two-phase jet kinetics (shape, impact on the reaction tank top) at injection and correctly simulate the fluid movements in the interaction vessel. Limits of the calculation domain are simulated by adiabatic and impervious (zero flux, no mass transfer) walls so that fluid/structure interactions and frictions are taken into account.

The liquid Li/Pb physical properties (conductivity, viscosity) have been refined and completed as function of the temperature, more particularly in the range [250°C – 500°C].

The sub-saturated injected water is modelled by a limiting condition at injector outlet (continuous flow, imposed constant pressure, imposed constant temperature) which ensures the correct injection pressure for each test. The liquid water flow is then controlled by the pressure drop evolution between the reaction tank and the injector.

A detailed sensitivity study has been performed on the Blast 5 test in order to analyse the influence of different code model parameters (flow regime, droplet size, friction coefficients between phases, two-phase water flow conditions at injector outlet).

The more satisfactory results (upwards water jet, pressure evolution in the reaction tank) are obtained assuming a two-phase (10% of vapour) water flow at injection and imposing liquid and vapour water to develop in the same velocity field. These conditions lead to increase fragmentation and diffusion of the water jet into the liquid Li/Pb metal, so that the interaction area with Li/Pb is enlarged and the consequent reaction tank pressurization is maintained longer, as in the experiment.

The same conditions are kept for the Blast 2, 3, 4 and 7 performed calculations.

The increased pressure level in the reaction tank due to a tube expansion diameter reduction (factor 6) is well reproduced in a Simmer calculation of the Blast 7 (without taking into account tube bundle). In that case, the maximum pressure level becomes greater than the pressure at injection leading to a pulsed water injection.

LIFUS 5 ANALYSIS

The Simmer meshing needs adaptations to represent the LIFUS 5 experimental device which differs from the previous BLAST:

- the interaction vessel is divided into four sectors by meridian plates not fixed to the vessel allowing then fluid motion from one sector to its neighbours,
- the water injector is placed in one sector which also contains an U-shape tube bundle,
- each sector supplies with an associated bended expansion pipe which is afterwards connected to a main larger expansion tube.

These 3D features have been modelled in the 2D/Rz Simmer geometry as following:

- the sector containing injector and tube bundle is represented with a central cylinder (volume = 0,25 total reaction tank volume), connected at the top to its associated expansion tube,
- the two adjacent sector are represented with a second concentric cylinder (volume = 0,5 total reaction tank volume), connected at the top to a bended and doubled cross section expansion tube,
- the last opposite sector is represented with a third concentric cylinder (volume = 0,25 total reaction tank volume), connected at the top to its associated bended expansion tube.

Porous walls are assumed between adjacent cylinders in order to allow mass transfer.

The U-shape tubes (20) bundle is also arranged, conserving the total tube volume fraction and the flow area, in three concentric and equidistant rings.

Injector modelling and water conditions at injection are similar to that defined in the previous Blast calculations.

This modelling allows to simulate the relevant phenomena shown throughout of the experimental results:

- the water jet fragmentation due to the tube bundle presence which greatly affects the pressure transient (level and chronology),
- the rapid vapour bubble radial propagation through all reaction tank sectors leading to a similar pressure evolution.

CONCLUSIONS

The BLAST tests analyses realized using SIMMER-III demonstrate the code ability to evaluate the consequences of a thermal interaction between a “hot” liquid Lithium/Lead metal and a “cold” water flow injection. The resulting pressure transient directly depends, of course, on the initial conditions of water injection and liquid metal pool and also on the liquid metal pool environment (containment structures, tube bundle, depressurization pipes,...). In particular, the two-phase water jet kinetics and expansion is greatly modified by the presence of a tube bundle, leading to a global pressure loading increase.

From a general safety point of view, these first analyses show the importance of the Lithium/Lead blanket design to reduce the accident consequences in case of an eventual cooling system failure.

REFERENCES

NT DRN/DER/SERSI/LECC 00/4072.

NT DRN/DER/SERSI/LECC 00/4073.

TASK LEADER

Pierre SARDAIN

DEN/DER/SERI/LFEA
CEA Cadarache
13108 St Paul Lez Durance Cedex

Tél. : 33 4 42 25 39 54
Fax : 33 4 42 25 36 35

E-mail : psardain@cea.fr

Task Title : SAFETY AND LICENSING

Development of minor components & instrumentation

INTRODUCTION

We have tested a rapid pneumatical valve in order to isolate a part of LiPb facility of DEMO. Our aim was to observe what could happen when a valve is closed very quickly in a facility with LiPb. The closing time of this valve was 0.1 second.

This time is very short for this application, where a time of 1 second would be satisfactory. With this close time we observed no important overpressure (7 bars max) and no abnormal vibrations.

2000 ACTIVITIES

PABLITO TEST FACILITY

The PABLITO loop is a testing circuit that makes use of lead lithium ($T_f = 235\text{ }^{\circ}\text{C}$).

The carried-out experiments on this circuit fall within the framework of the testing programmes on tritium breeding blankets with lithium lead of the future fusion reactors.

PABLITO was conceived in order to:

- familiarise with the manipulation and the conduct of a circuit Li-Pb (filling-up, emptying, circulation, checking of the elementary physical parameters),
- test on Li-Pb, the common appliances necessary for the functioning of a circuit of liquid metal (pumps, electromagnetic flow-meters, flow distortion flow-meters, pressure sensors, level probes, valves).

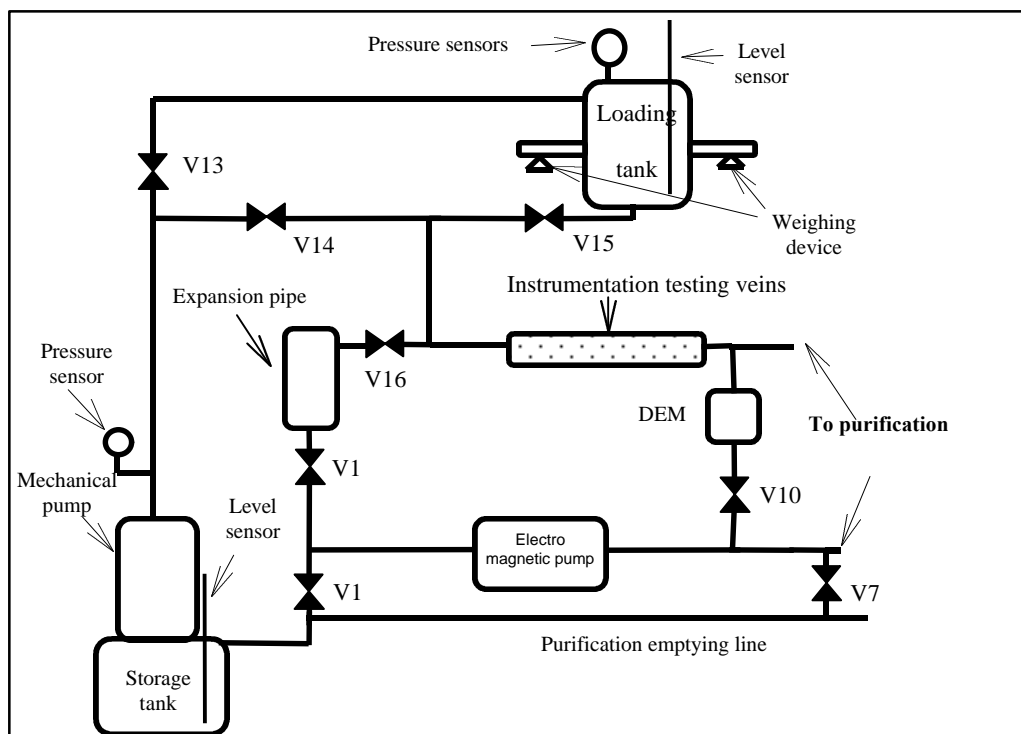
To do that, PABLITO has been equipped with a test pipe thus enabling the installation on request of the different test facilities.

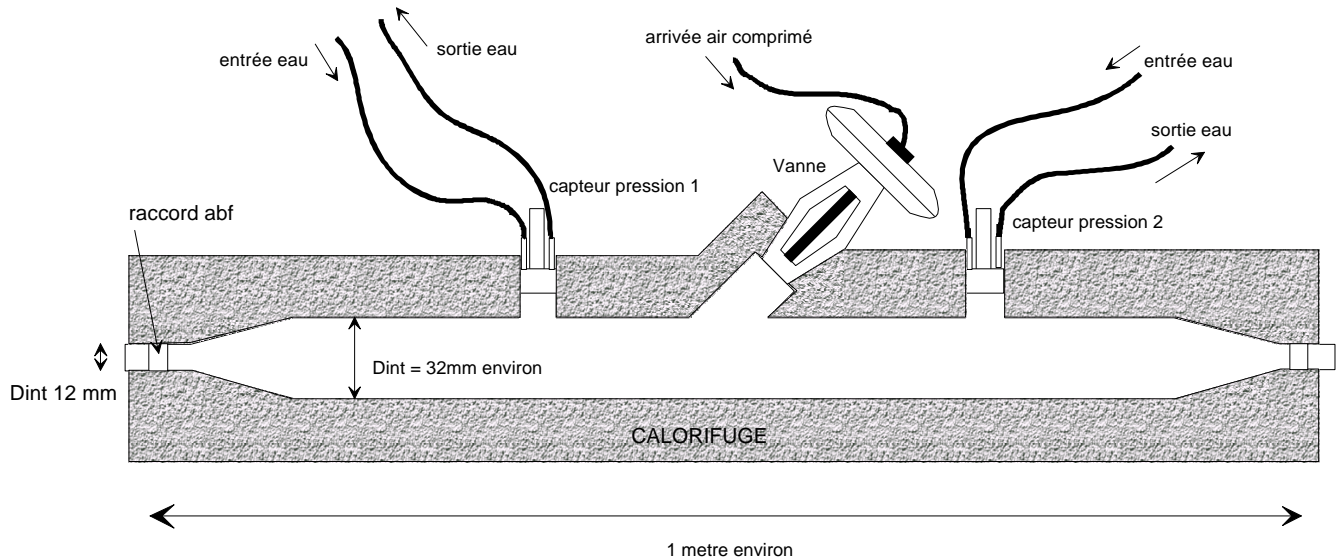
These testing pipes can contain different instrumentation components (sensors, valves, etc.).

RAPID VALVE TESTING DEVICE

Testing vein

We have installed on PABLITO a test pipe enabling us to test a rapid valve with a pneumatic activator. This test facility consists of one valve and two rapid pressure sensors with a flush membrane (cf. schema below).





Pressure sensors and their cooling device

The supply of pressure sensors has been a hard point in this construction. We have consequently opted for the use of the rapid pressure sensors with a flush membrane reprocessed from the STPI and having used in the past for sodium water reaction tests in GV pipes. These sensors of an American making (American Standard) cf. must be cooled with water.

The general characteristics of the utilised sensors are the following:

Drift of distilled water for the cooling	1,2 m ³ /h under 2 bars maxi
Maximum utilisation temperature	500°C after special test
Response time	15 micro-seconds
Resistance of the measurement bridge	350 Ohms
Insulation	500 Meghoms minimum
Resolution	infinite
Resistance to accelerations	Less than 0,01% per g

The cooling device is very simple. It is composed of:

- a capacity of approximately 50 litres in PVC,
- a pump able to assure a flow of 400 litres per hour under a 3 bars pressure,
- a regulator to assure a stable pressure of 2 bars in the sensors,
- a clarinet of water distribution toward the two sensors,
- a clarinet collecting the waters coming from the sensors,
- various valves enabling to isolate some parts of the circuit and to regulate the loss of charge in the circuit,

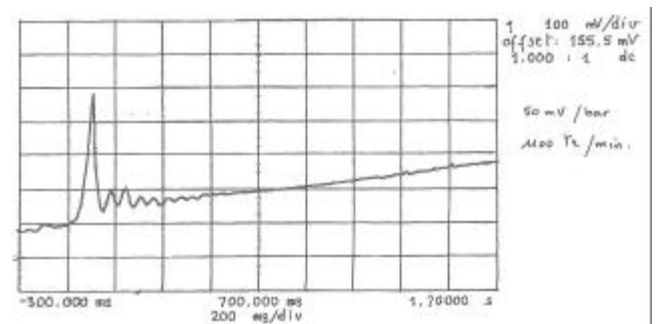
- a supporting sub-frame with a retention tray allowing to manipulate the whole at the bridge,
- a leakage detecting probe in the tray, enabling to lead safety actions.

TESTS AND RESULTS

The tests have been carried out according to the following procedure:

1. Circulation of the fluid at a given speed (in function of the pump's rotation speed).
2. Release of the closing of the pneumatic valve with the help of a manual activator.
3. Recording in function of the time, the pressure upstream and downstream from the valve, as well as the flow.
4. Purge and reopening of the valve.

The overpressures observed are like below:



Over pressure 8 bars with a velocity of the LiPb flow of 0.55 m/s.

CONCLUSION

We have noticed in a simple way the functioning of a quick closing valve in LiPb. With regard to the size of our installation, we have not observed any "waterhammer".

The measurement of the observed over-pressures is the same as the one in the calculations.

The improvement to be achieved on this kind of valve is the time of rise in pressure in the activator's chamber (a few seconds approximately). This value obviously adding to the 100 ms of the closing time, we have to take it into account in the scenarios of accident.

Finally, it is important to conceive gates with a more efficient insulation of the air pump in order to avoid the trapping of the oxides (longer activator, for example).

TASK LEADER

D. Piat

DEN/DER
CEA Cadarache
13108 St Paul Lez Durance Cedex

Tél. : 33 4 42 25 35 16
Fax : 33 4 42 25 79 49

E-mail : piat@drncad.cea.fr

Task Title : MHD EFFECTS

Test and modeling of natural convection MHD

INTRODUCTION

The objective of this task is to give a contribution to the understanding of the Pb-17Li flow behaviour in the WCLL blanket and in particular to assess the effects of MHD flow and to characterise them under representative magnetic field. Relevant parameters and scaling laws have to be obtained in order to evaluate the impact of MHD effects on Pb-17Li velocity and temperature distribution and consequently on the T-permeation towards the water coolant in WCLL blankets.

2000 ACTIVITIES

The 2000 activities aim at the understanding and the modeling of the MHD convection in the WCLL blankets. The problem has been simplified to the case of a vertically elongated parallelepipedic cavity. Two opposite vertical walls of the cavity are maintained at uniform temperatures (hot and cold faces), the other walls being in adiabatic conditions. The magnetic field is horizontal, either parallel or perpendicular to the adiabatic walls. All the walls are supposed electrically insulated.

This study includes an experimental part, a numerical part and an analytical part, all of them being presently in progress. This year has been mainly dedicated to the investigation of the case in which the magnetic field and the thermal gradient (or the heat flux) are perpendicular.

DEVELOPMENT OF THE DIFFERENT TOOLS

Several improvements of the 3D and the 2D numerical codes led to reduce computation time and to extend the using domain of the code use. For the $B \perp \text{grad}T$ case, the 3D calculations confirmed the 2D configuration of the flow according to the Sommeria-Moreau theory [1]. So, we developed a 2D version of the code including the heat and movement equations (but excluding the Ohm law) by replacing the Laplace force by the vorticity. Calculations take now only few hours and are validated by comparison with the 3D calculations.

The steady-state vertical flow in the median plane of the cell was fully characterized last year [2] by analytical modeling for the parallel and the perpendicular cases. This year has been devoted to the turning over flow and to the influence of the convective heat transfer in the perpendicular case only (where the phenomena are supposed to be 2D).

The figure 1 shows the solution of the stream function for $Ha=1000$ in a slender cavity with an elongated ratio of 3. The figure 2 gives to the temperature distribution in the case of a slender cavity with an elongated ratio of 3.

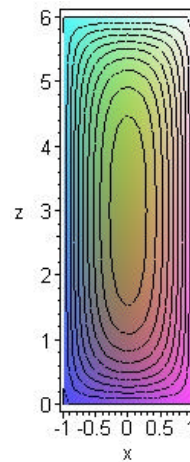


Figure 1 : Analytical result
of stream lines
($H=3, Ha=10^3$)

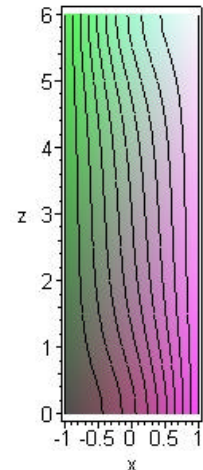


Figure 2 : Isothermal
lines in the weakly
convective case

The MASCOT-V convection cell is a parallelepipedic cavity of square horizontal section with a length of 4 cm and a height of 30 cm filled up with mercury [2]. All the walls are electrically insulated. Two vertical copper walls, facing each other must ensure the thermal homogeneity. The other two vertical walls as well as the cell bottom and plug are adiabatic and electrically insulated.

Variation range of the parameters:

- The magnetic fields varies from 0 to 0.7T, i.e. $0 < Ha < 800$.
- The experimental temperature gradient varies from 5 to 25 K, i.e. $5 \cdot 10^7 < Gr < 2 \cdot 10^8$.

The effective parameter representative of the WCLL blanket, Gr/Ha , can vary from 10^4 to the infinite. For the WCLL blanket case, the upper limit of this parameter is 10^6 .

CHARACTERIZATION OF THE GLOBAL HEAT TRANSFER

Experimental characterization

The heat transfer reaches a maximum for a moderate magnetic field (0.3T) and this maximum is accompanied by very low frequency oscillations.

In the range of low magnetic field, one can observe stages with sudden transitions. When the magnetic field increases, the stages are shorter and shorter and the oscillations become chaotic. Then the oscillation magnitude decreases with the magnetic field and becomes negligible for $B \approx 0,7T$.

It seems that the velocities are high enough to generate turbulence for low magnetic fields, and that a moderate magnetic field organises this turbulence in a 2D flow, helping so the heat transfer. At last, an intense magnetic field breaks down the flow, leading to a forced laminar flow and reducing the convective heat transfer.

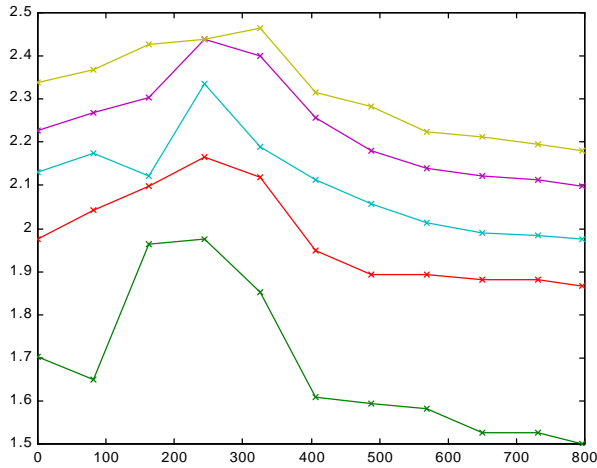


Figure 3 : Experimental heat transfer for different gaps of T corresponding to the numbers
 $Gr = (0, 4.4, 8.7, 13.1, 17.5, 21.9) \cdot 10^4$
 $Ra = (0, 0.88, 1.75, 2.62, 3.50, 4.37) \cdot 10^6$

Numerical characterization

The following diagram presents the results obtained for $\log_{10}(Nu-1)$ versus $\log_{10}(Ha)$, for different values of the Rayleigh number ($Ra = Pr \cdot Gr$, $Pr = 0.02$). The black squares and the blue diamonds respectively correspond to the 2D and the 3D calculations. A numerical correlation has been established (in red line):

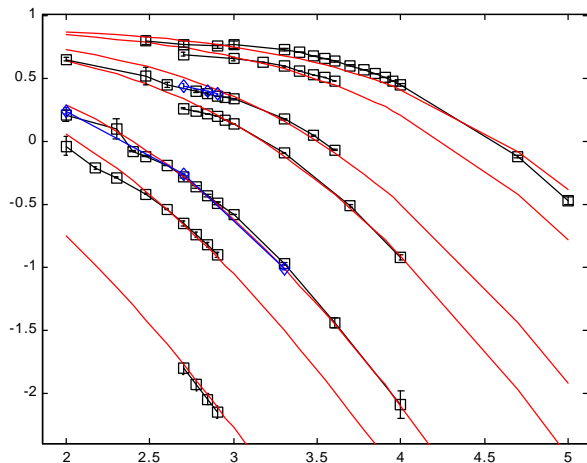


Figure 4 : Numerical heat transfer
Black squares = 2D ; blue diamonds = 3D ;
red lines = correlation

This graph validates the 2D model as well as the correlation in a large range of parameters.

LOCAL MEASUREMENTS.

Temperature and velocity measurements

The two following figures present the temperature and velocity profile on the median plane of the adiabatic wall in the case $\Delta T = 5$ K ($Gr = 4.37 \cdot 10^7$, $Ra = 8.75 \cdot 10^5$) et $B = 0.70$ T ($Ha = 731$).

The red and blue curves present the profile obtained from two set of probes (the probes corresponding to the red curve are placed 3 mm above the set of probes corresponding to the blue curve). The black curve shows the numerical results.

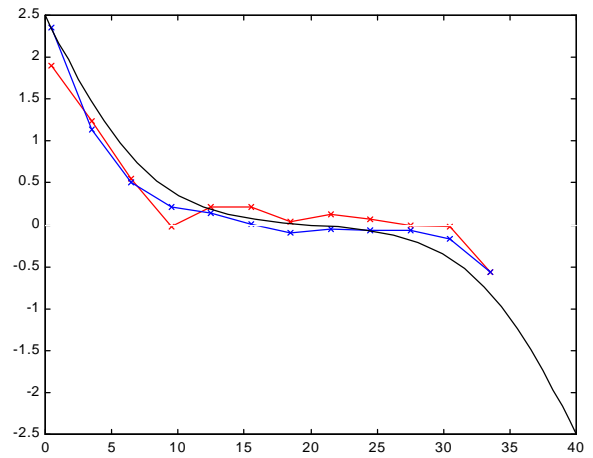


Figure 5 : Comparison between experimental and numerical results
Temperature profiles on the median plane of the cavity
 $\Delta T = 5$ K ($Gr = 4.37 \cdot 10^7$, $Ra = 8.75 \cdot 10^5$)
et $B = 0.70$ T ($Ha = 731$)

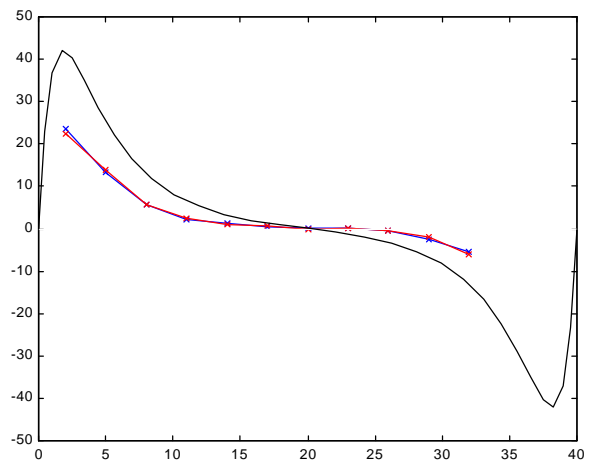


Figure 6 : Comparison between experimental and numerical results
Velocity profiles on the median plane of the cavity
 $\Delta T = 5$ K ($Gr = 4.37 \cdot 10^7$, $Ra = 8.75 \cdot 10^5$)
et $B = 0.70$ T ($Ha = 731$)

These measurements confirm the presence of a stratified fluid flowing mainly in the boundary layers.

Numerical results

From each point of the previous stability diagram, numerical calculation of the isothermal lines and stream lines are performed. The analysis of the results leads to different flow regimes when the Ra/Ha increases:

- a steady core flow regime with no diffusive isothermal lines in the turning over domains (for roughly $Ra/Ha < 10^2$),
- a stratified fluid with no motion in the core region, the flow being confined in the thermal boundary layers. We can observe a stratification tendency with only one eddy in case of high Ra , and with 3 eddies in case of low Ra , each of them having a stratified region in the core. If the first case seems to be stable, the second one is accompanied by a slight turbulence. We observe that the number of cells is always a odd number (1, 3, 5). This can be explained by the fact that two contiguous cells turning in the same rotary direction create by friction a vortex turning in the opposite direction,
- then a destabilization of the two previous stratified cases and the occurrence of chaos. One can wonder if the flow remains bi-dimensional in this case. A comparison with a 3D calculation is planned, but it will take a very long calculation time because of the high Rayleigh number requirement.

CONCLUSIONS

Both experimental and numerical tools give now important results on the heat transfer, on the flow arrangement and its stability. In the variation range of the experimental parameters, there is not always a good agreement with numerical results, specially for the heat transfer. This is probably due to the fact that the numerical boundary conditions (uniform hot wall and cold wall temperature) don't fit with the experimental reality and that this numerical code is not suitable for the calculation of small scale turbulence. Nevertheless, the joint use of these tools is of major importance for the understanding of the phenomena and the development of the analytical models presently in progress.

REFERENCES

- [1] "Why, when and how MHD turbulence becomes two-dimensional"
Somméria, R. Moreau, J. Fluid Mech. (1982), vol. 118
pp 507-518.
- [2] "Natural convection under intense magnetic field in vertical aspect ratio configuration", NT
DER/STPI/LCFI 99/044. G. Authié

TASK LEADER

Guy LAFFONT

DEN/DER/SRT/LCET
CEA Cadarache
13108 St Paul Lez Durance Cedex

Tél. : 33 4 42 25 73 14
Fax : 33 4 42 25 77 88

E-mail : guy.laffont@cea.fr

Task Title : BLANKET MANUFACTURING TECHNIQUES

First wall manufacturing by HIP forming technique

INTRODUCTION

Diffusion welding is considered as a manufacturing technique for the fabrication of DEMO European blankets. The structural material is a 9%Cr - 1%W martensitic steel.

The HCPB blanket module structure consists of a U shape first wall with rectangular channels cooled by flowing helium and of a series of horizontal cooled plates. Both components can be fabricated by the two-step HIP method that was studied by FZK.

The HIP forming method is an alternative fabrication route suitable for the first wall manufacturing. In this method, tubes are inserted between grooved plates and expanded during HIP to get the cooling channels. In the following of 1999 activities, the objective of the programme was to demonstrate the feasibility of the HIP forming technique on bent structures. For this purpose, a second bent first wall mock up was designed and fabricated.

2000 ACTIVITIES

FIRST FW BENT MOCK UP (TASK WP B3.1.2, 1999)

This mock up could not be manufactured in 1999 due to late delivery of Eurofer. It was manufactured and expertised in 2000. The manufacturing sequence is given in table 1 together with that of the second FW mock up.

*Table 1 : Manufacturing sequences
for bent first wall mock ups*

Step	First FW bent mock up	Second FW bent mock up
1	Bending plates	Machining grooves
2	Machining grooves & external profiles	HIP diffusion welding
3	HIP diffusion welding	Heat treatment
4	Heat treatment	Bending
5	-	Machining

For the first FW mock up, bending is made as the first step. As a consequence, adequate process parameters must be found to avoid excessive plate deformation (tube expansion and plate deformation occur simultaneously during HIP). It was found that using 15/17mm tubes ovalised to fit in the 16mm high channels was an efficient means to minimise the plate deformation. The measured deformation was less than 0.1mm.

Two Eurofer plates 24x130x500mm were bent at $90^\circ \pm 1$ by Forschungsgesellschaft Umformtechnik (Stuttgart). Bending location was at two thirds of the total length.

One plate was bent with a 50mm stamp radius. The other one was bent with a 75mm stamp radius. Three Eurofer tubes diameter 14/17mm were drilled to diameter 15/17mm. The tubes were soft annealed under vacuum in order to increase their ability to plastic deformation during bending (and also during HIP). The soft annealing treatment consisted in 2h step at 950°C for carbide dissolution followed by slow cooling (10°C/h) until 600°C and then natural cooling. The tubes were bent with a radius 75mm. The plates and the tubes were stacked and the tubes were ovalised. A view of the mock up components is given on Figure 1.

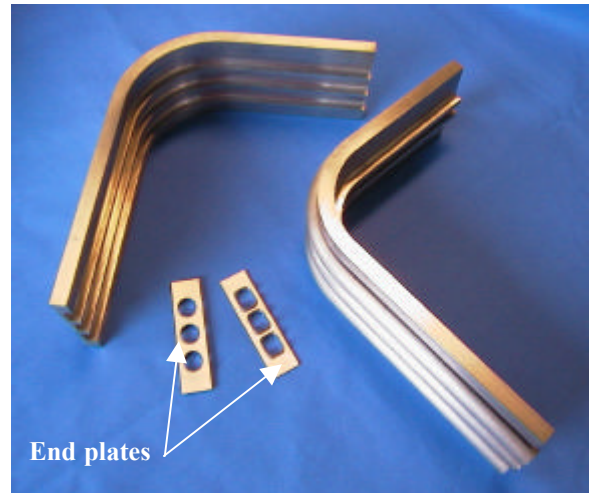


Figure 1 : First FW mock up components

The parts were degreased using an aqueous solution of 10% neutral PH detergent, then rinsed with tap water, rinsed with deionised water, rinsed with alcohol and dried with nitrogen. Tightness was achieved by TIG welding. Plates were firmly maintained one on each other during welding. This was necessary because the inner plate deformed slightly during machining. The mock up was outgassed at room temperature for 12h using a secondary vacuum pumping system. The HIP cycle was as shown on figure 2.

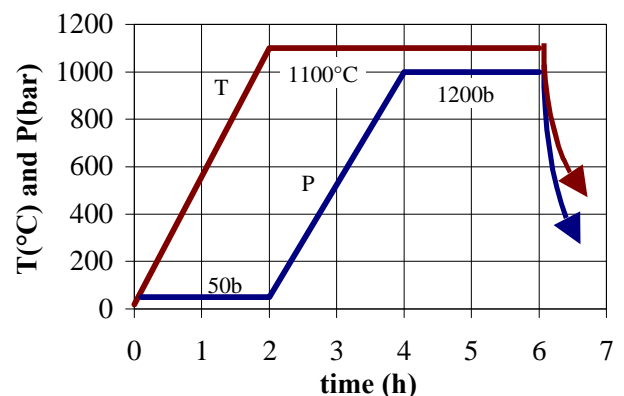


Figure 2 : HIP cycle for the first FW bent mock up

The mock up was expertised after HIPing. Tube expansion was not fully obtained (as shown on figure 3), which means that a leak appeared during HIP.

It has not been possible yet to determine the location of the leak. A chemical reaction between the filling metal used for tubes bending and Eurofer is suspected to have generated this leak.

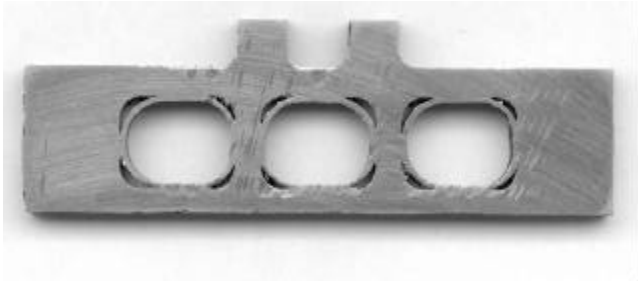


Figure 3 : Cross section of the first FW mock up after HIP

SECOND FW BENT MOCK UP (TASK TTBB2.3, 2000)

For the second FW mock up, bending is made after HIP (table 1). As excess material must be added to take into account deformation during bending, the plate thickness is much higher than the tube thickness, which eliminates the risk of unacceptable plate deformation. Components of the mock up are shown on figure 4.

Eurofer plates 24x168x450mm and tubes 14/16.5mm were used. The tubes were not soft annealed. The same surface preparation and HIP cycle than for the first mock up were applied. The HIP cycle was successful (figure 5).

No significant plate deformation was noticed. The mock up was heat treated to restore a fine grain size and to temper the material. Bending and expertise is foreseen by March 2001.

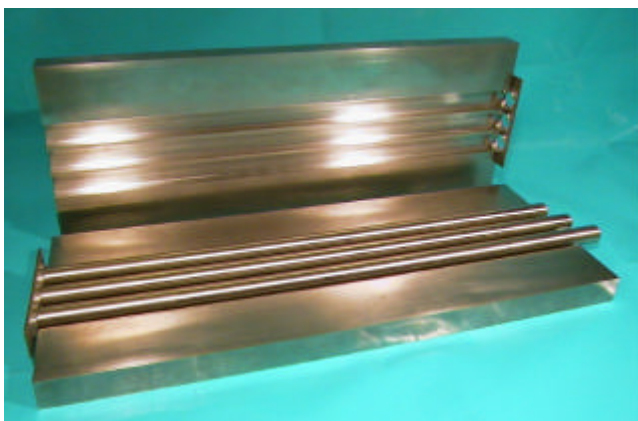


Figure 4 : Components of the second FW mock up before HIP



Figure 5 : Second FW mock up after HIP

CONCLUSIONS

The feasibility of the HIP forming method for the fabrication of HCPB blanket First Wall was studied.

A mock up was successfully HIPed. Bending and joint expertise is in progress.

REPORTS AND PUBLICATION

- [1] E Rigal, task WPB3.1.2 final report, NT DEM n°107/2000
- [2] E Rigal, task TTBB23 final report, to be issued.

TASK LEADER

Emmanuel RIGAL

DRT/DTEN/SMP/LS2M
CEA Grenoble
17, rue des Martyrs
38054 Grenoble Cedex 9

Tél. : 33 4 76 88 97 22
Fax : 33 4 76 88 54 79

E-mail : rigal@chartreuse.cea.fr

Task Title : DEVELOPMENT OF CERAMIC BREEDER PEBBLE BEDS - Characterization of Li_2TiO_3 pebble beds

INTRODUCTION

The characterisation of Li_2TiO_3 pebbles, in support of both their fabrication technology and the investigation of the performance of Li_2TiO_3 pebbles and pebble beds, plays a major role in the development of Li_2TiO_3 pebbles for the HCPB blanket.

It includes the determination of the geometrical, microstructural, crystal phase, purity, and mechanical strength characteristics of:

- the intermediate products in the sequence of the steps of the fabrication process,
- the pebbles from all produced batches,
- the pebbles once they have been subjected to the various out-of-pile tests of pebbles and pebble beds, and to HCPB mock-up tests.

2000 ACTIVITIES

Focus in 2000 was placed on the determination of:

CHARACTERISTICS OF THE Li_2TiO_3 PEBBLES OF THE 5 kg BATCH PRODUCED IN 1999 AT CTI

This batch, reference # CTI 1529 Ti 1040 CTI was constituted of 8 sub-batches. Microstructural and mechanical characteristics of the sub-batches 1-2, 3-4, 5-6, 7-8 are shown in Table 1.

They show a good agreement with the goal characteristics i.e. 90% T.D, 1-2 μm grain size, ~ 60 N average crush load, and a good reproducibility from one batch to the other one.

Impurity analysis using the Spark Source Mass Spectrometry technique is shown in Figure 1.

XRDA indicates the presence of monoclinic Li_2TiO_3 as major phase and traces of $\text{Li}_4\text{Ti}_5\text{O}_{12}$ in accordance with the lithium stoichiometry chosen for the material.

Impurity	CTI pebbles 1999 (ppm)
Al	60
B	0.05
Ca	50
Cl	2
Cr	100
Cu	2
Fe	200
K	2
Mg	5
Mn	2
Ni	30
P	0.5
S	1
Si	50

Figure 1 : Elemental impurity analysis of Li_2TiO_3 pebbles

CHARACTERISTICS OF THE ^6Li ENRICHED Li_2TiO_3 PEBBLES FOR THE HICU EXPERIMENT

The usual characteristics were determined, too, for the three batches of Li_2TiO_3 pebbles with 11%, 29.5%, and 0.06% ^6Li enrichments sintered at 1050°C and for the 29.5% ^6Li enriched pebbles sintered at 1100°C. Results are reported in [1].

Table 1 : Characteristics of the 5 kg-batch of CTI Li_2TiO_3 pebbles sintered at 1040°C
(Reference of pebbles : CTI 1529 Ti 1040 CTI)

Ref. of batch	Quantity (kg)	Pebble size (mm)	Porosity (%)		Bed density (g/cm^3)	Grain size (μm)	Specific surface area (m^2/g)	Average crush load (N)
			Open	Closed				
S 1-2	1.6	0.8 – 1.2	7.9	5.3	1.81	1 – 2.5	0.18	57
S 3-4	1.2	0.8 – 1.2	6.4	4.8	1.85	1 – 2.5	0.19	57
S 5-6	1.3	0.8 – 1.2	-	4.8	1.83	1 – 2.5	0.20	57
S 7-8	1.2	0.8 – 1.2	5.6	5.2	1.86	1 – 2	0.21	63

EXAMINATION OF Li_2TiO_3 PEBBLES AFTER THE FUNCTIONAL TESTS OF PEBBLE BEDS

In order to evaluate the performance of the Li_2TiO_3 pebbles option, relevant functional tests of pebble beds, both out-of-pile and in-pile, are carried out in collaboration with FZK, ENEA and NRG. Results of the tests are compiled in [2].

Characterization of the Li_2TiO_3 pebbles after the out-of-pile tests is performed at CEA in order to identify any changes and, thereby, help interpretation of test results.

Principal examinations were made after the following tests.

Annealing test at 970°C in air at CEA during three months

This test was made within the framework of the pebbles optimization.

It aimed at comparing the behaviour of the Li_2TiO_3 pebbles as a function of their sintering temperature, in other words, as a function of their microstructure.

The temperature and time conditions were defined by FZK as typical of DEMO end-of-life conditions at the higher temperature of the breeder in the HCPB blanket.

So far, the annealing behaviour of Li_2TiO_3 pebbles in the tests in air at CEA and the annealing behaviour in He + 0.1% H_2 stream (blanket reference purge gas) at FZK were found to be quite comparable, except for the colour of the pebbles that turned black in He + 0.1% H_2 .

Therefore, although the gas conditions of the CEA test are not as relevant as those of the FZK test, the conclusions and trends being inferred from the test results are still quite meaningful.

Comparison annealing tests at CEA were performed on Li_2TiO_3 pebbles sintered at 950°C for 1 hour, and at 1050°C for 1 hour, and on the pebbles sintered at 1040°C from the 5 kg-batch produced by pre-industrial means in 1999.

Characteristics of the specimens (weight loss, closed porosity, crush load, and grain size) were checked on the initial pebbles and on pebbles annealed in air at 970°C during 1 month, 2 months, and 3 months, respectively. Results are given in Table 2.

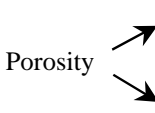
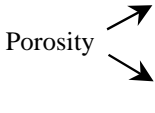
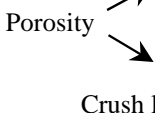
According to expectations, those results show that pebbles sintered at 1050°C are more stable on annealing than those sintered at 950°C as regards lithium vaporization (weight loss).

They confirm the significant grain growth observed in previous tests and the decrease of the closed porosity, which suggest a change in microstructure. Unexpectedly, there is no effect on the crush load.

Annealing test at 970°C in He + 0.1% H_2 at FZK during three months

The test was carried out with the reference Li_2TiO_3 pebbles of the 1999 production.

Table 2 : Behaviour of Li_2TiO_3 pebbles annealed at 970°C in air

		As-sintered	970°C 1 month	970°C 2 months	970°C 3 months
CTI 1529 Ti 950 CEA 950°C, 1 hour CEA sintering	Weight loss (%)	-	0.04	0.06	0.08
	Porosity 	Open (%)	-	-	-
		Closed (%)	-	-	4.2
	Crush load (N)	52 (20 – 101)	58 (36 – 131)	48 (26 – 76)	52 (23 – 83)
	Grain size (µm)	0.5 - 1	4 - 14	5.5 – 19	6 – 22
CTI 1529 Ti 1050 CEA 1050°C, 1 hour CEA sintering	Weight loss (%)	-	0.01	0.03	0.04
	Porosity 	Open (%)	-	-	-
		Closed (%)	-	-	2.7
	Crush load (N)	62 (27 – 110)	60 (39 – 77)	54 (32 – 79)	62 (41 – 82)
	Grain size (µm)	1 – 2	4 - 16	3.5 – 14	3.5 – 20
CTI 1529 Ti 1040 CTI 1040°C, 1 hour CTI sintering (5 kg batch)	Weight loss (%)	-	0.01	0.03	0.04
	Porosity 	Open (%)	-	-	-
		Closed (%)	-	-	3.1
	Crush load (N)	69 (31 – 107)	61 (39 – 99)	61 (35 – 88)	63 (37-99)
	Grain size (µm)	1 – 2	2.5 – 11	3.5 – 13	2.5 - 20

Evolution of crush load, specific surface area, grain size and porosity are investigated after 14, 48, 96 day annealing. One can observe a significant grain growth (see figure 2) along with a decrease in specific surface area, a slight decrease in porosity, an almost stable crush load, as well as the usual change in color of the pebbles. The surface aspect of the pebbles is unchanged. Results are in agreement with results of similar examinations at FZK [3].

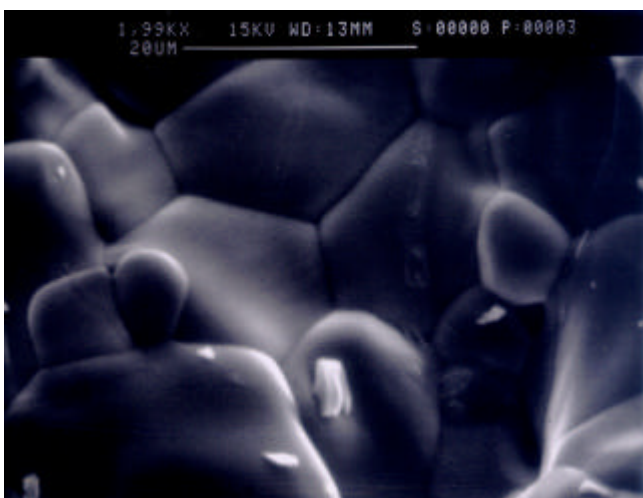
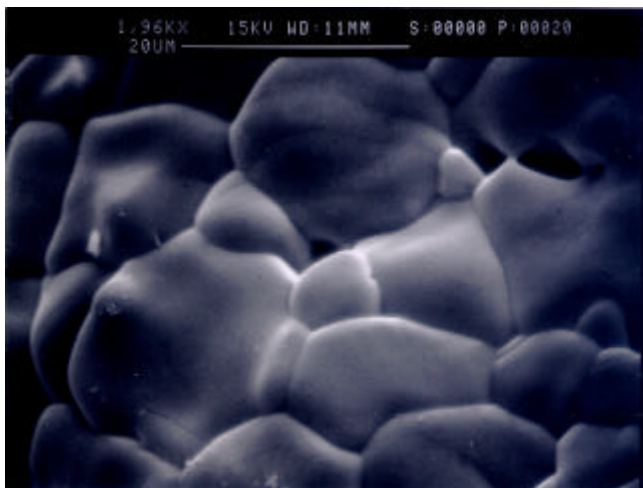
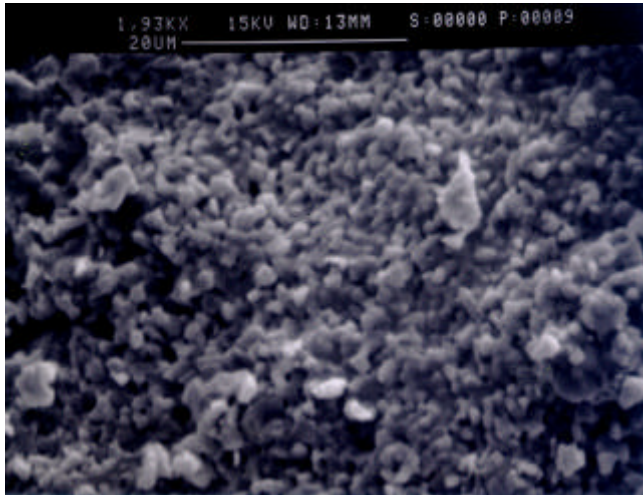


Figure 2 : Evolution of grain size of Li_2TiO_3 pebbles with annealing time
Top, 14 days – Middle, 48 days – Bottom 96 days

Uniaxial compression tests in He at FZK

A large number of tests were made in the range R.T to 850°C and stresses 3 to 6.6 MPa on the reference Li_2TiO_3 pebble beds in order to determine stress relationships and thermal creep strain relationships for both initial pebbles and long term annealed pebbles.

The peculiar behaviour observed for the Li_2TiO_3 pebbles (as compared to other ceramic pebbles and to the annealed Li_2TiO_3 pebbles) is not yet explained; the large increase in creep strain observed at the high temperatures is presently assumed to be due either to the material small grain size or to the low sintering temperature, as it is not observed on the large-grained annealed pebbles.

Further work is in progress to elucidate the phenomenon.

Figure 3 shows a cross section of the Li_2TiO_3 pebble bed agglomerated after the test at 800°C and 6.6 MPa.

One can see that pebbles are in close contact but are not “merged” together as are the Li_2TiO_3 pebbles sintered at 950°C under similar test conditions.

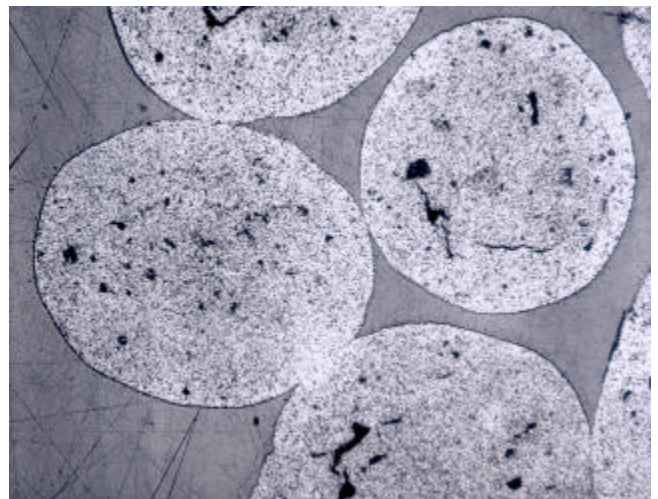


Figure 3 : Cross section of the Li_2TiO_3 pebble bed

CONCLUSION

The extensive work of characterisation of the Li_2TiO_3 pebbles allowed to optimise the parameters of the extrusion-spheronisation-sintering process so as to obtain Li_2TiO_3 pebbles which satisfy at best the requirements of the HCPB blanket. In addition, comparing the characteristics of the Li_2TiO_3 pebbles before and after the out-of-pile tests of pebble beds, performed so as to evaluate the performance of the Li_2TiO_3 pebbles option, was very useful to help understand any phenomena occurring during the tests.

Finally, the comparison showed an overall excellent behaviour of the current Li_2TiO_3 pebbles regarding the ceramic pebble bed key issues.

PUBLICATIONS

- [1] J.D.Lulewicz, N.Roux. Annual report on sub-task TTBB005-C and sub-task TTBB005-D. Internal report DTA/CEREM/CE2M/LECMA 00-DT-160 30/10/00
- [2] N.Roux. Compilation of blanket-relevant properties data for Li_2TiO_3 pebbles and pebble beds. Presented at CBBI-9, Toki (Japan) September 2000.
- [3] G.Piazza, J.Reimann, E.Günther, R.Knitter, N.Roux, J.D.Lulewicz. Behaviour of ceramic breeder materials in long time annealing experiments. Presented at 21st Symposium on Fusion Technology, Madrid (Spain) September 2000.

TASK LEADER

Jean-Daniel LULEWICZ

DRT/LIST/DECS/SE2M/LECMA
CEA Saclay
91191 Gif-sur-Yvette Cedex

Tél. : 33 1 69 08 48 24

Fax : 33 1 69 08 91 75

E-mail : jean-daniel.lulewicz@cea.fr

Task Title : DEVELOPMENT OF CERAMIC BREEDER PEBBLE BEDS - Validation of Li_2TiO_3 fabrication with pre-industrial means of the lab fabrication steps – Mastering/Optimizing

INTRODUCTION

Li_2TiO_3 emerged in the last few years as a promising ceramic breeder material for fusion reactor blankets. Li_2TiO_3 pebbles are being developed at CEA as a candidate ceramic breeder option for the helium-cooled pebble bed (HCPB) blanket investigated in Europe.

In view of the successful production at lab-scale using the extrusion-spheronization-sintering process of Li_2TiO_3 pebbles satisfying the HCPB blanket requirements, the validation using pre-industrial means of the lab-scale process was launched in 1999 with Ceramiques Techniques et Industrielles (CTI), culminating in the production of a 5 kg-batch of Li_2TiO_3 pebbles at the end of the year [1-2].

The good behaviour observed for the Li_2TiO_3 pebble beds in the functional tests performed in parallel [3] supported to continue in 2000 the development of the fabrication with focus on mastering and optimising the fabrication process parameters. Subsequently, a 6 kg-batch of Li_2TiO_3 pebbles, representative of the process as improved in 2000, was produced to supply the next tests. In addition, three special batches of Li_2TiO_3 pebbles corresponding to three ^6Li enrichments as required for the high fluence irradiation experiment in the High Flux Reactor at Petten were fabricated.

This work is summarized hereafter.

2000 ACTIVITIES

OPTIMISATION OF THE FABRICATION PROCESS OF Li_2TiO_3 PEBBLES

Several items were addressed [4]:

Study of the sensitivity of the process parameters on

- a) the characteristics of the Li_2TiO_3 powder
- b) the characteristics of the Li_2TiO_3 pebbles

The characteristics of the Li_2TiO_3 powder are mainly determined by the temperature of the second plateau of the heating cycle for the synthesis of Li_2TiO_3 from Li_2CO_3 and TiO_2 precursors.

This temperature was set to be 790°C in 1999. In this study two temperatures i.e., 780°C and 800°C bracketing the above value were used, the other conditions being kept constant.

In both cases, boats containing the reacting powders were distributed in various levels and various locations per level, in the industrial electrical furnace (see Fig.1).



Figure 1 : Electrical industrial furnace for powder synthesis and pebbles sintering

Relevant characteristics, i.e., weight loss on synthesis, Li_2TiO_3 powder apparent density, specific surface area, and particle diameter, as well as XRDA and impurity analysis were checked for all samples leading to the conclusions that a) the conditions throughout the furnace are quite uniform, and b) the tolerance on the temperature of synthesis of the Li_2TiO_3 powder is not strict, which is a tremendous advantage.

The shaping conditions were further studied, and the sensitivity of the sintering temperature on the key characteristics of the pebbles was investigated : open/closed porosity, specific surface area, and grain size.

Here again, the tolerance on the sintering temperature was found to be not very drastic [4] which is very advantageous from the industrial scale fabrication standpoint.

Optimisation of the fabrication equipment

This item was given great consideration [4]. Several devices of the facility were redesigned : extruding machine (reduction of dead volume, utilization of a multi-hole nozzle made of alumina) see Fig 2, device to cut the cylindrical granules, spheroniser (coating of the walls and of the rotating plate with Teflon and organic material respectively).

Consequently, the operating conditions were re-adjusted (formulation of the extrusion paste, procedure to dry the granules, spheronising time and speed, sintering cycle).

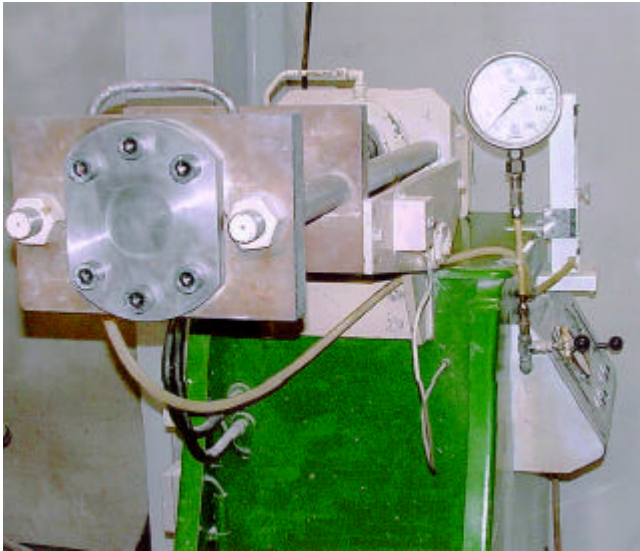


Figure 2 : Extruding machine

Minimisation of the content of the activable impurities

Elemental impurities in the Li_2TiO_3 powder and pebbles are measured using Spark Source Mass Spectrometry. In the Li_2TiO_3 pebbles produced in 1999, major impurities were Fe, Cr and Ni with 200, 100, and 30 ppm contents respectively.

Calculations of the related induced long-term activities suggested to decrease Ni to the larger extent possible.

Among these three elements, Ni induces the more activation, though it is not too critical in view of its limited content.

To this end, as much as possible of the stainless steel equipment was replaced : stainless steel sieves were changed to nylon ones, the steel nozzle was changed to an alumina one, the spheroniser steel walls were coated with Teflon, the spheroniser steel plate was coated with an organic material [4].

As a result, the impurities level was considerably decreased as compared to 1999 and is now quite acceptable (see subtask TTBB005-C).

PRODUCTION OF ^6Li ENRICHED Li_2TiO_3 PEBBLES SPECIMENS FOR THE HICU EXPERIMENT

The HICU experiment, the high fluence irradiation to lithium burn-up and dpa conditions representative of DEMO end-of-life for the HCPB breeder, is foreseen in 2001 in the High Flux Reactor at Petten.

In order to meet the goals of the experiment, ^6Li enriched materials have to be irradiated, i.e., 11% ^6Li , and 29.5% ^6Li Li_2TiO_3 pebbles, as well as depleted ones, i.e., 0.06% ^6Li pebbles so as to evidence the only dpa effect.

Fabrication of the three specimens required three different productions by the industrial firm.

The enriched specimens were obtained from enriched Li_2CO_3 powders prepared by mixing in appropriate proportions 95% ^6Li Li_2CO_3 and 7.5% ^6Li Li_2CO_3 powders.

A few adjustments of the process conditions were necessary to comply with the deviation of the characteristics of the ^6Li enriched Li_2CO_3 powders from the normal ones. In particular, the current sintering temperature of 1050°C led to a density lower than expected, and specimens sintered at 1100°C were prepared too.

FABRICATION OF A 6 kg BATCH OF Li_2TiO_3 PEBBLES

In order to master the fabrication process parameters as improved in 2000, as well as to dispose of the amount of Li_2TiO_3 pebbles necessary to supply the campaign of functional tests of Li_2TiO_3 pebble beds and HCPB mock-up tests foreseen in 2001, a 6 kg-batch of Li_2TiO_3 pebbles was produced at the end of 2000, see Fig.3.

Detailed characterisation, and performance evaluation of these pebbles are part of the 2001 program work.

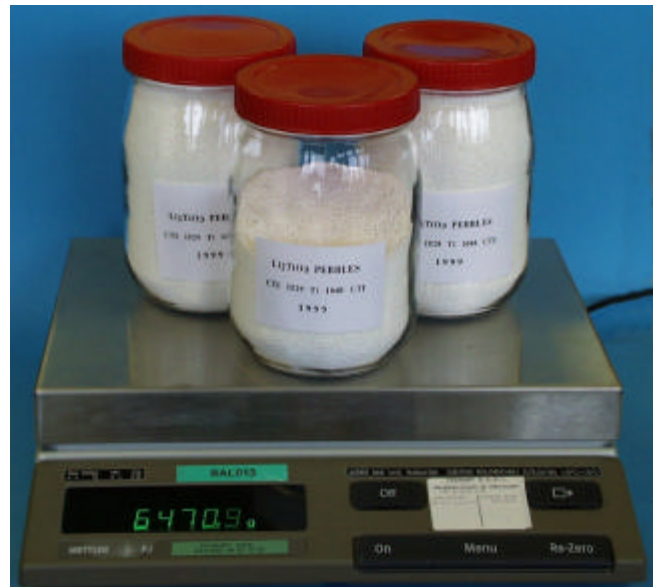


Figure 3 : 6 kg-batch of Li_2TiO_3 pebbles produced in 2000

CONCLUSION

The activity at CEA as regards the optimisation of the process parameters for the fabrication of Li_2TiO_3 pebbles meeting the requirements of the HCPB blanket was successfully achieved, and it was completed in accordance with the foreseen time schedule.

Li_2TiO_3 pebbles specimens were delivered in due time to the European partners for the out of pile functional tests of pebble beds, and for the irradiation experiments.

REFERENCES

- [1] J.D.Lulewicz, N.Roux. Current results of the validation using pre-industrial means of the steps of the lab-scale extrusion process for the fabrication of Li_2TiO_3 pebbles. Proceedings CBBI-8, Colorado Springs (2000) p.25.
- [2] J.D.Lulewicz, N.Roux. 1999 work on the validation with pre-industrial means of the steps of the lab-scale process for the fabrication of Li_2TiO_3 pebbles by extrusion. Internal report CEA/CEREM/CE2M/LECMA 99-DT-130.
- [3] J.D.Lulewicz, N.Roux, G.Piazza, J.van der Laan. Behaviour of Li_2ZrO_3 and Li_2TiO_3 pebbles relevant to their utilization as ceramic breeder for the HCPB blanket. ICFRM-9 Colorado Springs, 1999, to be published in J.Nucl.Mat (2000).
- [4] J.D.Lulewicz. Advances in the pre-industrial fabrication of Li_2TiO_3 pebbles by the extrusion-spheronization-sintering process. Presented at CBBI-9, Toki (Japan) September 2000.

TASK LEADER

Jean-Daniel LULEWICZ

DRT/LIST/DECS/SE2M/LECMA
CEA Saclay
91191 Gif-sur-Yvette Cedex

Tél. : 33 1 69 08 48 24
Fax : 33 1 69 08 91 75

E-mail : jean-daniel.lulewicz@cea.fr

Task Title : DEVELOPMENT OF BREEDING BLANKETS

INTRODUCTION

Silicon carbide composites (SiC_f/SiC) appear as one of the most promising low activation materials for structural applications in breeding blanket for fusion power reactors [1]. Taking advantage of the SiC_f/SiC composites properties, the TAURO blanket concept has been developed by CEA in the last years [2]. It is a self-cooled liquid metal breeder blanket using SiC_f/SiC as structural material and Pb-17Li (90% ^6Li enriched) as both coolant and breeder/multiplier. Appropriate design methodologies are necessary to correctly assess the limits of present-day composites in order to provide guidelines for further R&D.

In particular, specific behavioural models are needed to reproduce their complex non-linear mechanical response. At the same time, SiC_f/SiC composites present different properties depending on the loading direction. Isotropic resistance criteria valid for metals are therefore inadequate.

A new resistance criterion has then been defined and is presented in this work. Examples of application of the improved design analysis methodology to the TAURO dimensional analyses have been also carried out and the differences in the results obtained using more simplistic assumptions have been stressed.

2000 ACTIVITIES

MODELLING OF THE MECHANICAL BEHAVIOUR OF SiC_f/SiC COMPOSITES

The non-linear mechanical behaviour of SiC_f/SiC composites depends on the interactions between fibers and matrix during loading. These interactions lead to a progressive material damage in terms of matrix microcracking and matrix/fibers decohesion and the mechanical behaviour of the composite is then qualified as being elastic-damageable.

Continuum Damage Mechanics (CDM) -based theories [3] are the most suitable for developing a behavioural model capable of being incorporated into analytical or numerical schemes and of determining a structural response. They provide explicit relations at the macroscopic scale between the stress and strain variables.

Thus, the experimental tests needed to identify such models are, usually, classical tension/compression tests. The constitutive law of a damageable elastic material can be derived starting from two potentials: the thermodynamic potential that supplies the state equations and the dissipation potential that supplies the damage evolution laws.

Much attention has been paid in recent years to the prediction of the stress-strain relation in ceramic matrix composites and specifically in SiC_f/SiC .

Among the CDM-based theories, the ONERA model [4] appeared to be the most suitable approach for an implementation in the FEM code CASTEM 2000.

The identification of the model has been carried out using the experimental data obtained on the SiC_f/SiC composites produced by SNECMA and Figure 1 shows a satisfactory simulation with CASTEM 2000 of an in-axis incremental tension/compression test.

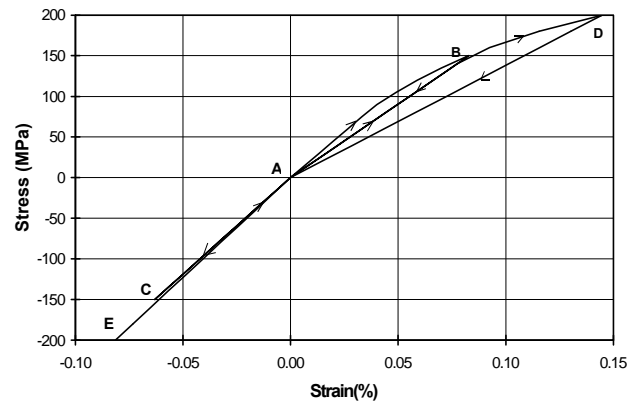


Figure 1: Simulation of in-axis incremental tension-compression test on SiC_f/SiC using the FEM code CASTEM implemented with the ONERA model [4]

Resistance criteria for SiC_f/SiC composites

The ONERA has also recently proposed a resistance criterion specifically developed for SiC_f/SiC composites which takes into account the two different failure modes of SiC_f/SiC composites (isotropic failure under compression and anisotropic failure due to damage accumulation under tension).

In order to differentiate between compressive and tensile behaviour, the ONERA criterion uses the spectral decomposition of the stress tensor:

$$\sigma = \sigma^- + \sigma^+$$

These tensors are then expressed in the orthotropy system of the material:

$$\sigma_{\text{orth}}^- = n_{\text{orth}}^{-1} \sigma^- n_{\text{orth}}$$

$$\sigma_{\text{orth}}^+ = n_{\text{orth}}^{-1} \sigma^+ n_{\text{orth}}$$

$$\sigma_{\text{orth}}^- = n_{\text{orth}}^{-1} \sigma^- n_{\text{orth}}$$

In term of these tensors the ONERA criterion is written as:

$$\sqrt{\dot{\sigma}_{\text{orth}} : M_1 : \dot{\sigma}_{\text{orth}}} + \sqrt{\dot{\sigma}_{\text{orth}}^+ : M_2 : \dot{\sigma}_{\text{orth}}^+} = 1$$

The matrix M_1 and M_2 are constructed starting from the stiffness matrix S of the material:

$$M_1 = \alpha : S$$

$$M_2 = \begin{bmatrix} m_{11}S_{11} & m_{12}S_{12} & 0 \\ m_{12}S_{12} & m_{22}S_{22} & 0 \\ 0 & 0 & m_{66}S_{66} \end{bmatrix}$$

The agreement between the failure envelope predicted by the ONERA criterion and the experimental data is very good (Figure 2).

However, the identification of the parameter m_{12} needs a bi-axial test.

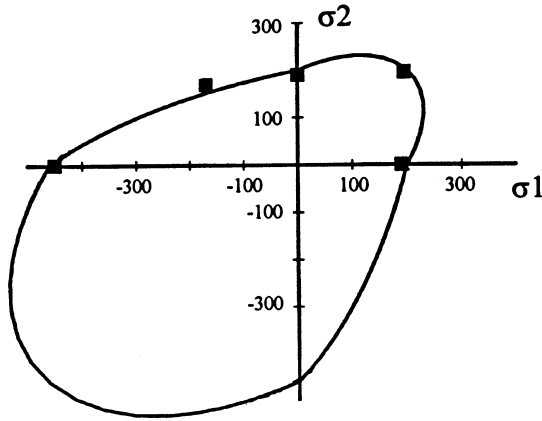


Figure 2 : Failure envelope in the $(\sigma_{XX}, \sigma_{YY})$ plane as defined by the ONERA criterion compared with experiment

The main difficulties of the above criteria are related to the complexity of the mechanical tests needed for their identification. A resistance criterion that, while being based on physical considerations, presents the advantages and ease of use of quadratic criteria and can be easily identified is therefore proposed. This new criterion has been applied to the thermo-mechanical analyses of the TAURO blanket and is referred hereafter as the “TAURO design criteria”.

TAURO criterion for evaluating stresses through the thickness:

Stresses through the thickness can be evaluated assuming brittle elastic behaviour and using the maximum stress criterion:

$$\sigma_{ZZ}^- \leq \sigma_{ZZ} \leq \sigma_{ZZ}^+$$

$$|\tau_{XZ}|, |\tau_{YZ}| \leq \tau_{\max}$$

where σ_{ZZ}^- and σ_{ZZ}^+ are respectively the compressive and tensile limits for normal stress and τ_{\max} is the limit for shear stresses.

TAURO criterion for evaluating stresses in plane:

For plane stresses, a criterion derived from the Von Mises stress is proposed. The idea is, once again, to distinguish between a “positive” and “negative” energy on the basis of the spectral decomposition of the stress tensor. The Von Mises criterion can be written as:

$$\frac{1}{2} \left\{ 3\text{Tr}[\dot{\sigma}\dot{\sigma}] - \text{Tr}^2[\dot{\sigma}] \right\} \leq \sigma_0^2 \text{ or}$$

$$\frac{1}{2} \left\{ 3\text{Tr} \left[\frac{\dot{\sigma}\dot{\sigma}}{\sigma_0^2} \right] - \text{Tr}^2 \left[\frac{\dot{\sigma}}{\sigma_0} \right] \right\} \leq 1$$

where σ_0 is the maximum allowable stress (which is the same for compressive and tensile loading). We can then split the tensor $\dot{\sigma}$ into its positive and negative eigenvalues:

$$\dot{\sigma} = \dot{\sigma}^+ + \dot{\sigma}^-$$

$$\dot{\sigma}^+ \dot{\sigma}^- = 0$$

which leads to:

$$\frac{1}{2} \left\{ 3\text{Tr} \left[\frac{\dot{\sigma}^+ \dot{\sigma}^+}{(\sigma_0^+)^2} \right] + 3\text{Tr} \left[\frac{\dot{\sigma}^- \dot{\sigma}^-}{(\sigma_0^-)^2} \right] - \text{Tr}^2 \left[\frac{\dot{\sigma}^+}{\sigma_0^+} \right] - \text{Tr}^2 \left[\frac{\dot{\sigma}^-}{\sigma_0^-} \right] - 2\text{Tr} \left[\frac{\dot{\sigma}^+}{\sigma_0^+} \right] \text{Tr} \left[\frac{\dot{\sigma}^-}{\sigma_0^-} \right] \right\} \leq 1$$

or:

$$\left(\frac{\sigma_1^+}{\sigma_0^+} \right)^2 + \left(\frac{\sigma_2^+}{\sigma_0^+} \right)^2 + \left(\frac{\sigma_1^-}{\sigma_0^-} \right)^2 + \left(\frac{\sigma_2^-}{\sigma_0^-} \right)^2 - \frac{\sigma_1^+ \sigma_2^+}{(\sigma_0^+)^2} - \frac{\sigma_1^- \sigma_2^-}{(\sigma_0^-)^2} - \frac{\sigma_1^+ \sigma_2^-}{\sigma_0^+ \sigma_0^-} - \frac{\sigma_1^- \sigma_2^+}{\sigma_0^- \sigma_0^+} \leq 1$$

where σ_0^+ and σ_0^- are, respectively, the assumed limit under tensile and compressive loading. The only two parameters (σ_0^+ and σ_0^-) needed to identify this criterion can then be obtained by means of classic tension/compression tests.

Figures 3 shows the comparison of the failure envelope defined by the TAURO criterion with that one defined by the ONERA criterion.

The agreement between the two criteria, and therefore the agreement with experimental results, is quite satisfactory.

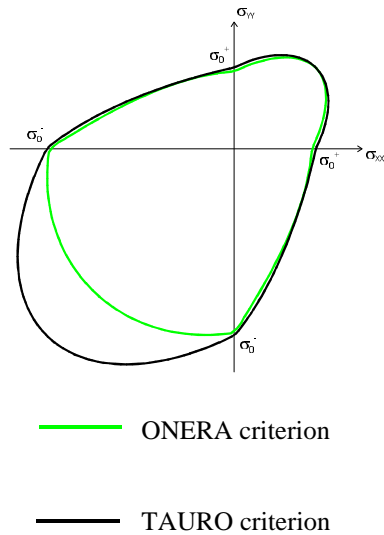


Figure 3 : Comparison of the failure envelopes defined by the TAURO criterion and the ONERA criterion in the (s_{xx}, s_{yy}) plane

Dimensional analysis of the TAURO blanket

Thermo-mechanical analyses of the TAURO blanket performed previously [5] have been repeated using the new SiC_f/SiC specific behavioural model and design criteria presented here above, the final objective being to obtain a better estimate of the limits and potentialities of SiC_f/SiC as structural material for fusion reactors.

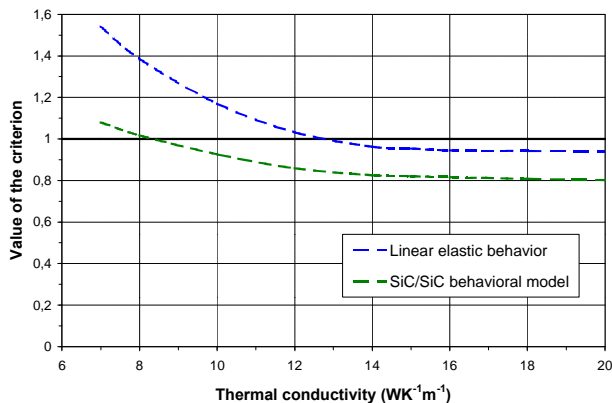


Figure 4 : Comparison between the results obtained assuming linear elastic behaviour and using the SiC_f/SiC specific behavioural model

A parametric analysis has been carried out in order to find the admissible values of the thermal conductivity through the thickness that would still allow the TAURO blanket to withstand thermal loads on the FW.

The blanket appeared capable to withstand thermal loads even with a thermal conductivity of about 8.5 W/mK. As a comparison (Figure 4), a minimum allowable thermal conductivity of about 13 W/mK would be founded assuming a linear elastic behaviour.

CONCLUSION

The use of SiC_f/SiC composites as structural material for breeding blankets involves the development of appropriate design methodologies capable of taking into account their complex non-linear mechanical behaviour. Specific models for SiC_f/SiC composites have been developed in the last years. One of these models, developed at the ONERA has been chosen for implementation in the FEM code CASTEM 2000. Among other advantages of this model, it can be pointed out that its explicit 3D formulation reduces computational times and the possibility of identifying all the model's parameters by means of classical uniaxial tension/compression tests. The simulation of experimental tests carried out with CASTEM 2000 showed that the model is capable of reproducing the non-linearity of the stress-strain relation of the composite as well as the anisotropy of its mechanical behaviour. Specific resistance criteria are also necessary in order to achieve a correct design of SiC_f/SiC structures. New resistance criteria, based on physical consideration, have been developed in this work. The main difficulties are, for the time being, related to the maximum allowable stresses to be used for the dimensional analyses. The actual stress limits could be completely defined only once the influence of neutron damage on the mechanical properties of the composite will be evaluated. Preliminary values have however been proposed.

The suggested solutions have then been applied in the design studies of the TAURO blanket. It has been shown that the use of appropriate calculation methodologies is necessary in order to achieve a correct design of the blanket and a more realistic estimate of the limits of present-day composites. The obtained results can also be extended to all nuclear components making use of SiC_f/SiC structures.

REFERENCES

- [1] L. Giancarli et al., « R&D issues for SiC_f/SiC composites structural materials in Fusion Power Reactors Blankets », IAEA-TC Meeting on FPPD, Culham 24-27 March 1998 (to be published in Fus. Eng. & Des.).
- [2] G. Aiello et al., « A parametric analysis of the TAURO SiC_f/SiC breeder blanket », CEA internal report SERMA/LCA/RT/99-2582/A, 1999.
- [3] L. M. Kachanov. Introduction to Continuum Damage Mechanics. Martinus Nijhoff Publishers, 1986.
- [4] J.-F. Maire, P.-M. Lesne, « An Explicit Damage Model for the Design of Composite Structures », Composite Science & Technology, 58, 1998.
- [5] L. Giancarli, S. Molon, J.-F. Salavy, J. Szczepanski, « Improvements of the TAURO Breeding Blanket Design », CEA internal report SERMA/LCA/1964, 1996.

REPORTS

H. Golfier, G. Aiello, L. Giancarli, « Progress on the TAURO blanket system », CEA internal report SERMA/LCA/RT/00-2837/A, October 2000.

G. Aiello, L. Giancarli, H. Golfier, « Modelling and design criteria for the analyses of SiC_f/SiC structures in nuclear fusion reactors », CEA internal report SERMA/LCA/RT/00-2866/A, November 2000.

G. Aiello, L. Giancarli, « SiC_f/SiC composites as structural material in Fusion Power Reactors in-vessel components », CEA internal report SERMA/LCA/RT/00-2920/A, February 2001

TASK LEADER

Luciano GIANCARLI

DRN/DMT/DIR
CEA Saclay
91191 Gif-sur-Yvette Cedex

Tél. : 33 1 69 08 21 37
Fax : 33 1 69 08 66 42

E-mail : luciano.giancarli@cea.fr

UT-SM&C-COAT

Task Title : DEVELOPMENT OF AN OXIDE LAYER ON Fe-Al COATINGS

INTRODUCTION

The fabrication of the tritium permeation barrier (TPB) required in the WCLL blanket concept of the fusion reactor is studied and evaluated in the frame of the TTBA-003 task on the basis of aluminised coatings is performed on a martensitic steel using two methods : hop dip galvanizing or Chemical Vapour Deposition (CVD).

In that context, the laboratory has optimised a CVD coating performed in two steps [1] and consisted of a Fe-Al layer formed by a specific pack-cementation method at a temperature of 750°C and an Al₂O₃ top layer deposited by a Pyrosol process at "low" temperature (400 – 500°C). Different permeation tests have shown that this material is efficient as hydrogen permeation barrier.

The aim of the UT-SM&C-COAT is to study the possibility of forming the oxide top layer by a direct oxidizing of the Fe-Al coating. The purpose is to study alternative solutions to simplify the CVD route for an economical purpose, even if the CVD process qualified now has been considered as a method offering a good industrial potential in the conclusions of the coated TPB fabrication assessment [2]. The feasibility of oxidizing Fe-Al base coatings has been studied using different methods :

- classic thermal oxidation,
- in-situ oxidation performed during the pack-cementation operation itself, by using oxidizing atmosphere during the final step,
- pyrolysis of a water aerosol,
- ion oxidation.

In all cases, the maximal temperatures have been limited to 750°C because of the tempering treatment of the martensitic steel substrate and to avoid a modification of the Fe-Al coating characteristics.

2000 ACTIVITIES

CLASSIC and IN SITU OXIDATION METHODS.

The coatings oxidized by the two methods have been investigated by different techniques last year : SEM, EDS, ESCA, XRD. Their characterization has been completed by a Glow Discharge Optical Spectrometry (GDOS) analysis to determine the qualitative and quantitative profiles of different selected elements as a function of depth.

The following table summarizes the Al/Fe ratio calculated as a function of depth and the thickness of the oxide evaluated using the oxygen profile.

As shown in table 1, the main GDOS results are:

- the Al/Fe ratio shows an important Al enrichment of the superficial layer,
- the Al diffusion depth is more important in the case of the oxidized coatings with regards to the Fe-Al reference,
- the thickness of the native oxide is of about 25 nm in the case of the Fe-Al reference coating ; but the oxide thickness formed by oxidation is very different according to the method used : it is much more important in the case of the classic oxidation (350 nm) than in the case of the in situ method (75 nm).

Table 1 : Al/Fe ratio as a function of depth and thickness of the oxide layer

	Fe-Al reference	Classic oxidation	In situ oxidation
Depth (nm)	Al/Fe ratio		
0	1.37	0.35	1.87
25	0.50	4.0	0.38
50	0.48	3.9	0.36
75	0.46	1.7	0.32
100	0.46	0.94	0.30
125	0.45	0.64	0.29
150	0.46	0.50	0.30
175	0.45	0.41	0.29
200	0.45	0.36	0.29
	Oxide thickness (nm)		
	25	350	75

ION OXIDATION METHOD.

The treatments have been performed on T91 martensitic steel specimens prepared with a mirror polished surface finishing.

Fe-Al reference coating

The Fe-Al reference coating that has been used as base material to test the oxidizing method has been performed by pack cementation in the conditions described in the Coating Qualification Report [1].

Operating conditions for the ion oxidation treatment

The feasibility of the method has been tested in a pilot-scale Plasma-Assisted CVD (PACVD) reactor equipped with a low frequency power supply and with a furnace.

The treatment uses O₂ as reactive gas. The specimens are placed on the substrate holder which is polarized and heated by a resistive heating device.

In effect, the plasma should activate the oxidation reaction, but the tests performed last year only with the plasma assistance and without additional heating showed that the operation conditions are not efficient enough to form an oxide layer on the Fe-Al coating [3].

The process has been performed under reduced pressure (~ 0.8 mbar) at a temperature of 630°C. A power of 150 W has been delivered for the plasma assistance. A treatment of 3 hours has been tested.

Investigation results

A qualitative analysis performed on the surface by EDS technique clearly shows the presence of the oxygen peak in addition to the Al, Fe and Cr elements, in comparison with the Fe-Al reference coating but no quantitative results relative to light elements like oxygen can be given with this method.

The Al, Fe and Cr concentration profiles in the coating have been controlled after ion oxidation as a function of depth by the EDS analysis performed on the polished cross-section of the specimen. They show that a slight diffusion of aluminium occurred from the substrate to the surface during the treatment, because the Al diffusion depth is thinner after oxidizing (6 µm instead of 12 µm). But the Al concentration in the superficial layer has not changed and the diffusion depth is so more correlated with the coating thickness revealed by the SEM observation after chemical attack. : it seems that the compounds formed in the 6 µm thick layer are stable and are not modified by the oxidizing treatment conditions.

These results are confirmed by the X Ray Diffraction analysis performed at glazing incidence. The spectra relative to the Fe-Al coating before and after the ion oxidation treatment show that the FeAl compounds are still present after oxidizing. The Fe-Al reference coating presents some little peaks correlated with Al₂O₃. These peaks are still present in the oxidized coating and the presence of Fe₂O₃ compounds can be also noticed.

Comparison with the other oxidation process

All these results illustrate the evolution of the Fe-Al reference coating performed by pack-cementation after a ion oxidation treatment performed at 630°C with plasma and thermal assistance. The use of an additional heating has an obvious effect on the oxidation capability of this treatment with regards to the plasma assistance alone. But, the effect of the plasma is also important when comparing with the thermal methods.

The comparison with the results obtained with the classic or the in situ oxidation methods tested last year [3] gives the following remarks :

- the formation of alumina is obtained in all cases, but it seems to be more pronounced in the cases of the thermal methods, with regards to the Fe-Al reference coating, than in the case of ion oxidation,
- for these two oxidation methods, the formation of magnetite was only revealed by the ESCA surface analysis and not by the XRD investigation at glazing incidence : this means that the amount of Fe₂O₃ is probably higher in the case of ion oxidation, which may not be so interesting since the barrier effect seems to be related to the alumina material,
- the classic and in situ methods modified the Al concentration profiles by increasing the Al diffusion depth and decreasing the Al concentration in the superficial layers ; the evolution of the Al profile is quite different during ion oxidation.

So, the formation of an oxide layer is possible with all these methods, but they lead to quite different characteristics. The plasma assistance has in particular a great influence on the oxidation mechanisms with regards to more classical thermal methods.

FABRICATION of SPECIMENS

Specific specimens compatible with the experimental device of ENEA devoted to the measurements of gas permeation rate have been fabricated.

Discs have been machined in a T91 martensitic steel plate : they are characterized by a thickness of only 1 mm for a diameter of 47 mm. Both faces are prepared with a mirror polished surface finishing to ensure a good high vacuum tightness.

A total of 4 discs has been coated and oxidized in the conditions defined in Table II for the two methods : classic oxidation and in situ oxidation.

CONCLUSION

Different methods have been tested to get a direct oxidation of the Fe-Al coating in order to replace the Pyrosol deposition of alumina.

Three of them enable to form an oxide layer :

- classic thermal oxidation,
- in situ oxidation performed during the pack cementation operation,
- ion oxidation with thermal assistance.

The characteristics of the oxidized coatings are quite different according to the method used.

From a material point of view, the thicker oxide layer is obtained with the classic thermal method. But, from a process point of view, the in situ method presents real advantages because it is performed during the same step than the pack-cementation treatment. The whole process could be carried out in a single operation including the Fe-Al deposition and the oxidation, which offers interesting scale-up considerations for the treatment of large components. In that view, the ion oxidation method is not so attractive, since it requires an experimental device equipped with pumping system and electric power supplies and because its oxidation efficiency is not drastically improved with regards to the other thermal methods.

So, the classic thermal oxidation and the in situ oxidation methods produced a direct oxidation of the Fe-Al coating. Nevertheless, the barrier efficiency of the oxide layer formed in each case should be evaluated and compared to the results obtained with the Fe-Al/Al₂O₃ coating qualified in the TTBA-003 task.

REPORT AND PUBLICATION

- [1] C. CHABROL, F. SCHUSTER "Coating qualification report", Note technique DEM n°98/32, 15/07/98.
- [2] C. ESCAVARAGE "Coated TPB Fabrication Assessment", FRAMATOME report n° NVPM DC 00 0247 IMU, 9/05/2000.
- [3] C. CHABROL, V. BENEVENT, F. SCHUSTER "Development of an oxide layer on a Fe-Al CVD coating", Note Technique DEM n° 99/94, 20/12/99.

TASK LEADER

Claude CHABROL

DRT/DTEN/SMP/LPTS
CEA Grenoble
17, rue des Martyrs
38054 Grenoble Cedex 9

Tél. : 33 4 76 88 99 77
Fax : 33 4 76 88 99 85

E-mail : Chabrol@cea.fr

Task Title : DIFFUSION COEFFICIENT MEASUREMENTS IN LIQUID METALS

INTRODUCTION

OBJECTIVE

The knowledge of the diffusion coefficient of the main constituents of a material in a liquid metal is necessary to make a corrosion model of this material in this liquid, in particular when the limiting step of the whole corrosion process is the diffusion of a dissolved species in the diffusion boundary layer of the liquid.

To determine the diffusion coefficient of a metallic element in a liquid metal, a method using a rotating cylinder specimen with a well defined forced convection, which gives a good control of mass transfer, has been adapted and a device has been built [1].

Experiments performed with this technique have first allowed to confirm that the corrosion process of 9-11 wt% Cr martensitic steels by Pb-17Li liquid alloy is controlled by the iron diffusion in the liquid boundary layer. Secondly, iron diffusion coefficient in Pb-17Li at temperatures between 475°C and 517°C was determined.

The objective of the study now is to determine the iron diffusion coefficient in pure lead in order to compare this value with those of the literature and to draw influence of the Li content in Pb on the iron diffusion coefficient. The device and procedure will have first be adapted to work with Pb due to the high oxygen solubility in Pb.

2000 ACTIVITIES

The rotating cylinder technique can be used for the determination of a diffusion coefficient when the corrosion kinetics is governed by the convective diffusion of the dissolved species in the liquid boundary layer. But one major difference between lead and lead-lithium is the oxygen solubility. While it is very low in Pb-17Li due to the presence of lithium, it is high in Pb: at 500°C: it is between 3 to 7 10^{-3} wppm in Pb-17Li compared to about 20 wppm in Pb at the same temperature.

Therefore, if an iron specimen is immersed at this temperature in a lead bath saturated in oxygen, the iron specimen will be oxidised. Thus the mechanism of corrosion is no longer controlled by the dissolution of the metallic element in the liquid boundary layer and the rotating cylinder device cannot be used to determine a diffusion coefficient.

Therefore, preliminary to use this technique with lead, a way to remove the oxygen from the lead bath must be developed: it was the activity in 2000.

REVIEW OF THE METHODS TO REMOVE OXYGEN FROM Pb

Different methods are stated in the literature to remove oxygen from liquid lead:

- A method consisting in a bubbling of an argon/hydrogen gas mixture in the liquid lead bath at temperatures higher than 350°C [3-5]. However, no oxygen measurements in Pb during the bubbling are reported as well as no data exist to make a correlation between the hydrogen content in the bubbling gas and the oxygen content in the Pb bath. It is reported that hydrogen easily reduces PbO_2 in water and Pb sub oxides. Pb_3O_2 and Pb_2O_3 are reduced in PbO or Pb at temperatures higher than respectively 230°C and 235°C.
- A second method consists in adding in the Pb bath some elements like Mg, Ca, Ge, Li, Zn...which allow to decrease oxygen content in Pb by forming very stable oxides [6,7]. The drawback of this technique is that some foreign elements which can modify the corrosion mechanisms are introduced in the liquid.
- The third method uses a cold trap or a Ti-Zr hot trap at 600°C. The cold trap temperature determines the oxygen content in the Pb bath. The hot trap has the disadvantage to induce some pollution in the Pb bath. In the literature, no oxygen content measurements in Pb bath during the tests of these techniques are reported.

For this study, we have used the first method to remove oxygen from Pb because no foreign metallic element which could modify the corrosion mechanism is introduced in the bath.

EXPERIMENTAL DEVICE TO REMOVE OXYGEN FROM Pb

A schematic view of the apparatus is represented in Figure 1. A 350 mm high and 35 mm diameter crucible is filled with lead and placed in a airtight container. A bubbling gas system consisting of tube with four 1 mm holes at its extremity and a finger for thermocouple are fixed to the container cap and plunged in the lead. This device is placed in a furnace and connected to a vacuum pump and a feeding circuit of hydrogenated argon.

The container and the crucible are first cleaned and then the crucible is placed in the container under vacuum.

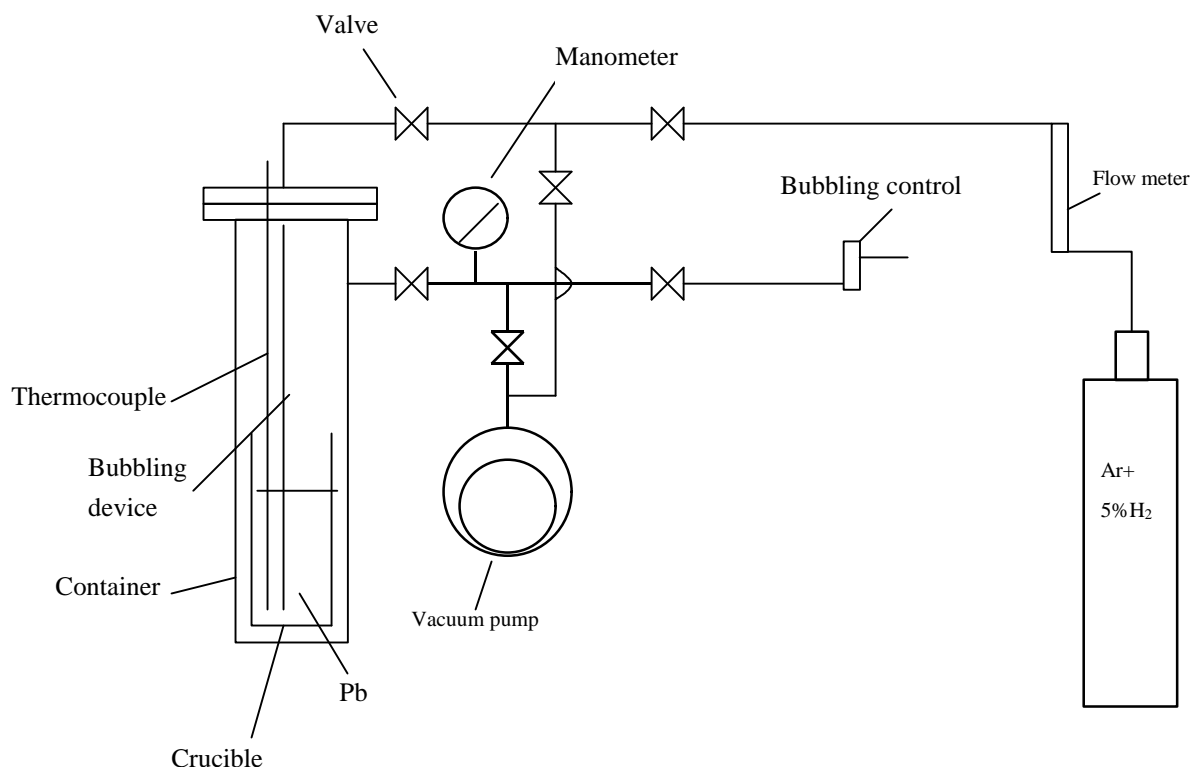


Figure 1 : Crucible with lead and Ar /H₂ gas bubbling system

The container with the crucible are heated under dynamic vacuum up to 400°C for 24 hours for degassing. After that, in a glove-box under a controlled atmosphere, the crucible is filled with lead. The bubbling tube and the finger for thermocouple are then immersed in the liquid Pb. Finally, still in the glove box, after the Pb freezing, the crucible is placed in the container which is then closed.

The bubbling gas which has been used is an argon with 5 vol.% H₂ mixture. The temperature of the lead bath during the bubbling was 450°C.

As we have not an oxygen probe, we cannot measure the oxygen content in the lead bath. Thus, at the end of the bubbling sequence the container with the crucible is opened in a glove box under controlled atmosphere and an iron specimen is immersed in the liquid lead for few hours at 550°C. If the specimen surface after removing the lead has a metallic aspect, it is considered that the oxygen content in Pb is sufficiently low.

RESULTS

Four tests have been performed.

At the beginning of the first test, probably due to a too high pressure variation, lead has been entertained in the tube for gas entrance. This tube which is at room temperature has been plugged. The device has been dismantled and cleaned. After reassembling the device and heating the container with lead bath, a 1L h⁻¹ gas bubbling at 1 bar pressure in the liquid has been installed. Lead vapours condensated in gas exit tube leading again to the plugging.

During the second test, the lead has been partly thrown out of the crucible.

The third test has been performed in the same way than the tests 1 and 2, except that the pressure and the flow rate of the bubbling gas were respectively 0.5 bar 0.5 L h⁻¹.

This test lasted 48h. After the test, an iron specimen was immersed for 8 hours in the lead at 550°C.

After immersion, the lead was removed from the specimen surface.

This latter was covered by an oxide layer. Therefore, the oxygen content in the lead after the bubbling was still too high.

The last test has been performed in the same conditions than the test 3 but it lasted 100 hours. After, a specimen was immersed for 16 hours in the lead at 550°C.

The specimen surface had a metallic aspect: the oxygen content in the bath after the bubbling sequence was too low to allow the formation of an oxide layer on iron.

A procedure has therefore been found to sufficiently decrease the oxygen content in the lead to avoid the oxidation of an iron specimen.

Prior to introduce a iron cylinder specimen in the lead in order to determine the diffusion coefficient of iron, an argon with 5% H₂ gas mixture must be introduce by bubbling the liquid lead bath at 450°C for at least 100 hours.

CONCLUSION

One important difference between the liquids lead and lead-lithium is their oxygen solubility. While it is very low in Pb-17Li due to the presence of lithium, it is high in Pb: at 500°C it is between 3 to 7 10^{-3} wppm in Pb-17Li compared to about 20 wppm in Pb at the same temperature. Therefore, if an iron specimen is immersed at this temperature in a lead bath saturated in oxygen, it will be oxidised. As the determination of a diffusion coefficient in a liquid by means of the rotating cylinder specimen method is possible only when the limiting step of the corrosion process is the convective diffusion of the dissolved species, this method can be used only with liquid lead with a low oxygen content.

A review of the different methods for removing the oxygen from the liquid lead has been made. To avoid the presence in the lead bath of any impurity which could modify the corrosion process, the method consisting in a bubbling of an argon/hydrogen mixture in the bath has been used.

A device has been adapted to introduce a bubbling gas in a crucible containing lead and placed in an airtight container. A procedure has been found to sufficiently remove oxygen from lead to avoid oxidation of an iron specimen.

REFERENCES

16th SOFT (1990) 901-905

- [1] N. Simon, Etude des interactions de l'alliage liquide plomb-lithium avec les aciers austénitiques et martensitiques, Thesis, Université Paris VI.
- [2] T. Dufrenoy, V. Lorentz, A. Terlain, Determination of the diffusion coefficient of iron in Pb-17Li alloy, CEA Report RT-SCECF 520 (December 1999)
- [3] J. Desreumaux, S. Marques, Solubilité et comportement de l'oxygène dans le plomb, le bismuth et l'alliage eutectique plomb bismuth. Etude bibliographique, RT-DER/STPI/LPCP-99/008
- [4] A. Takinen, Oxygen-metal (Ag, Au, Bi, Cu, In, Sb, Sn, Te) interactions in dilute molten lead alloys, Acta Polytechnica Scandinavia, Ch. 146, 3-44 (Helsinki 1981)
- [5] M. Broc, J. Sannier, G. Santarini, Experimental studies on the use of liquid lead in molten salt nuclear reactor, Nuclear Technology, Vol. 63, 197-208 (1983)
- [6] F. D. Richardson, L. E. Webb, Oxygen in molten lead and the thermodynamics of lead oxide-silica melts, Trans. Inst. Min. Metall. 64 (1954) 529-554

- [7] M. Jacquin, M. Cappelaere, Corrosion des métaux, alliages et matériaux réfractaires par le plomb fondu, DCA/SECE/SECML/10746, HT-12/66/77 (1977)

REPORT

T. DUFRENOY, HERBERT

Determination of the diffusion coefficient of iron in liquid Pb. Rapport CEA RT-SCCME (March 2001)

TASK LEADER

Thierry DUFRENOY

DEN/DPC/SCCME/LECNA
CEA Saclay
91191 Gif-sur-Yvette Cedex

Tél. : 33 1 69 08 16 16
Fax : 33 1 69 08 15 86

E-mail : thierry.dufrenoy@cea.fr

Task Title : LIQUID METAL CORROSION UNDER MAGNETIC FIELD

INTRODUCTION

OBJECTIVE

Corrosion of materials exposed to liquid metals depends on many parameters such as temperature, hydrodynamics, thermal gradient,... In the water-cooled liquid metal blanket designed for fusion reactors, the corrosion behavior of steels in contact with the Pb-17Li alloy has been investigated and it was shown that the dissolution of martensitic steels was significantly affected by the alloy velocity. In the high magnetic field confining the plasma, the flow of the liquid alloy is characterized by the presence of a core velocity in the central region and various boundary layers in the vicinity of the channel-walls which exhibit a strong velocity gradient [1]. The mass transfer between a solid and a liquid being controlled by the velocity gradient at the wall, a modification of the corrosion process may thus be expected in the presence of the magnetic field [2]. It is important to study this phenomenon and quantify the effect of the field on the corrosion of steels in contact with the Pb-17Li alloy.

In order to achieve this purpose, it is proposed to perform corrosion tests in Pb-17Li under magnetic field in flows driven by a rotating disk inside a cavity. Such a study is of interest because the hydrodynamics in this configuration can be well described by numerical simulation (reported in [3, 4]) and thus the influence of the field on the mass transfer can be well characterized. However, the velocities numerically predicted must be validated by experiments to have a correct evaluation. The objectives of the present work are to measure experimentally the flow velocities and to compare the results with those obtained by simulation. The hydrodynamic characterization was made in mercury and the conclusions drawn in the frame of this study will be used in the Pb-17Li alloy afterwards.

2000 ACTIVITIES

In the work performed in 2000, velocity measurements were carried out in mercury - with and without magnetic field - by using an ultrasonic method and the results were compared with those obtained by numerical analysis.

EXPERIMENTAL METHOD

A special device with a rotating specimen has been built to validate the numerical code used to predict the velocity gradient distribution in the cavity.

It works with water or mercury instead of lead-lithium so that tests can be performed at room temperature.

It is the same as the one used for future Pb-17Li experiments but the cavity is made of Plexiglas instead of steel and specific zones for the location of the ultrasonic sensor have been included. The figure 1 presents a view of the device.

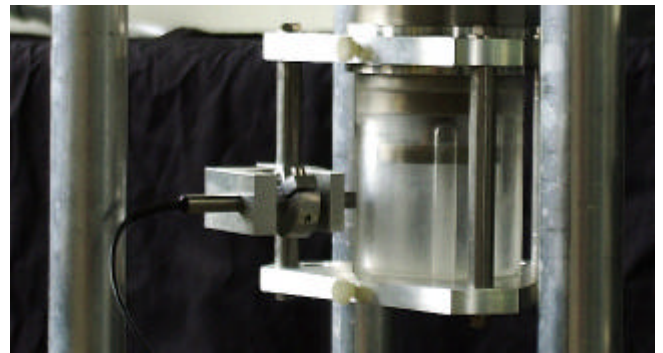


Figure 1 : View of the cavity, the probe support and the ultrasonic sensor

The velocity measurements have been performed with an ultrasonic sensor. An ultrasonic beam produced in a cylindrical sensor (8 mm in diameter) penetrates the liquid bath through the external wall of the Plexiglas cavity. When the ultrasonic beam inside the liquid (water or mercury) encounters a particle, it is reflected with a frequency proportionally modified with the velocity of this particle. The difference of frequency between the incident and the reflected beams gives the particle velocity along the beam trajectory. When the particle has a density very close to the fluid density, it can be assumed that its velocity is identical to that of the fluid velocity. If the particle concentration is sufficiently high and if the size of the analyzed medium is not too large, it is possible to know the velocity distribution across the liquid from one wall to the other. Three types of difficulties can be identified in the use of the ultrasonic method:

- The first one is to have particles with suitable density. For water, a powder of starch (density 1.1 g/cm³) was used for the measurements. For mercury, natural particles of mercury oxide (density 11.7 g/cm³) were used.
- The second type of difficulty comes from the fact that the ultrasonic beam has a relatively large size (8 mm), producing some difficulties in the analysis of local velocity measurement.

The third one is related to the principle of the measurement itself, which allows only the knowledge of the projection of the velocity on the line of the ultrasonic beam. As a consequence, special computation must be achieved to calculate this projection in order to use the numerical results and compare this projection with the experimental ones.

To test the validity of the experimental approach of the velocity measurements inside the cavity, water and mercury flows were characterized without magnetic field in the same range of Reynolds numbers. The both series of measurements are compared with the velocity distribution given by the numerical procedure (the numerical analysis is detailed in [5-6]). An excellent agreement is seen between the three profiles which exhibit a good location of the two maxima for each curve (same position for water, mercury measurements and calculation results) and a good precision for the intensity of the velocity, this precision being better in the vicinity of the maximum. On the other hand, the size of the boundary layer is well comparable in the three cases. The disturbances observed in the case of mercury are probably due to the small concentration of natural oxide particles inside the bath.

The water velocity distribution obtained without magnetic field is similar to the one obtained in the presence of a magnetic field. This result, which is expected as water is not influenced by a magnetic field, shows that the ultrasonic method to measure the liquid velocity is not affected by the presence of the magnetic field.

RESULTS

Hydrodynamics of flow without magnetic field

The hydrodynamics analysis of a flow without magnetic field has been realized in water and mercury inside the Plexiglas cavity. A good agreement has been obtained between the experimental results and numerical simulation (carried out by using the commercial code FLUENT and detailed in [2, 3]) for both the profile and the intensity of the velocity distribution. The tangential component is very well measured whereas the radial component presents some experimental instability, which can be attributed to the very low value of this component.

Hydrodynamics of flow under a magnetic field

The device was placed inside the solenoid which allows to impose a longitudinal magnetic field, continuously adjustable between 0 and 0.4 T. Two series of tests, one with low Reynolds number (6670) and one with high Reynolds number (26680) were carried out with interaction parameter N values ($N = Ha^2/Re$, Ha : Hartman number and Re : Reynolds number) varying from 0 to respectively 10 and 2.5.

As the wetting of mercury on steel substrate is very poor, the contact resistance between the two elements is sufficiently high to consider the disk insulated from the mercury. Therefore, in the present study, the analysis of the experimental results is compared with the classical case of insulating disk and the experimental conditions correspond to the case of an insulating cavity with an insulating rotating disk.

A first series of tests was performed for a low value of the Reynolds number ($Re = 6670$). An increasing of the velocity is observed when the Hartmann number rises from 0 to 260, which is in perfect agreement with the theory (Fig. 2-a).

This effect is correlated with the very known effect of the magnetic field, which tends to suppress any gradient and thus homogenizes the velocity distribution. A thin boundary layer (i.e. the Hartmann layer) vanishes the velocity at the bottom wall of the cavity. It can also be seen that the symmetry of the velocity distribution is improved when the Hartmann number increases. For a given Reynolds number, the experimental definition of the velocity distribution is better when the Hartmann number increases. This can be attributed to two phenomena: the first one is related with the increasing of the velocity which is better for the precision of the measurement, the second one results from the stabilizing effect of the magnetic field which tends to homogenize the velocity distribution. In the figure 2-b, the results show that the experimental distribution of the velocity along the ultrasonic beam fits very well with the theoretical results.

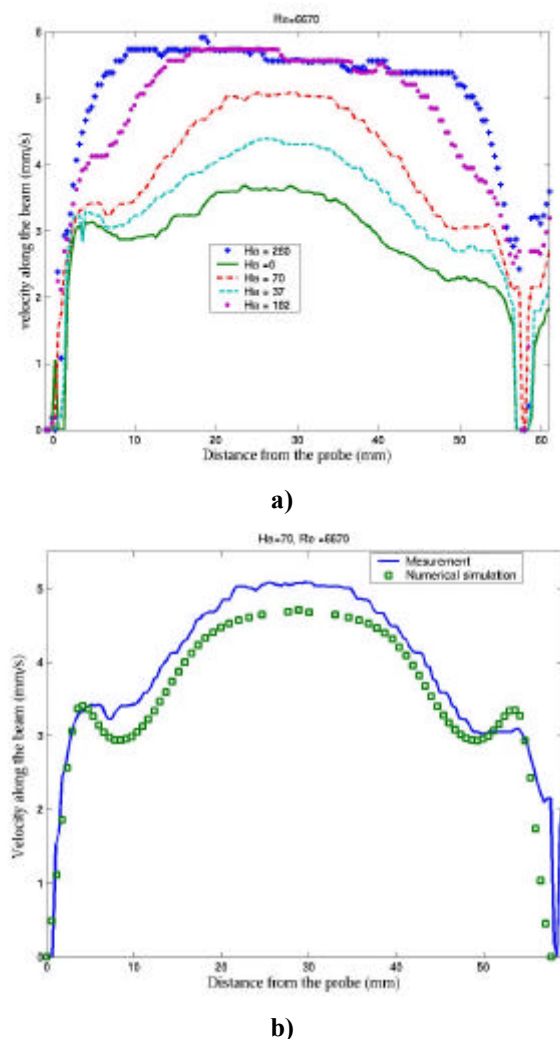


Figure 2 : Evolution of the velocity profiles in mercury under magnetic field ($Re = 6670$)
 a) Experimental results for different Hartmann numbers
 b) Comparison between experimental and numerical results for $Re = 6670$ and $Ha = 70$

The second series of results (Figure 3) is obtained for a large value of the Reynolds number ($Re = 26680$) corresponding to a rotation of the disk of 40 turns per minute). The theoretical and experimental curves fit very well.

The value of the velocities increases with Ha . Unlike the previous case, the asymptotic value of the velocity (equal to half of the value of the disk velocity) is not completely reached because, for a given value of the Hartmann number, the interaction parameter equal to $N = Ha^2/Re$ (ratio of the inertia forces to the electromagnetic forces) decreases when the Reynolds number increases.

The asymptotic values of the velocity can only be reached for large values of N and Ha .

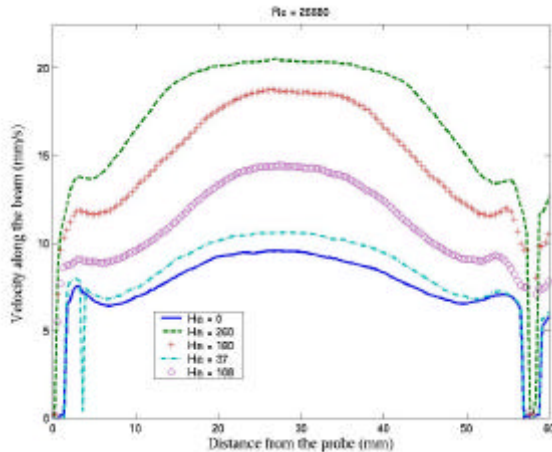


Figure 3 : Evolution of the velocity profiles in mercury under magnetic field ($Re = 26680$), for different Hartmann numbers.

For sufficiently high value of the Hartmann number, it is shown that the wall velocity gradient becomes independent of this parameter.

This can be easily explained by the fact that the tangential velocity in the cavity is at a level which is exactly the half value of the driving disk velocity.

In that condition, the distribution of the induced electric current which only depends on the velocity distribution, is also fixed and thus the electromagnetic torque reaches an asymptotic value which does not change when the magnetic field is increased.

For that steady state situation, the viscosity torque exerted by the wall on the fluid does not change, which fixes an asymptotic value of the velocity gradient at the wall.

Another result concerns the evolution of the maximum of the tangential component of the velocity versus the magnetic field intensity (i.e., versus the Hartmann number), in a cross section of the cavity. The theoretical distribution of this maximum velocity, in the case of insulating walls corresponding to the present experiment, reaches half of the value of the tangential velocity of the driving disk in the asymptotic situation of high Hartmann number.

The comparison of the experimental and theoretical distributions of this maximum of velocity for a small Reynolds number ($Re = 6670$) shows a very good agreement.

CONCLUSION

Velocity measurements were carried out in flows driven by a rotating disk, under and without magnetic field.

Then, the experimental values were compared to those obtained theoretically in order to validate the numerical simulation. The main results obtained via this study were the following.

- The specific device built to measure the velocity inside the cavity by ultrasonic method was very satisfying. A very good reproducibility of the experimental results was obtained.
- The experimental method was validated by comparing the velocity distribution obtained without magnetic field in water and mercury inside an insulating cavity made of Plexiglas. In addition, the good agreement between the both experimental approaches confirms the possibility to use ultrasonic method for velocity measurement inside mercury. Such measurements were never carried out before in rotating mercury flows.
- The validation of the numerical analysis was made by using a Plexiglas cavity filled with mercury and a stainless steel rotating disk. Due to the bad electric contact between the disk and the mercury, the wall cavity was assumed to be insulating. The agreement was very good for the two values of Reynolds number (low and high) considered in the experiments and for different values of the Hartmann number. Therefore, the theoretical approach used to predict velocities is well validated. It can be used in the future to describe the velocity field in the Pb-17Li alloy for which experimental measurements cannot be performed.
- In the future, it will be necessary to improve the electric contact between the mercury and the disk by coating its surface with gold. Then, the velocity measurements will be compared with those predicted in the case of a conducting disk. Finally, the study will be devoted to the Pb-17Li alloy and the corrosion tests will start.

REFERENCES

- [1] S. Molokov, Fully developed liquid metal flow in multiple ducts in a strong uniform magnetic field, Eur. J. Mech. B-Fluids 12-6 (1993) 769-787.
- [2] F. Barbier, A. Alemany and S. Martemianov, On the influence of a high magnetic field on the corrosion and deposition processes in the liquid Pb-17Li alloy, Fus. Eng. Des. 43 (1998) 199-208.
- [3] F. Barbier, A. Alemany and A. Kharicha, Corrosion in moving liquid Pb-17Li under magnetic field: Hydrodynamic modeling in rotating flows, CEA report, RT-SCECF 510 (December 1999).

- [4] A. Kharicha, A. Alemany and F. Barbier, Influence of the magnetic field and the conductance ratio on the hydrodynamic of a fluid driven by a rotating disk in a cylindrical enclosure, Proceedings of the 4th International PAMIR Conference on Magnetohydrodynamic at Dawn of Third Millennium, Presqu'île de Giens, France, September 18-22, 2000, 1 (2000) 405-410.

REPORT

F. BARBIER, A. ALEMANY, A. KHARICHA,
Hydrodynamics in liquid metal flow driven by a rotating disk under magnetic field: experiment and simulation, RT-SCECF 545 (November 2000).

TASK LEADER

Françoise BARBIER

Person to contact:
Anne TERLAIN

DEN/DPC/SCCME/LECNA
CEA Saclay
91191 Gif-sur-Yvette Cedex

Tél. : 33 1 69 08 16 18
Fax : 33 1 69 08 15 86

E-mail : anne.terlain@cea.fr

Task Title : COMPATIBILITY OF REFRACTORY MATERIALS WITH LIQUID ALLOYS

INTRODUCTION

OBJECTIVE

In a fusion reactor, the plasma-facing region is submitted to a high particles flux generated in the plasma and thus High Heat Flux Components (HHFC) operate high heat flux. Solutions must be found to extract these high heat fluxes ($> 5 \text{ MW/m}^2$), especially on the divertor which is a key component of a fusion power plant. Several divertor concepts based on different coolants are proposed. Among them, the liquid metal-cooled divertors are evaluated because their high thermal conductivity is attractive. The advantage is also the variety of suitable liquid metals, exploited here to select a liquid metal with low chemical reactivity with air. The Pb-17Li alloy ($T_{\text{melting}} = 235 \text{ }^\circ\text{C}$) could be a good candidate.

Concerning the potential materials for the divertor, W-alloys appear to be the best choice as armor material whereas the same W-alloy, Mo-alloys (e.g., TZM), martensitic steel and possibly the SiC_f/SiC are the best performing structural materials. Several designs were evaluated: round W-alloy tubes surrounded by W-alloy monoblock, square W-alloy tube with castellated plasma-facing wall, square W-alloy tube with porous plasma-facing wall. Whatever the concept, the coolant liquid metal is in contact with W-alloy surfaces. Therefore, one major issue concerns the high temperature compatibility between liquid metal and W-alloys (interface temperature up to $1350 \text{ }^\circ\text{C}$ in the static liquid metal gap are expected). Up to now, the compatibility of tungsten with Pb-17Li was not considered in details. Concerning the solubility of W in Pb-17Li, only a few experiments were performed with W-crucibles. It was concluded that the solubility of this element in the eutectic was less than 1 wppm at $600 \text{ }^\circ\text{C}$.

Referring to pure lead, no phase diagram is available for the Pb/W couple and no intermediate phases exist in the system. Literature data reported no attack of tungsten after 306 hours at $950 \text{ }^\circ\text{C}$ and 100 hours at $1000 \text{ }^\circ\text{C}$ in pure Pb. Referring to Guminski model very low solubilities are expected for refractory metals in lead. Thus, it is thought dissolution of tungsten like molybdenum should be limited in Pb-17Li. However, there was no systematic study. In addition, it has to be noted that discrepancies exist about solubilities determined for some refractory metals in Pb-17Li. Moreover, during the solid-liquid interaction, dissolution can take place at the interface but other phenomena such as compound formation at the surface or liquid metal penetration in the solid leading to embrittlement can also be observed. With regard to W-alloys, literature data are very limited to have a good description of the corrosion in Pb-17Li. Thus, an investigation must be carried out on this system.

2000 ACTIVITIES

W-alloy specimens were exposed to static Pb-17Li at different temperatures up to 1500 h. After exposure, the corrosion behavior was analyzed.

MATERIALS

The tungsten alloy (W-1 wt% La_2O_3) was delivered by Plansee company in the form of rods. Its typical composition was W – 1 wt% La_2O_3 with impurities (wppm): 20 Mo – 15 Fe – $< 10 \text{ Si}$ – $> 10 \text{ Cr}$. Samples (diameter: 4.78 mm, length: 40 mm) were machined from the rods.

EXPERIMENTAL PROCEDURE

The Pb-17Li pieces were cleaned with a wire brush to remove the oxide scale. After cleaning of the W specimens in acetone and ethanol, weight and geometrical measurements were made. All the operations to introduce the W specimens in crucibles with molten Pb-17Li were carried out in a glove box with purified argon gas. Once the Pb-17Li alloy was melted, the liquid was poured into a Mo crucible.

Three crucibles (corresponding to different corrosion temperatures) were used and about 800 g of Pb-17Li was filled into each Mo crucible. Three W samples were mounted into a specimen holder. Then, each specimen holder was immersed into the crucible with the molten alloy. After cooling, the Mo crucible with specimens was sealed by electron beam welding. The as-sealed crucibles were placed into 316L steel or 601 nickel alloy containers which were subsequently electron beam welded.

The corrosion tests were performed at three temperatures: 450, 600 and $800 \text{ }^\circ\text{C}$. Their duration was 1500 hours. After the tests, the containers and the crucibles were opened, the Pb-17Li melted and the samples extracted from the alloy in the glove box.

CHARACTERIZATION

After test, the specimens were weighted after removing the residual lead alloy adhering to the surface by dipping them in a chemical mixture (1/3 ethanol, 1/3 acetic acid, 1/3 hydrogen peroxide).

Optical microscope and scanning electron microscope (SEM) with analysis by energy dispersive spectroscopy (EDS) were used to perform observation and analyses. Chemical analyses of the Pb-17Li alloy after corrosion tests were performed by inductively coupled plasma mass spectrometry (ICP-MS).

RESULTS AND DISCUSSION

It was not possible to measure the weight variation of the corrosion samples after the tests because tungsten was significantly etched by the chemical mixture used to remove the lead alloy adhering to the surface. As a consequence, no information was obtained by this method to detect whether tungsten has lost weight (corrosion by dissolution) or gained weight (corrosion by formation of reaction products) during contact with Pb-17Li. Another experimental procedure must be considered to make weight measurements in the future.

After the tests, the concentrations of Mo and W in Pb-17Li were respectively 2-3 ppm and less than 0.5 ppm whatever the temperature. These analyses indicate that the Mo crucible is not completely inert with the Pb-17Li alloy. Concerning the concentration of tungsten in Pb-17Li at the end of the tests, the value is very low (< 0.5 wppm) and no change is detected with the corrosion temperature. Such values might indicate that the dissolution of tungsten in Pb-17Li is not important. However, we must draw attention to the experimental conditions. Under isothermal conditions, the element concentration becomes equal to the solubility after a period of time. Assuming the solubility of W in Pb-17Li is very low, the dissolution rate can decrease with time and reach zero. Therefore, the corrosion of tungsten by direct dissolution process can be minimized in our tests. Corrosion experiments in non-isothermal conditions would be necessary to establish if dissolution occurs significantly at temperatures where the solubility is greater than the bulk concentration.

Apart from dissolution effects, the changes in surface morphology and composition due to liquid metal penetration or compound formation are important in themselves. Figures 1 and 2 show cross-section micrograph of respectively a reference specimen and a specimen after exposure at 800°C in Pb-17Li. No attack is detected. Whatever the temperature, no reaction products are observed at the interface. This is confirmed by the X-ray images which indicate no modification in the distribution of the different elements. These results are different of those obtained with tungsten in contact with pure liquid lead [1]. In that case, it was found that the presence of oxygen in lead modifies the interaction mechanism leading to the oxidation of tungsten. In the case of the Pb-17Li alloy, the solubility of oxygen is very small [2] and the oxygen concentration is much lower than that contained in the molten lead used in [1]. Moreover, a fundamental characteristic is the presence of lithium in the alloy: the oxygen affinity for lithium is higher than for tungsten so that lithium oxide is more stable than tungsten oxide. As a consequence, tungsten cannot be oxidized in contact with Pb-17Li and our results agree well with that.

Another concern when solids are exposed to molten metals is the penetration of the liquid along the grain boundaries. The cross sections and X-ray images do not indicate the formation of a liquid channel from the surface of tungsten. Therefore, liquid penetration of Pb-17Li along W grain boundaries is unlikely to occur. Nevertheless, further investigations about the microstructure of tungsten are needed.

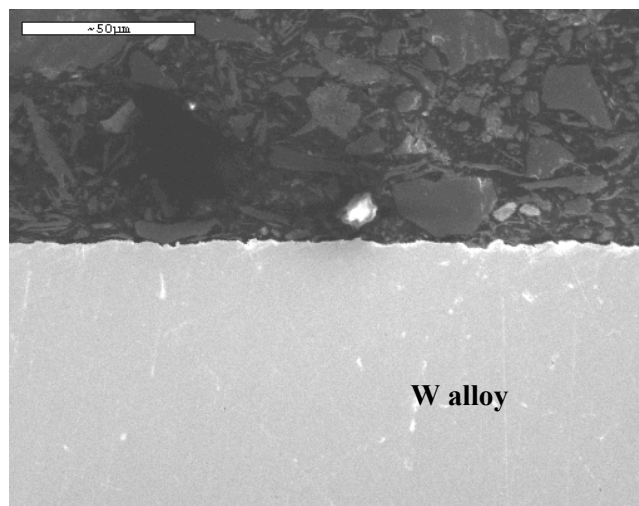


Figure 1 : Surface of the tungsten alloy before exposure to the Pb-17Li liquid alloy

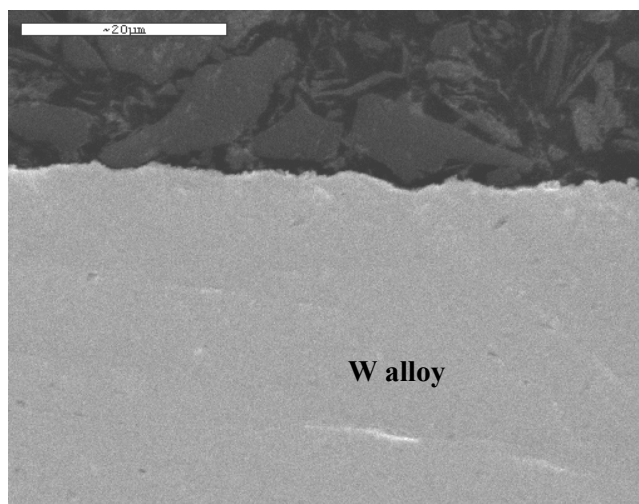


Figure 2 : W alloy /Pb-17Li alloy interface after corrosion test at 800 °C

CONCLUSION

The corrosion behavior of a W alloy has been studied by immersion tests in static liquid Pb-17Li in the temperature range 450-800 °C and for exposure times up to 1500 h. The amount of tungsten found in Pb-17Li at the end of the corrosion tests was very small (< 0.5 wppm) indicating that the dissolution of this element was likely very limited. However, it has to be noted that the dissolution process may be minimized in the present isothermal tests due to the very low solubility of tungsten in the melt. In order to evaluate the dissolution rate, test should be carried out in non-isothermal conditions.

The interaction with the molten alloy did not lead to the formation of reaction products on the tungsten surface. No attack and no composition change were found at the solid-liquid interface. The preliminary observations did not exhibit any liquid metal penetration in the tungsten. Nevertheless, the microstructural study must be carried out more in depth.

Further investigations are required for complete evaluation of the corrosion behavior (improvement of the experimental method for weight measurements, observations of the grain boundaries, determination of the W solubilities in Pb-17Li at higher temperatures...).

REFERENCES

- [1] G. Benamati, P. Buttol, V. Imbeni, C. Martini and G. Palombarini, Behaviour of materials for accelerator driven systems in stagnant molten lead, J. of Nucl. Mater. 279 (2000) 308-316.
- [2] M.G. Barker, J. A. Lees and T. Sample, Determination of the solubility of oxygen in Pb-17Li, 4th International Conference on Liquid Metal Engineering and Technology, LIMET 4, Avignon, France, 1 (1988) 206.1-206.8.

REPORT

F. BARBIER, H. HERBERT, Corrosion behaviour of W alloy in static Pb-17Li, RT-SCECF 543 (November 2000)

TASK LEADER

Françoise BARBIER

Person to contact:
Anne TERLAIN

DEN/DPC/SCCME/LECNA
CEA Saclay
91191 Gif-sur-Yvette Cedex

Tél. : 33 1 69 08 16 18
Fax : 33 1 69 08 15 86

E-mail : anne.terlain@cea.fr

Task Title : WETTING OF MATERIALS BY LIQUID METALS

INTRODUCTION

OBJECTIVE

In the fusion reactors, liquid metals or alloys are considered as tritium breeding materials and/or coolants. For these uses, the wetting and the reactivity of the liquid with the solid have to be known to assess the efficiency and lifetime of a system. For instance, extrapolation of corrosion test results can be done only when the time for achieving the solid wetting by the liquid is known otherwise the lifetime could be overestimated. Or the efficiency of a cooling system depends on the wetting of the walls to cool by the liquid. In chemical process, one crucial parameter to design a packed contactor is the mass transfer surface area which is closely related to the wetting characteristics of the packing by the liquid.

The work performed previously [1] has shown that the sessile drop and transferred drop techniques are well suited to study the wetting of a liquid metal by a solid and in particular the Pb/Fe and Pb/Fe-7Cr systems, even if some specific adaptations have had to be developed due to the significant Pb vapour pressure. It was shown that, whatever the atmosphere (secondary vacuum pure He or He+H₂) in the experimental devices, at temperatures close to 400°C, pure liquid lead does not wet Fe or Fe-7Cr (F-82H) (contact angle higher than 90°). This result has been attributed to the presence of an oxide layer acting as a barrier for the wetting. Moreover, it has been observed that these materials are wetted by liquid Pb at 400°C (40°-50° contact angle) if, just before the wetting test, they are subjected to an in situ heat treatment at a higher temperature.

The objective of the work carried out this year, has been to study the wetting and the reactivity of the same materials, Fe and Fe-7Cr, by the Pb-17Li liquid alloy. Moreover, the behaviours of all the systems studied during 1999 and 2000 have been compared in order to draw the influence of Li content in Pb on the wetting.

2000 ACTIVITIES

EXPERIMENTAL RESULTS WITH THE SESSILE DROP TECHNIQUE

The sessile drop technique has been used in the usual way [1]: a piece of Pb-17Li, put on the polished substrate, is heated up to 500°C under a secondary vacuum in a vertical metallic furnace. To limit the liquid Pb-Li evaporation, a He+H₂ gas mixture atmosphere (1 bar) is introduced in the furnace. The temperature is thus increased up to obtain the drop spreading.

The first experiments conducted in this way have shown that this experimental procedure is not satisfactory because the oxide layer on the drop surface is too thick to allow the contact angles to be measured accurately.

For this reason, another technique allowing to produce the drop inside the furnace and to put it down on the substrate has been used afterwards.

EXPERIMENTAL RESULTS WITH THE "DISPENSED DROP" TECHNIQUE

A metallic furnace, heated by molybdenum resistances and inside which a 10⁻⁵ Pa vacuum can be achieved, is equipped with a device consisting in an alumina crucible and a piston.

At the bottom of the crucible, there is a 0.6 mm diameter capillary through which a drop can be made at the capillary end and dispensed on a substrate by using the piston (Figure 1). The experimental procedure is the following:

- the crucible with Pb-17Li is heated under vacuum at a higher temperature than the Pb-17Li melting point;
- when the temperature of the test is reached, the liquid alloy is pushed out of the crucible via the capillary to make a drop. The alloy extrusion through the capillary allows to avoid the presence of a continuous superficial oxide layer;
- the drop attached to the capillary is then put in contact with the substrate by moving the crucible;
- the crucible is raised to detach the drop from the capillary. After that, the drop spreads on the substrate.

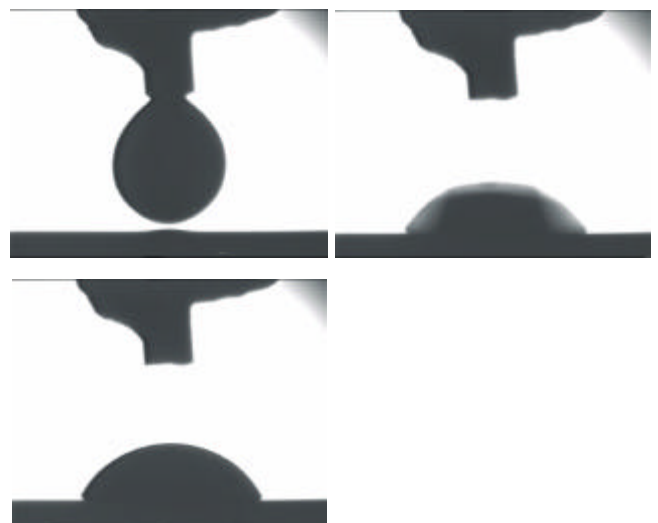


Figure 1 : Experiment 4 (Fe/Pb at 400°C)
Camera images of the "dispensed drop" technique

Two types of experiments have been performed:

- one for which before the drop formation at 400°C, the substrate is heated between 820°C and 850°C under vacuum ($\sqrt{10^{-4}}$ Pa) for a few minutes because it has previously been shown [1] that such a heat treatment allows to remove the oxide layer on Fe and Fe-7Cr substrates. After this treatment, the temperature is lowered at 400°C and the wetting test begins,
- another in which the substrates have not been heat treated at high temperature before the test. The crucible with Pb-17Li alloy and the substrate are heated at 400°C under vacuum atmosphere in which the test is performed.

RESULTS AND DISCUSSION

All the contact angle values measured with Pb or Pb-17Li drops under a high vacuum atmosphere (10^{-7} mbar) on Fe or Fe-7Cr substrates heat treated at high temperature or not are recalled in the Table 1.

Table 1 : Contact angles, obtained by the dispensed drop technique, of liquid Pb and Pb-17Li on Fe and Fe-7Cr at 400°C under a 10^{-7} mbar vacuum

Liquid	Substrate			
	Fe	HT Fe ⁽¹⁾	Fe-7Cr	HT Fe-7Cr ⁽¹⁾
Pb	71°	45°-50°	90°	60°±3°
Pb-17Li	---	49°±1°	68°±2°	61°±3°

(1) Substrate with a *in situ* heat treatment at 800°C under vacuum just before the wetting test

The Pb and Pb-17Li contact angles on heat treated iron have similar values (between 45° and 50°). These values are very close to those obtained by other authors with Pb on Fe preliminary heated treated under dry H₂ before test. (40° - 45°).

The oxygen partial pressure in the furnace is such that we can expect from Ellingham diagramme that iron oxides are not stable and therefore that Pb or Pb-17Li is in contact with a metallic iron surface. The addition of Li in Pb does not modify significantly the Pb/Fe system wetting characteristics. The contact angle values which have been determined are common for a liquid metal / solid metal system with negligible solubility as it is the case for the Pb/Fe and Pb-17Li/Fe system.

The contact angles of Pb and Pb-17Li on the heat treated Fe-7Cr substrate are similar. One interpretation is that the initial oxide layer has been removed during the heat treatment and the liquids are in contact with a metallic surface as for Fe substrate. However, it cannot be excluded that a very thin oxide layer or a pollution remains at the Fe-7Cr surface even after the heat treatment. It could explain the difference between the wetting of Fe and Fe-7Cr. It is also to notice that heat treatment at high temperature can induce modifications of the chemical composition of the Fe-7Cr material near its surface.

The comparison of the contact angle of Pb and Pb-17Li at 400°C on the Fe-7Cr material without preliminary heat treatment shows that the presence of Li in Pb increases the wettability of the Fe-7Cr material. The Li in Pb-17Li can react with the superficial oxide layer to reduce it at least partially. The final contact angle is not far from the one observed when Fe-7Cr has been preliminary heat treated (68° to compare to 61°).

The spreading kinetics are generally rapid which is a feature of a non reactive spreading: the kinetics is very rapid (spreading times less than 40 ms). The reactivity between Pb or Pb-17Li is limited to a grain boundary grooving (Figure 2). This phenomenon is limited compared to the dissolution process. Moreover, it is important to consider when the mean grain size of the material is of the same order of magnitude than the grooving depth: in that case, it can induce grain loosening.

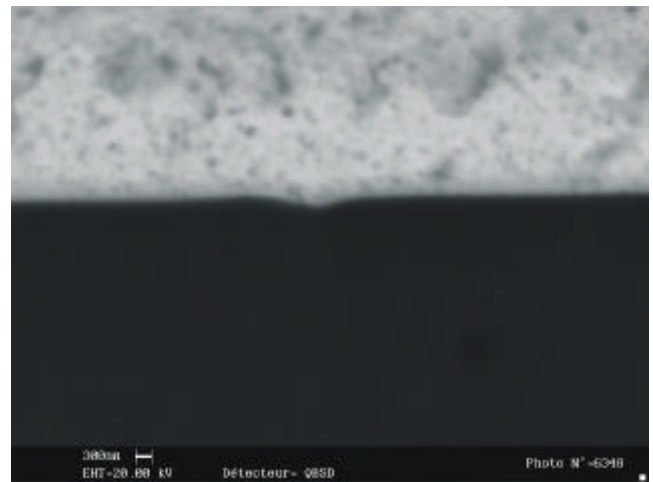


Figure 2 : Groove at the Pb-17Li/Fe interface at 400°C after 60 min

CONCLUSION

The low difference between the contact angles obtained with Pb and Pb-17Li liquids on the heat treated Fe or Fe-7Cr shows that on these substrates the effect of Li on the wetting is low. On the other hand, the presence of Li increases the wettability of the Fe-7Cr substrate with its initial oxide layer: the contact angle is decreased by about 20° (Table 1). Furthermore, Pb just as well Pb-17Li wet better the heat treated Fe ($\theta \approx 45^\circ$ to 50°) than Fe-7Cr ($\theta \approx 60^\circ$). We can also notice that our experimental results suggest that intermediate oxidation states between the metallic surface ($\theta \ll 90^\circ$) and the initial oxidised surface ($\theta \gg 90^\circ$) exist. Only *in situ* spectroscopic studies could allow to characterise these states. The spreading kinetics are very fast, which is characteristic of a non reactive spreading. The reactivity between Fe and Pb is limited to a Mullins type grooving. The reactivity between Fe and Pb-17Li in the sessile drop configuration is also mainly grooving at grain boundaries. The Fe-7Cr substrates undergo a very limited intergranular corrosion but at 400°C, the grooves are hardly visible with a Scanning Electron Microscope ($d < 100\text{nm}$).

REFERENCES

- [1] P. Protsenko, M. Jeymond, L. Coudurier, N. Eustathopoulos, Etude du mouillage des substrats a base de fer par des alliages de Pb, Decembre 1999.

REPORT

P. PROTSENKO, M. JEYMOND, N.
EUSTATHOPOULOS, A.TERLAIN
Wetting and reactivity in the Pb-17Li/Fe and Pb-17Li/Fe-
7Cr systems, RT SCECF 550 (November 2000)

TASK LEADER

Anne TERLAIN

DEN/DPC/SCCME/LECNA
CEA/Saclay

Tél. : 33 1 69 08 16 18

Fax : 33 1 69 08 15 86

E-mail : anne.terlain@cea.fr